DESIGN AND ANALYSIS OF MULTIBAND PLANAR ANTENNA FOR FUTURE 5G WIRELESS DEVICES

A Thesis Submitted in Fulfillment of the Requirement for the Award of the Degree of

DOCTOR OF PHILOSOPHY

in

ELECTRONICS AND COMMUNICATION ENGINEERING

Submitted By

NAVEEN KUMAR

Registration No: 951506005

Under Supervision of

Dr. Rajesh Khanna

Professor, ECED, TIET, Punjab, India

THAPAR INSTITUTE
OF ENGINEERING & TECHNOLOGY
(Deemed to be University)

Department of Electronics and Communication Engineering

THAPAR INSTITUTE OF ENGINEERING AND TECHNOLOGY,

PATIALA, PUNJAB - 147004

February 2021

DECLARATION

I, **NAVEEN KUMAR,** hereby certify that the thesis entitled **"DESIGN AND ANALYSIS OF MULTIBAND PLANAR ANTENNA FOR FUTURE 5G WIRELESS DEVICES"** which is being submitted by me to **Department of Electronics and Communication Engineering, Thapar Institute of Engineering and Technology (TIET), Patiala, Punjab, India** in fulfillment of the requirements for the award of the degree of ¨Doctor of Philosophy¨ under the guidance and supervision of **Dr. Rajesh Khanna,** Professor, ECED, TIET. The content presented in this thesis does not incorporate without proper acknowledgement any material previously published or written by any other person except where due reference is made in the text.

Naveen Kumar

Registration No.: 951506005 **Date:** 28/07/2021

CERTIFICATE

It is certified that the work contained in the thesis titled **"Design and Analysis of Multiband Planar Antenna for Future 5G Wireless Devices"** by Naveen Kumar [Registration No. 951506005] has been carried out under my supervision and that this work has not been submitted elsewhere for the award of any other degree.

Dr. Rajesh Khanna (Supervisor)
Professor,
Electronics and Communication Engineering Department,
Thapar Institute of Engineering and Technology Patiala, Punjab – 147004

Date: 28/7/21

ACKNOWLEDGEMENT

It is all by the grace of God that I got the opportunity to pursue Ph.D. degree. I am thankful and acknowledge the help and support given directly or indirectly by all those around me.

I would like to express my gratitude to my thesis supervisor **Dr. Rajesh Khanna**, Professor, ECED, TIET for providing excellent guidance, encouragement, inspiration, constant and timely support throughout this thesis work. The invaluable advice and support I received from him on academic and personal level have made me a better person both professionally and personally.

I would like to express my sincere gratitude to administration and management of Thapar Institute of Engineering and Technology (Deemed to be University) for supporting me during my studies. I am thankful to the Director, TIET, Patiala for his constant encouragement and support. I greatly acknowledge my doctoral committee members: Dr. Anil Kumar Verma, Professor, CSED, TIET; Dr. Amit Mishra, Assistant Professor, ECED, TIET; Dr. Jaswinder Kaur, Assistant Professor, ECED, TIET for sharing their valuable inputs in completing this work. I'm thankful to Dr. Anil Arora, Assistant Professor, ECED, TIET for his help and support to arrange testing of the antenna prototypes at Delhi University. I'm grateful to Dr. Alpana Agarwal, Professor and Head, ECED, TIET for providing her kind support throughout my studies. The staff of ECED is also always co-operative and helpful and I acknowledge my thanks to them.

Special thanks to my friends and colleagues: Gourav Mahipal, Manvi Sharma, Aarti Bansal, Navneet Kaur, Hitender Gupta, Sachin Yadav, Tajinder Kaur, Atipriya Sharma, Deepa Negi, Neha Ahuja, Vivek Singh Bawa, Abhishek Thakur, Sandeep Verma who were always there to help and support me. I'm grateful to Raksha for her constant support and encouragement which helped me in completing my work. I'm thankful to Dr. Divitha Seetharamdoo, Dr. Ozuem Chukwuka Anthony, and Syed Ali Kazim from Universite Gustave Eiffel, Villeneuve d'Ascq, France for their help and support.

Last but not the least, I would always like to thank my parents Sh. Narinder Kumar and Smt. Satya Devi for their continuous support and patience. Special thanks to my brother Er. Rohit Saini and his companion Mrs. Jaspreet Kaur for their support.

Naveen Kumar

ABSTRACT

As the wireless communication systems are advancing continuously in terms of technology, size, features, data rate etc., the need to support multiple communication technology poses space constraints. The gadgets and devices that we are seeing these days are compact in size which not only supports voice communication but also serve as a multimedia system supporting applications like Voice over Internet Protocol (VoIP), multi-person video calling, high-speed internet, online high-end games, virtual reality-based apps etc. For the advanced apps/softwares there is the need of high data rate which further demands more bandwidth from the communication technology in use.

Antenna is an important component of any wireless device and can affect the system performance if not properly designed. With the development of next generation of mobile communication technology i.e. Fifth Generation (5G), new frequency bands have been added to be used for mobile communication. For the first time, the bands in mmWave range between 30 GHz to 90 GHz have been earmarked for 5G use cases. This results in need to design antennas which can support the lower as well as mmWave bands for 5G communication. This motivation led to the work presented in the thesis.

The thesis is focused to achieve four objectives: first one is to analyze and design a single element planar antenna. The antenna type chosen is Planar Inverted-F Antenna (PIFA) and the radiating element is analyzed using Theory of Characteristic Mode (TCM) analysis to design the antenna systematically. The TCM analysis showed what current modes are the significant modes which can be excited efficiently to achieve the desired frequency band coverage. The overall structure of PIFA is also analyzed using TCM to find out the location of the radiating element on the ground plane. Second objective is to design a MIMO antenna system using the radiating element designed in first objective. So, two element and four element MIMO antennas are designed, simulated and analyzed for MIMO performance. One of the PIFA design is with L-shaped radiating element (Ant 1) and second one is with L-shaped L-slot radiating element (Ant 2). Ant 1 works in 3.5 GHz, 12 GHz, and 17 GHz bands while Ant 2 works in 3.5 GHz, 4.2 GHz, and a wide mmWave band.

Without the use of any isolation enhancement technique, the isolation level between certain antenna elements is above -15 dB level which is not good for MIMO antennas. So, the third objective is to enhance the isolation between the antenna elements by using

isolation enhancement technique. The technique used is to introduce a complimentary metamaterial unit cell placed between the antenna elements on the ground plane. The novel metamaterial unit cell is designed to exhibit metamaterial properties in 3.5 GHz band. This is because it has been observed that the isolation level is poor in 3.5 GHz band and inclusion of metamaterial unit cell in MIMO antenna design enhances the isolation by 8 dB in 3.5 GHz band.

The fourth objective is to fabricate the proposed antenna structures and measure the antenna parameters using Network Analyzer and Anechoic Chamber. The measured and simulated results for all the proposed MIMO antenna designs shows good agreement with each other. As per our knowledge, the antenna design supporting both sub-6 GHz and mmWave bands is not reported before in the literature. So, the proposed MIMO antenna is novel as the same radiating element supports both sub-6 GHz and mmWave bands making the whole structure compact and leaving more space for other device components.

Keywords: 5G, isolation, mmWave, metamaterial, MIMO.

TABLE OF CONTENTS

List of Figures

List of Tables

Nomenclature

ε	Permittivity
ε_r	Relative Permittivity/ Relative Effective Dielectric Constant
λ	Wavelength
λ_o	Wavelength of resonant frequency
μ	Permeability
J	Current Distribution
α_n	Eigenvalue of n^{th} Characteristic Mode
J_n	Eigen current of n^{th} Characteristic Mode
S_{ij}	S-parameters of i and j ports
$\eta_{i,rad}$	Radiation Efficiency of i^{th} port
δ	Loss tangent
n	Refractive index
z	Impedance
c	Speed of light
ρ_e	Envelope correlation coefficient

Acronym and Abbreviations

3G	Third Generation
4G	Fourth Generation
5G	Fifth Generation
AMPS	Advanced Mobile Phone Services
CCL	Channel Capacity Loss
CMA	Characteristic Mode Analysis
CST	Computer Simulation Technology
DCS	Digital Communication System
DGS	Defected Ground Structure
DG	Diversity Gain
DNG	Double Negative
DRA	Dielectric Resonator Antenna
EBG	Electromagnetic Band Gap
ECC	Envelope Correlation Coefficient
ENG	Epsilon Negative
FDD	Frequency Division Duplexing
GHz	Gigahertz
GPS	Global Positioning System
GSM	Global System for Mobile Communication
HD	High Definition
HFSS	High Frequency Structure Simulator
IoT	Internet of Things
LTE	Long Term Evolution
MEG	Mean Effective Gain
MHz	Megahertz
MIMO	Multiple input Multiple Output
MNG	mu Negative
MSA	Microstrip Antenna
MTM	Metamaterial
NL	Neutralization Line
NR	New Radio
PCS	Personal Communication Service

PCB	Printed Circuit Board
PIFA	Planar Inverted-F Antenna
SAR	Specific Absorption Rate
SIW	Substrate Integrated Waveguide
SRR	Split Ring Resonator
SDL	Supplementary Downlink
SUL	Supplementary Uplink
TARC	Total Active Reflection Coefficient
TCM	Theory of Characteristic Mode
TDD	Time Division Duplexing
UMTS	Universal Mobile Telecommunication Service
VNA	Vector Network Analyzer
WiMAX	Worldwide Interoperability for Microwave Access
WLAN	Wireless Local Area Network
WRC	World Radio Congress

Chapter 1 Introduction

1.1 Introduction

In the late 1980's, the first-generation wireless systems were developed such as Advanced Mobile Phone Services (AMPS) but as the need for digital technology increased, the second-generation wireless systems came into view such as Global System for Mobile Communication (GSM) and Digital AMPS. The third generation was deployed in the 21st century due to the requirement of high-speed digital communication technology. Then fourth generation was introduced to provide mobile broadband services which has higher data rate than its predecessors. Recently research and development of standards and technologies has been started for next generation of mobile communication which is fifth generation [1].

Since the start of wireless communication with first communication system to the latest Smartphones and gadgets, there is an exponential increase in complexity of systems. Figure 1.1 presents the generations of mobile communication with their major technological advancements. The Dawn of 5G Era has started with various industries and research institutes are working towards defining, designing and developing the systems, technologies and specification/standards for the fifth Generation (5G) systems. There will be significant rise in user data traffic in the next few years and to cope up with this there is a need to develop advanced techniques, services and devices for the upcoming 5G technology [2].

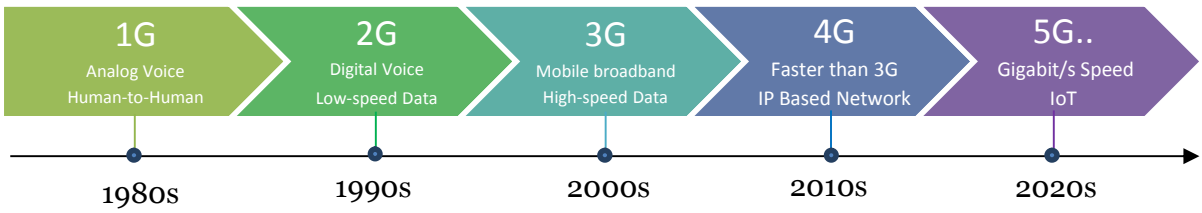

Figure 1.1: Generations of Mobile Communication

There will be significant change to be seen in the next generation of mobile technologies. 5G is proposed to be the key technology behind implementation of IoT. A device such as refrigerator, dishwasher, air conditioner and many more appliances will be able to get connected to the network all the time regardless of location and without human intervention. In order to make it happen, the 5G infrastructure can have simultaneous connectivity for

millions of device connections. Smart Cities, Smart Grids, Smart Transport, Machine to Machine Connectivity, Telemedicine are some of the potential technologies that will become a possibility as a result of 5G [3].

Mobile communication has seen an enormous growth in the field of wireless communication in recent years. Nowadays, portable devices have gained much popularity due to multimedia support, High Definition (HD) videos, smart apps, able to click photos, play music, able to receive and make calls etc. The technology not only focuses on multiple functions but also the prototype of the mobile handset. A low-profile structure that gives smarter designs is the main need in today's era [4]. Therefore, a mobile phone that is not used only for calling but also as an entertainment device and makes our life comfortable and easier, is required.

So, the requirements for future antennas are wider bandwidth, higher gain, directionality, MIMO capability, beamforming etc. Several antenna structures have been proposed by researchers worldwide, working at different frequencies of 5G communication. Some researchers developed MIMO antennas while others presented novel techniques to achieve high gain and wider bandwidth.

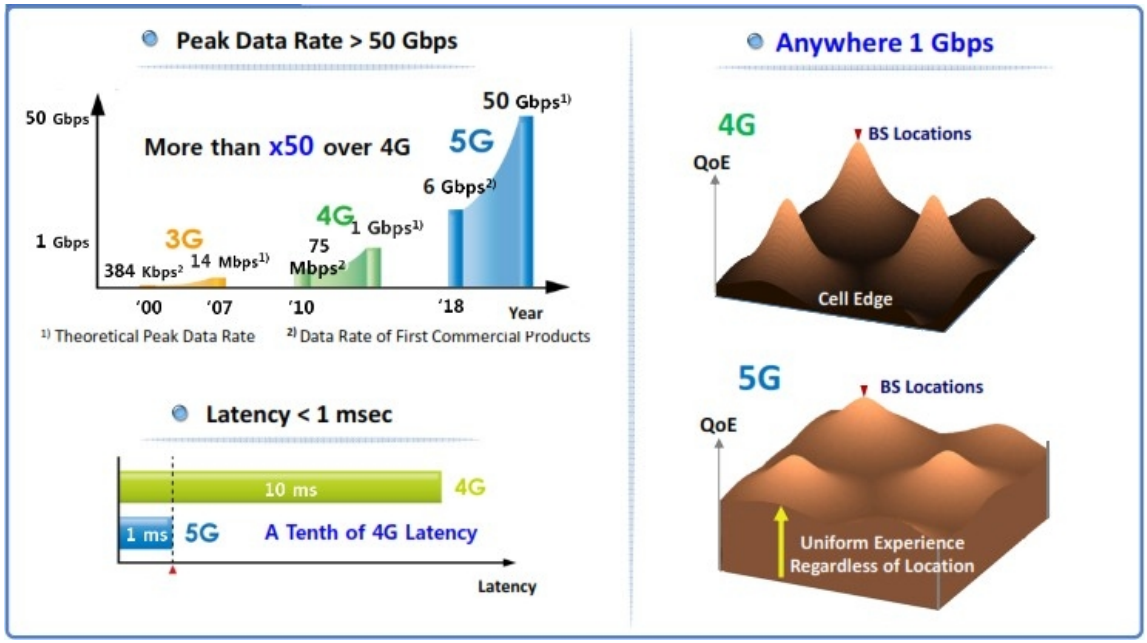

Figure 1.2: 5G Service Vision [5]

Figure 1.2 shows 5G service vision which was proposed by Samsung in their white paper published in 2015. Many research labs, industries share similar vision for future 5G communication. As the demand for digital technology increases, a system that can support high transmission bandwidth and provide high-quality multimedia is required. To meet these challenges, mobile phones were equipped with small antennas that can support multiple

frequency bands and have low profile structure so that they can be easily placed in the housing of the mobile phones [4].

As the development of 5G wireless standards and systems progresses, the frequency bands for next generation mobile communication below 6 GHz will be important to make the smooth transition from 4G LTE to 5G technologies. Although 4G LTE will undergo through a continued evolution for mobile broadband by using advanced techniques such as carrier aggregation and higher-order modulations to improve bandwidth characteristics beyond present limitations.

In the current communication scenario, the mobile technologies which are working in spectrum bands above 6 GHz will be utilized by the mobile industry to achieve additional bandwidth which results in obtaining higher data rates and high capacity from the future communication systems. It is expected that future 5G wireless systems will mostly be employed in such environments which allows dense and much localized deployment, potentially making Time Division Duplex (TDD) more viable. The bands between 6 GHz and 40 GHz are important to consider for 5G systems due to propagation characteristics in these bands [3].

These days wireless networks are becoming heterogeneous due to significant development in the technologies for radio access. The portable devices with multimedia support, High Definition (HD) videos, numerous apps/softwares, high end gaming, augmented reality, virtual reality etc. are gaining popularity. This will lead to significant rise in user data traffic in the next few years [5]. To cope up with this, advanced techniques, services, and new devices needs to be developed for the upcoming 5G services. At World Radio Congress (WRC 15) meeting, several countries submitted proposals for the frequency bands which can be considered for future 5G communication. Industries and research institutes are working towards defining, designing and developing the systems, technologies and specification/standards for 5G systems supporting high data rate.

In the year 2018, 5G New Radio (NR) bands in sub-6 GHz range were allocated for future mobile broadband services and few bands above 6 GHz range were also allocated for 5G communications in the year 2019. All these developments have led to the need for multi-element antenna systems in wireless devices. In MIMO system the transmitter and the receiver use more than one antenna to create multiple uncorrelated channels between them. These MIMO antenna devices need to be compact in size supporting various functions. Hence, a low-profile structure that results in compact devices and aesthetically good designs, is the need of the hour [4].

Table 1.1 presents the frequency bands allocated for 5G communication both in sub-6

GHz and mmWave frequency range. The sub-6 GHz range is also termed as FR1 and mmWave range is termed as FR2. The bands in mmWave range are all operating in TDD mode and offer wide bandwidth.

Table 1.1 Frequency Bands allocated for 5G Mobile Communication *[6]*

Operating Band	**Frequencies**		**Duplex Mode**
	Uplink (MHz)	**Downlink (MHz)**	
n1	1920 – 1980	2110 – 2170	FDD
n2	1850 – 1910	1930 – 1990	FDD
n3	1710 – 1782	1805 – 1880	FDD
n5	824 – 849	869 – 894	FDD
n7	2500 – 2570	2620 – 2690	FDD
n8	880 – 915	925 - 960	FDD
n12	699 – 716	729 - 746	FDD
n20	832 – 862	791 - 821	FDD
n25	1850 – 1915	1930 – 1995	FDD
n28	703 – 748	758 – 803	FDD
n34	2010 – 2025	2010 – 2025	TDD
n38	2570 – 2620	2570 – 2620	TDD
n39	1880 – 1920	1880 – 1920	TDD
n40	2300 – 2400	2300 – 2400	TDD
n41	2496 – 2690	2496 – 2690	TDD
n50	1432 – 1517	1432 – 1517	TDD
n51	1427 – 1432	1427 - 1432	TDD
n66	1710 – 1780	2110 – 2200	FDD
n70	1695 - 1710	1995 – 2020	FDD
n71	663 - 698	617 – 652	FDD
n74	1427 - 1470	1475 – 1518	FDD
n77	3300 – 4200	3300 – 4200	TDD
n78	3300 – 3800	3300 – 3800	TDD
n79	4400 - 5000	4400 – 5000	TDD
[7]n257	26500 – 29500	26500 – 29500	TDD
n258	24250 – 27500	24250 – 27500	TDD
n260	37000 – 40000	37000 – 40000	TDD
n261	27500 - 28350	27500 - 28350	TDD

Table 1.2 Frequency Bands allocated for various Communication Standards [7]

Wireless Communication Service		**Allocated Frequency Band**
GSM 900	Global System for Mobile	890-960 MHz

	Communication	
DCS 1800	Digital Communication System	1710-1880 MHz
PCS 1900	Personal Communication System	1850-1990 MHz
UMTS 2000	Universal Mobile Telecommunications Systems	1920-2170 MHz
3G IMT-2000	International Mobile Telecommunications – 2000	1885-2200 MHz
4G LTE	Fourth Generation Long Term Evolution	704-716 MHz, 734-746 MHz 1710-1755 MHz, 2110-2155MHz 2300-2400 MHz 2500-2570MHz, 2620-2690 MHz
ISM 2.4	Industrial, Scientific, Medical	2400-2484 MHz 5150-5350 MHz 5725-5825 MHz
UWB	Ultra-wide Band	3.1 – 10.6 GHz
IoT [8]	ISM bands Potential Band(s)	2400-2484 MHz, 5150-5350 MHz, 5725-5825 MHz 12 GHz, 17 GHz

1.2 Common Antenna Types for Portable Devices

For portable or handheld devices there are many kinds of antenna structures being used depending on the space constraint and application type. The advancements in the design of the antennas is driven by the requirements of the mobile communication market. Most of the antennas are designed to support major communication standards worldwide such as GSM, DCS, PCS, UMTS (3G), 4G LTE, and next will be 5G. On the other hand, some of the designs are also used for non-cellular frequency bands such as WLAN, Bluetooth, GPS and WiMAX.

Couple of the most used planar antenna types are:

- Microstrip Antenna (MSA)
- Planar Inverted-F Antenna (PIFA)

1.2.1 Microstrip Antenna (MSA)

The antennas which uses microstrip line to feed the radiating element are termed as

Microstrip Antennas. They are also known as microstrip patch antenna (MPA) because they can be easily printed on PCB using common PCB prototyping procedure. In Microstrip structure there is a dielectric substrate which has ground plane on one side and the antenna radiating geometry on the other side as shown in Figure 1.3 [4]. These antennas are easy to handle, light in weight and support linear as well as circular polarization. On the other hand, the typical drawbacks are low gain, narrow bandwidth, and low power handling capacity. Multiband operation can be obtained by applying various techniques such as defected ground structure [9], slotted radiating element [10] [11],

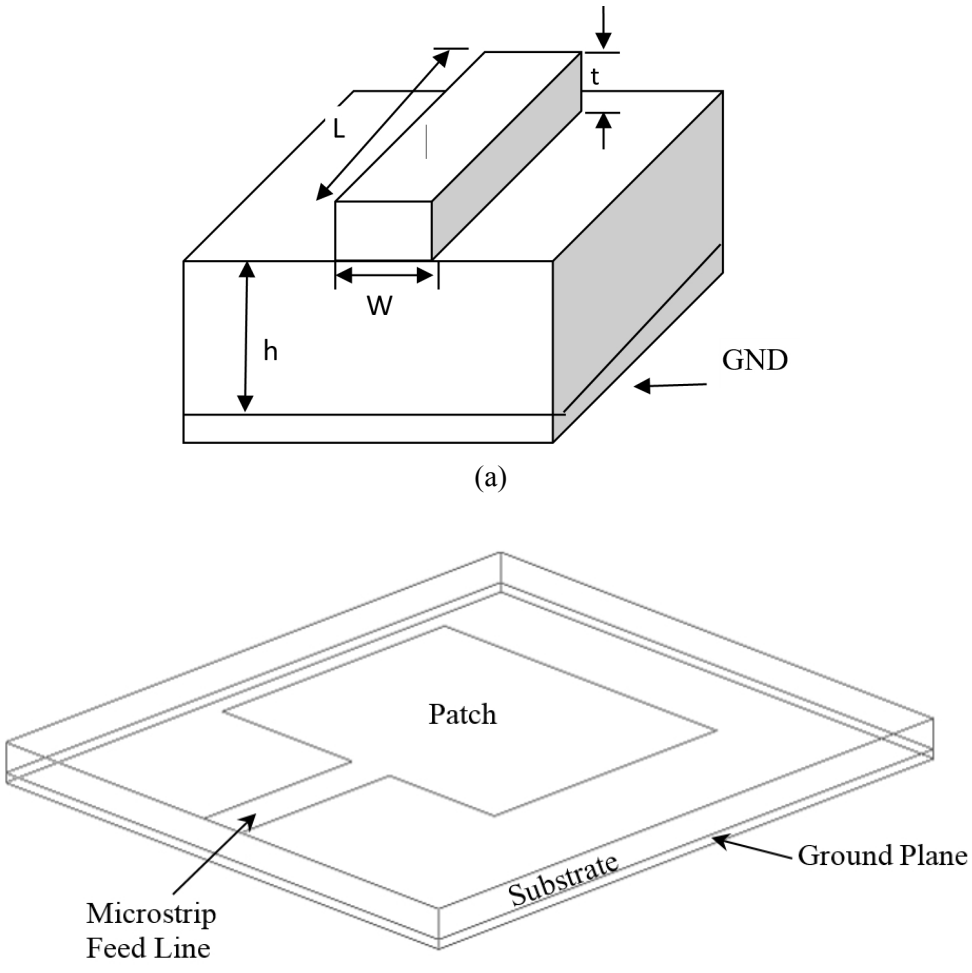

Figure 1.3: (a) Microstrip line (b) Conventional Microstrip antenna (MSA)

1.2.2 Planar Inverted F Antenna (PIFA)

The bandwidth of Inverted-F Antenna (IFA) is very narrow and to improve the bandwidth of the antenna, a conductor plate replaces the wire radiator, hence PIFA was invented. Another term used for PIFA short-circuited microstrip antenna as a plate is used to short circuit the ground plane and the radiating element as shown in Figure 1.4 [4]. The ground

plane size has a significant role in designing PIFA and can be used to optimize the antenna for wide-band and multi-band frequencies. Due to low profile, compact size, easy integration, and light weight, the PIFA is used in number of applications especially in mobile phone handsets [12].

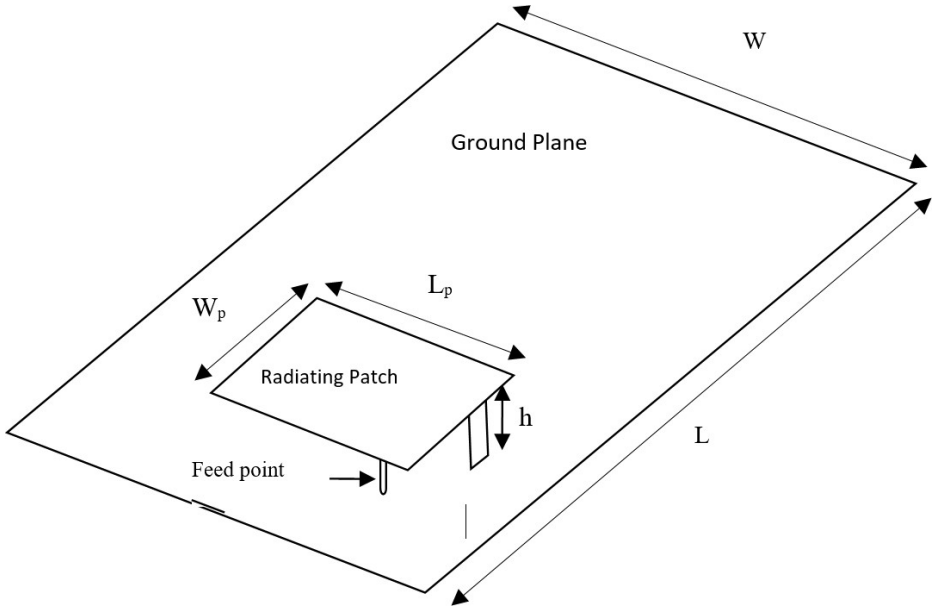

Figure 1.4: Conventional Planar Inverted-F antenna (PIFA)

Different shaped slots are etched on ground plane and/or radiator, to obtain different configurations in order to achieve single and multiple resonant frequencies. The bandwidth of the antenna can be improved by transforming the horizontal element from a wire to a plate which also results in PIFA structures. These designs have self-resonating structure and by varying dimensions and position of the shorting and feed plate, the antenna performance can further improve [12].

Compared to conventional antenna types, PIFA offers unique advantages such as compact size making it possible to house inside the mobile device body. Also, PIFA offers low back radiation which results in lower Specific Absorption Rate (SAR) values towards the user's body [12]. In both vertical and horizontal polarization states, the PIFA structure shows moderate to high gain. Apart from various advantages the efficiency of PIFA is reduced by various losses such as mismatch, external parasitic resonances, ohmic, feed line transmission etc.

The advancement of the configuration of the handset antenna from monopole antennas to PIFA shows that the wire is the vital component of a handset antenna, while the slot(s) and stub(s) compensate for the mismatch between different components and enhance the characteristics of radiation [13].

1.3 MIMO Antenna Isolation Techniques

In handheld devices having small form factor, the MIMO antenna configuration may result in closely placed antenna elements [14]. This can lead to high coupling levels which further degrades the efficiency and channel capacity of MIMO system. There are several techniques which can enhance the isolation and diversity performance of the MIMO antennas [15] [16].

1.3.1 Defected Ground Structure

For planar antennas the ground plane affects the overall performance as the surface current flows through the ground plane too and for lower frequencies it also acts as a radiating structure. Since, for the proper functioning of the MIMO antenna system, the elements need to have same ground plane, as a result of which there may be higher mutual coupling between the antenna elements due to the induced current on the ground plane. The mutual coupling reduction can be achieved by creating some ground plane defects [17] [18]. The function of the defect is as reject filter which suppress the coupled fields. This method of mutual coupling reduction is termed as defected ground structures (DGS). The ground plane can have the defects in various shapes and sizes such as open-ended slots, slits, shielding walls etc. [19] [20]. Figure 1.5 shows one type of DGS for two element MIMO antenna system.

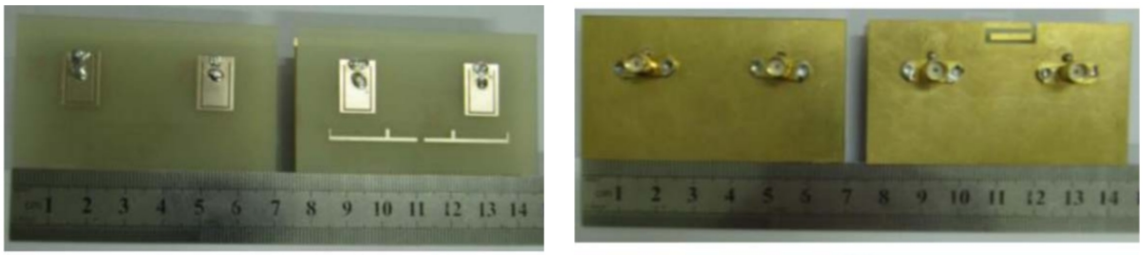

(a) (b)

Figure 1.5: (a) Front side of two PIFAs without/with isolation structures (b) Back side of two PIFAs without/with isolation structures [17]

1.3.2 Decoupling Networks

The antenna elements of MIMO system having mutual coupling between them can use decoupling networks to reduce the coupling. The input ports of adjacent antennas would be

decoupled by such networks, thereby reducing the correlation between the radiation pattern resulting in increase their radiation efficiency. A matching network is usually used as a decoupling network to provide adequate input port matching [21] [22] and several designs have been implemented with this approach for example as shown in Figure 1.6. Lumped and distributed components have been used adeptly to increase isolation between nearby antennas [23].

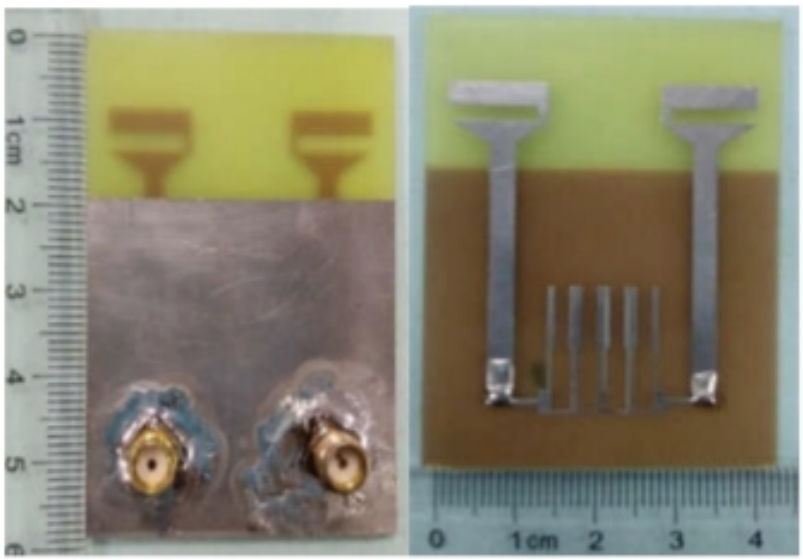

Figure 1.6: Front and Back view of MIMO Antenna with Decoupling network on top layer [23]

1.3.3 Neutralization Line

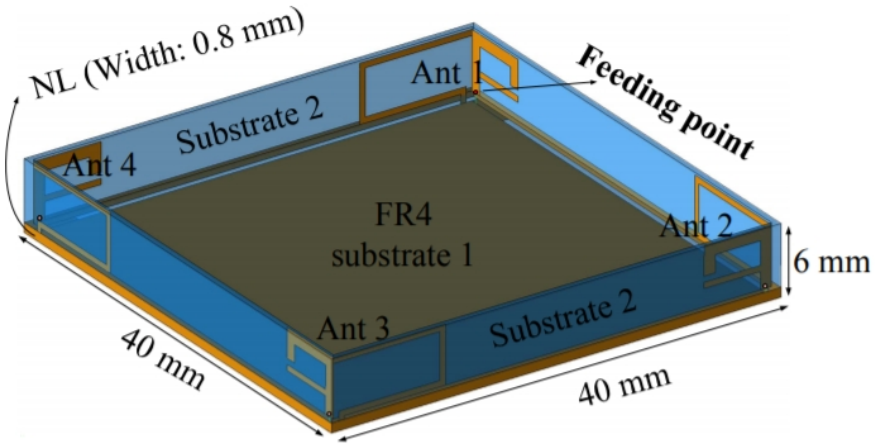

Figure 1.7: Configuration of MIMO Antenna with Neutralization line (NL) [24] © 2018, IEEE

The increase in the mutual coupling and correlation between the antenna elements is caused by induction of some currents on its nearby antenna element. Another technique to

improve isolation is to use neutralization line (NL) in which the current is captured at a particular position at the excited element, then the phase is reversed by choosing a suitable length of the NL [24] [25] [26]. In this strategy, choosing the point is crucial. With minimum impedance and highest current, the point on the radiating antenna should then be. The NL technique's effective bandwidth depends on the variance of the impedance at the selected position. On the surface of the radiating antenna, the starting point of the NL is then chosen as a low impedance point with stable impedance in the operating band.

1.3.4 Parasitic Elements

Another approach to minimize mutual coupling is by using parasitic elements to remove part (or most) of the coupled fields between antenna elements. This improves the efficiency, isolation and correlation coefficient between the antenna elements. An inverse coupling field will be generated by the parasitic component which reduces the original one, decreasing the overall coupling to the victim antenna. Typically, these parasitic components are not physically bound to the antennas, as if they were attached to the ground system to create a kind of resonator. Figure 1.8 shows an example of using a parasitic PIFA element. These modules are configured to monitor the bandwidth and frequency band of isolation. The objective of the use of parasitic elements is to minimize the mutual coupling by generating reversing fields to the original ones produced by the stimulated antenna [27].

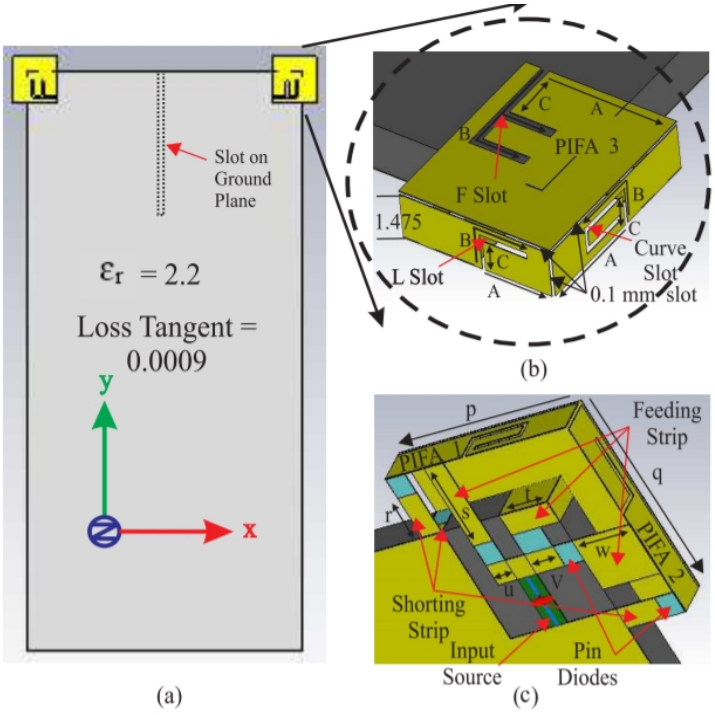

Figure 1.8: Geometry of MIMO antenna with parasitic PIFAs (a) Front View (b) Slot on the ground plane (c) Shorting and Feed strip position of PIFA [27] © 2016, IEEE

1.3.5 Metamaterials

Metamaterials (MTM) are the artificial materials whose properties are not found in nature but can be engineered. Materials that possess negative dielectric permittivity and negative magnetic permeability are known as Double Negative (DNG) materials or Metamaterials. J. B. Pendry showed that the mu negative (MNG), epsilon negative (ENG), and double negative (DNG) material can be obtained by using periodic thin wire structures and/or split-ring resonators (SRRs) effectively [28]. MTM can enhance the performance parameters of an antenna such as gain, bandwidth, polarization conversion, beam steering and size reduction [29, 30, 31, 32, 33, 34, 35, 36, 37, 38].

Also, for MIMO antenna designs the isolation can be enhanced by employing MTMs [33] [39] [40] [41]. High isolation levels can be achieved with proper designing of MTM structures in desired frequency bands. Figure 1.9 illustrates one example of the use of the MTM structure to enhance isolation. If properly constructed, the band gaps may act as a band-reject filter and reduce the mutual coupling between the antenna elements.

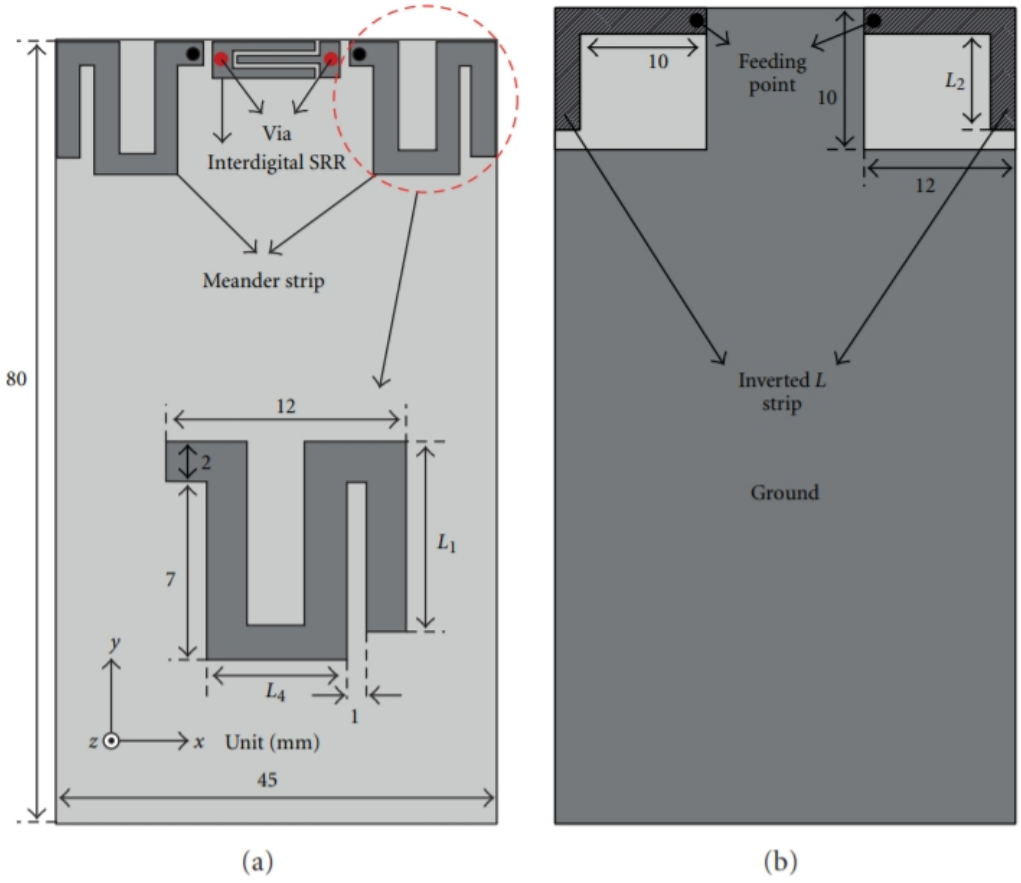

Figure 1.9: Proposed antenna structure (a) Top View with SRR between the antenna elements (b) Bottom view with feed points [29]

1.4 Theory of Characteristic Mode (TCM)

Though state-of-the-art commercial full-wave electromagnetic solvers are available to the researchers to model and analyze electromagnetic structures including antennas, systematic antenna design on complex platforms can only be performed using the theory of Characteristic Modes (TCM) [42, 43]. It is an interesting approach extensively used in mobile industry which helps us to design more efficient and higher performance antennas [44, 30, 31]. TCM describes current distribution on a conductive body as superposition of several characteristic modes. Moreover, the use of TCM for MIMO antenna designs has shown to outperform conventional design methods [43].

In recent years, Theory of Characteristic Mode (TCM), also known as Characteristic Mode Analysis (CMA) is being applied to design various types of antennas for numerous applications. TCM was first discussed by Garbacz [45] and its refined work was presented by Harrington and Mautz [46]. Even after these initial works on TCM, it was not significantly used in the analysis and design of antennas for many years. But in recent years TCM gained popularity and its use for systematic antenna design [43], bandwidth enhancement [47, 48], MIMO system design [44], optimizing feed location [49], multi-mode antenna design [50, 51] became prominent, chassis modes are also analyzed and used for efficient MIMO system design [52, 53] [54]. TCM offers a modal study of conductors by evaluating eigenvalues from a set of weighted eigen function equations [43]. As per TCM, the following equation shows different parameters for current distribution (J) as it is further decomposed into a set of orthogonal modes:

$$J = \sum_n a_n J_n = \sum_n \frac{1}{1+j\alpha_n} V_n J_n \qquad (1.1)$$

where a_n is the weighing coefficient, V_n is the excitation coefficient of nth characteristic mode, α_n is the Eigenvalue of nth characteristic mode, J_n is the eigen current of nth characteristic mode

The electromagnetic properties of the conductor can be explored by analyzing the eigenvalues and eigen vectors (or eigen currents). Comparing traditional antenna design techniques and TCM approach, it can be observed that TCM provides a systematic process to design an antenna while former approach mainly relies on experience and trial-and-error [43].

1.5 MIMO Antenna Performance Parameters

1.5.1 Envelope Correlation Coefficient (ECC)

The ECC is described as a metric of isolation between closely positioned antenna elements. In other words, the mutual coupling of the antenna elements can be measured in terms of the ECC. There are two techniques for computing ECC, one is from the far-field radiation patterns [55] and the other is from the S-parameters [56].

Practically, the first method is far more complicated and requires a lot of processing of numerous data points compared to the second method [14]. So, the S-parameters based method is preferred mostly for high efficiency antennas. Also, accurate ECC values can be calculated by including antenna radiation efficiency term [57]. According to S- parameters method, ECC (ρ_e) between antenna elements (i, j) of N-element MIMO system is calculated by following equation [14]:

$$\rho_e(i,j,N) = \left| \frac{\sum_{n=1}^{N} S_{i,n}^{*} S_{n,j}}{\prod_{k=i,j}\left(1-\sum_{n=1}^{N} S_{k,n}^{*} S_{n,k}\right)^{1/2}} \right|^2 \frac{1}{\eta_i \, \eta_j \, \eta_N} \tag{1.2}$$

where $S_{i,n}$, $S_{n,j}$, $S_{k,n}$, $S_{n,k}$ are S-parameters

η_{ir}, η_{jr}, η_{Nr} are radiation efficiencies of the ports.

1.5.2 Diversity Gain (DG)

Another important diversity performance parameter of MIMO system is Diversity Gain (DG) which is calculated as:

$$D = 10 e_\rho \tag{1.3}$$

where $e_\rho = \sqrt{(1 - |0.99\rho_e|^2)}$

1.5.3 Total Active Reflection Coefficient (TARC)

When multiple antenna elements forming a multi-port antenna system operates simultaneously, the performance of antenna elements affects adjacent elements. The actual system behavior is not completely predicted by S-parameters alone. TARC is defined as "the ratio of the square root of the total reflected power to the square root of the total incident power" as seen below [58]:

$$\Gamma_a^t = \sqrt{\sum_{i=1}^{N} |b_i|^2} / \sqrt{\sum_{i=1}^{N} |a_i|^2} \quad (1.4)$$

TARC can be calculated from the scattering matrix of the MIMO antenna. For 2 element antenna system, TARC can be calculated using following equation [14]:

$$\begin{aligned} \Gamma_a^t &= \sqrt{(|a_1(s_{11} + s_{12}e^{j\theta})|^2 + |a_1(s_{21} + s_{22}e^{j\theta})|^2)} / \sqrt{2|a_1|^2} \\ &= \sqrt{((s_{11} + s_{12}e^{j\theta})|^2 + |(s_{21} + s_{22}e^{j\theta})|^2)} / \sqrt{2} \end{aligned} \quad (1.5)$$

where θ is the phase of input signal.

After obtaining the S-parameters of the MIMO antenna system, the phase of the input signal is varied between 0 and 180 degrees. This variation in phase gives us an insight to the antenna resonant behavior and results in corresponding plots for effective bandwidth evaluation.

1.5.4 Mean Effective Gain (MEG)

Another key consideration for the MIMO antenna system is Mean Effective Gain, which depicts the effect of the antenna on the link budget. MEG is defined as "the average power received by the antenna to the sum of the average power that would have been received by two isotropic antennas in the same environment" [14].

MEG is a measure of antenna performance in a real propagation environment. The equation to calculate MEG using S-parameters of MIMO antenna system is given below:

$$M\ \ G_i = 0.5\eta_{i,r} \quad = 0.5\left[1 - \sum_{j=1}^{M} \left|S_{i}\right|^2\right] \quad (1.6)$$

where $\eta_{i,rad}$ is radiation efficiency for i^{th} port, M is number of antenna elements in MIMO system, S_{ij} is the S-parameter

1.5.5 Channel Capacity (CC)

Channel capacity is a measure of number of bits per Hz of bandwidth [14]. In other words, it is defined as the maximum rate of information transfer over a communication channel without interference and it is also known as Shannon's theorem. It is a way to compare MIMO system performance with single antenna. It is influenced by other diversity performance parameters and it grows linearly with increase in number of antenna elements in

MIMO system [8]. The measure of system degradation can be evaluated in terms of channel capacity loss (CCL). It is calculated using the following equations:

$$C(Loss) = -\log_2 \det(\eta) \tag{1.7}$$

where η = 2 x 2 correlation matrix

$$\eta = \begin{bmatrix} \sigma_1 & \sigma_1 \\ \sigma_2 & \sigma_2 \end{bmatrix} \tag{1.8}$$

CCL can also be calculated using S-parameters:

$$\sigma_{ii} = 1 - \left(|S_{ii}|^2 - |S_{ij}|^2\right) \tag{1.9}$$

$$\sigma_{ij} = -\left(S_{ii}^{*} S_{ij} + S_{ji} S_{ii}^{*}\right) \tag{1.10}$$

1.6 Motivation of Thesis

With the transition from 4G to 5G technology, the data rates will also increase as the demand for higher data rate increases. Therefore, the need for antennas supporting high data rates arises and this can be achieved by Multi-Input Multi-Output antenna systems. Along with support high data rates, new frequency bands are also being allocated for 5G communication which demands novel antenna solutions to support sub-6 GHz as well as mmWave bands. Having multiple antenna elements forming MIMO system may result in performance parameter degradation due to mutual coupling.

Based on the discussions in the previous sections, several MIMO antenna designs have been proposed in this thesis covering 5G NR bands below 6 GHz and in mmWave frequency range. TCM is used for systematic design of the antenna element. Isolation is enhanced by using complimentary metamaterial unit cell on the ground plane placed between the antenna elements.

1.6.1 Research Gaps

- In last couple of years many researchers have proposed antenna designs for 5G future devices operating at different frequency bands above 6 GHz. Several antenna structures have been designed and analyzed such as circularly polarized patch antenna [59], Dielectric resonator antenna (DRA) [60], Magneto-Electric Dipole [61], Patch antenna using EBG [62], Patch Antenna array [63], Reconfigurable antenna [64] [65], Fabry Perot Resonator [66], Printed

Slot Antenna [67, 68], Hybrid MIMO antenna [69], SIW Slot array [68]. Most of the designs are single element designs with moderate gain values. Future 5G devices will require high gain and multiple antenna elements to support higher capacity and higher data rates. So, MIMO designs need to be explored and developed for candidate frequencies of 5G wireless communication.

- The technologies such as 4G, WLAN and future 5G Services are developed to support higher data rates and to achieve this multiple antenna elements are required in wireless devices. In [14] several MIMO parameters are discussed and various antenna designs at different frequencies are presented. In [34], [59], [69], [70], [71], [72] many novel designs for MIMO applications have been proposed and analyzed. But in most of the designs mutual coupling is just near acceptable value. Work can be done to improve MIMO parameters like isolation, ECC, Diversity Gain etc. To improve MIMO parameters, several techniques have been proposed recently such as using slots on ground plane [73], Metamaterials (MTM) [29], [32], [33]. Conventionally MTMs are used to enhance antenna parameters like gain, size reduction, bandwidth etc. Also, MTM can be used in MIMO structures to improve isolation.
- Theory of Characteristic Modes (TCM)analysis provides an innovative and systematic design process for developing MIMO antenna systems. Recent research work lacks analysis of the antenna structures to design efficient structures systematically [43].

1.7 Objectives

Based on the research gaps identified above the main objectives of the thesis are:

1. To propose and analyze a single element planar antenna of MIMO system.
2. Design of a MIMO system with more number of elements for future 5G services.
3. To optimize and enhance various antenna parameters like gain, bandwidth, efficiency and MIMO characteristics of the proposed antenna.
4. To fabricate and test the proposed antenna.

1.8 Research Methodology

The research will be carried theoretically and through simulations using commercial software simulation package such as High Frequency Structure Simulator (HFSS), Computer Simulation Tool (CST), FEKO. These softwares will be used for design and simulation of proposed antenna structures. Then analysis and optimization of the antenna structures is done to achieve desirable antenna characteristics and performance.

Following methodology is followed to achieve objectives of the research work:

- Designing of single element antenna structure of MIMO system in the simulation software.
- Analysis and optimization of proposed structure using Theory of Characteristic Modes (TCM).
- Fabrication and testing of the proposed single element design.
- Designing a MIMO system by extending single element structure into a greater number of elements.
- Analysis and optimization of proposed MIMO system to achieve desirable characteristics.
- Fabrication and testing of the proposed MIMO system.
- Designing of a suitable Metamaterial (MTM) structure at operating frequency.
- Introducing the MTM structure between the antenna elements of the MIMO system to enhance performance of the system.
- Fabrication and testing of the final proposed MIMO antenna system.

1.9 Thesis Outline

The thesis is organized as follows:

Chapter 1 provides a general introduction to the thesis topic. The basics of Metamaterial and Theory of Characteristic Mode are discussed briefly. Various MIMO antenna performance parameters are also defined and discussed.

Chapter 2 discusses various MIMO antenna designs available in literature and also different isolation enhancement techniques.

Chapter 3 presents the systematic design of the antenna radiating element starting with a rectangular conductor plate and performing TCM analysis. The to modify the radiating element structure to achieve desire modal behaviour. For isolation enhancement between the MIMO antenna elements, a novel metamaterial unit cell structure is designed and analyzed exhibiting metamaterial properties for 3.5 GHz band.

Chapter 4 presents the proposed multiband MIMO antenna for sub-6 GHz 4G/5G bands and IoT band in 17 GHz range. Simulated and measured results are presented and discussed.

Chapter 5 presents the proposed multi-wideband MIMO antenna for sub-6 GHz and mmWave bands. Simulated and measured results are presented and discussed.

Chapter 6 concludes the research work and present few suggestions for future work.

1.10 Summary

The chapter includes the introduction about the topic of research which is 5G communication. A brief history of mobile communication technologies is presented. Some of the possible future applications which will use 5G technology are also discussed and various needs with respect to such applications is outlined. MIMO antenna systems will make 5G communication data rates a reality, so for MIMO antennas the isolation enhancement techniques are briefly discussed. The systematic design approach for mobile handset antennas is presented and explained briefly which is called Theory of Characteristic Mode (TCM). MIMO antenna performance parameters are presented and explained to better understand the performance indicators. The motivation for the research work along with the methodology is also presented.
In chapter 2, a comprehensive literature survey is presented which helped us throughout the research work. The research gaps were found after studying the literature and based on those gaps the research objectives were derived.

Chapter 2 Literature Survey

2.1 Introduction

The advancements in wireless technologies and the increase in wirelessly connected devices led to significant rise in research of novel antenna structures. MIMO systems are becoming a need to support high data rate in all kinds of gadgets and devices irrespective of their size. A device such as laptop or smartphone or smart watch or wireless earphones needs to be connected to the internet and support high data rate communication. Therefore, the need for multi-band MIMO antennas arises which are designed as per the space available in a device. Novel MIMO parameters enhancement techniques are to be employed while designing MIMO antennas to achieve good diversity performance. This chapter presents and discusses the state-of-the-art of antennas for 5G communication. There are three sections: first section includes the review of single band antennas for 5G devices, second section include the review of MIMO antennas for sub-6 GHz bands for 5G, and third section include the review of MIMO antennas for sub-6 GHz and mmWave bands for 5G.

2.2 Literature Review of Single Element Antennas for 5G

Ka Ming Mak et. al. [59] presented a patch antenna which is circularly polarized can be used in future 5G mobile phones. Antenna miniaturization is performed, and beam width enhancement is also achieved. The size of the proposed antenna is significantly reduced by loading slots on the patch and folding the edge also, this allows the proposed antenna to be installed in a compact handheld device. Patch antenna is surrounded with a dielectric substrate to obtain wider beam width and this arrangement also supports the antenna. Measured value of (HPBW) is 124^0, the 3-dB axial ratio bandwidth is 3.05%, and overall impedance bandwidth is 10%.

Hau Wah Lai et al. [61] proposed a novel technique which uses a H-shaped tapered ground. This technique helped in reducing the thickness of a proposed magneto electric (ME) dipole antenna. The antenna height is significantly reduced from 0.25 λ_0 to 0.11 λ_0 (where λ_0 is the wavelength resonant frequency). The multi-layer PCB technology can be used to easily realize

the proposed novel antenna structure which is low cost and easy to fabricate. Impedance bandwidth achieved by the proposed antenna is 18.74% (4.98 GHz to 6.01GHz). Radiation patterns are stable which also have low back radiation and cross polarization.

Almir Souza e Silva Neto et al. [62] presented an antenna using an EBG (Electromagnetic Band Gap) structure operating at 28 GHz band for 5G Applications. Bandwidth is enhanced using EBG structure. RT Duroid 5880 substrate is used to design the proposed antenna and on the ground plane multi-cylinders with radius of 0.2 mm are drilled while substrate is not drilled.

Ferrero et al. [64] presented a reconfigurable antenna for 5G communication which covers DCS, PCS, UMTS, LTE (1800 MHz, 2600 MHz, 3500 MHz) permanently. Reconfigurability enables several other bands to be covered by the proposed antenna such as LTE 600/700 and GSM 850/900. Overall size of the antenna is compatible with current mobile terminals. A digital tunable capacitor is used to reconfigure the antenna characteristics. But reconfigurable antennas require extra circuitry such as battery, capacitor or diodes for tuning etc. This makes overall antenna structure to be bulky and not suitable for its use in some mobile devices.

Prem Narayan Choubey et al. [67] proposed a Triangular CSR (Complimentary Split Ring) Slot antenna using Substrate integrated waveguide. The antenna operates in 28 GHz and 45 GHz bands for 5G communication. For obtaining high gain, two and four elements arrays are designed. Wider impedance and gain bandwidth have been achieved by exciting 2nd order modes. Overall size of antenna is also very low profile. Efficiency is also higher than 80% for both resonances.

Hassan Tariq Chattha et.al. [73] proposed a novel single element two port PIFA. Two feeding plates are placed which are perpendicular to each other, by using single radiating patch and two isolated feeding ports, polarization diversity is achieved. Two ports have good isolation between them which is achieved with introduction of a rectangular slot on the ground plane. Two functions can be achieved by the proposed PIFA covering the and LTE (2.5 GHz -2.7GHz) and WLAN (2.45GHz) bands with overall bandwidth from 2.35 GHz to 2.80GHz. Therefore, the proposed structure shows diversity and MIMO performance using a simple PIFA structure.

N. Ojaroudiparchin et al. [74] proposed an insensitive antenna for future 5G systems which

uses new method of designing an antenna. An air-filled slot-loop structure is used to reduce the effect of lossy FR4 substrate and to improve performance of the antenna. Antenna is insensitive to different permittivity values as the main substrate used is air. So, while using different types of substrates the antenna showed similar performance like for gain, radiation, efficiencies etc. Antenna operates at 22 GHz which is a candidate band for 5G communication. Proposed antenna showed more than 90% efficiencies at resonant frequency.

2.3 Literature Review of Single band MIMO Antennas for 5G

Youngki Lee et al. [29] proposed an antenna with MIMO functionality using a multilayered structure. Three substrates are used and split ring resonator (SRR) cell is introduced in inter-digital form to improve isolation between the antenna elements. Designed antenna works on LTE band 40 with desired bandwidth coverage. The peak gains of the antenna are low but ECC is 0.16 which is well acceptable level of 0.5.

R. Hafezifard et al. [32] developed two meander line antennas on Metamaterial loaded substrate between the elements to reduce mutual coupling. The proposed antenna array showed size reduction and low mutual coupling due to the use of Metamaterial structure. Mutual coupling lower than -30 dB throughout the band of operation is achieved and omnidirectional radiation patterns are observed. Use of Metamaterial layer also helped in achieving wider bandwidth of 790 MHz and high gain of 6.5 dBi.

O. M. Haraz et al. [63] proposed a patch antenna array having 8 X 8 elements. The proposed design provides space and polarization diversity for 5G future networks. The shape of antenna elements is rectangular which uses single spatial feed mechanism and have dual linear polarization. The maximum gain value obtained by the proposed array is 21 dBi at resonant frequency of 28 GHz.

Kamili J. Babu et al. [72] presented a MIMO antenna with two elements operating at 6.8 GHz with wider bandwidth coverage. A patch element is employed between the antenna elements to reduce mutual coupling below -33 dB at resonance. Overall size of the antenna is not much compact as per resonant frequency. ECC value is well below 0.15 for the entire band of operation. To bandwidth enhancement is achieved by defected ground structure

(DGS).

Osama M. Haraz et al. [75] presented a single-band PIFA structure with three radiating elements working at 28 GHz for the future mmWave5G wireless communications. The proposed MIMO system has 3 single-band PIFA elements. The minimum value of isolation achieved is 13 dB between the antenna elements. A wideband coverage from 27.73 GHz to 28.54 GHz (807 MHz) is obtained by the antenna. MIMO parameters are calculated and have acceptable values such as mean effective gain (MEG), diversity gain (DG), envelop correlation coefficient (ECC), and multiplexing efficiency (ME).

2.4 Literature Review of Multi-band MIMO Antennas for 5G

Mohammad S. Sharawi et al. [8] presented some of the new performance metrics for analyzing printed MIMO antennas. Some of the recent work on printed MIMO multi-band antennas using isolation enhancement techniques is also presented and discussed. MIMO Performance parameters such as ECC, DG, MEG, TARC, and System capacity are discussed and several antenna designs are discussed which works at different bands of frequency.

S Luo et al. [25] designed a microstrip patch MIMO antenna operating in 5 GHz band. The antenna has two elements and uses a NL structure to ehance the isolation level. Still the isolation level between the element is -13 dB which is not below the acceptable level of -15 dB for proper MIMO system performance. The peak gain is 8.3 dBi which is quite good but the overall size of the antenna is not compact.

Guohua Zhai et al. [34] proposed a mushroom structure with double layer for improving isolation between 4 element antenna structures. Substrate integrated cavity-backed slot antenna elements have been used which use a double layer of mushroom wall framework between the elements. The ECC value is very low, i.e. 0.02 for the entire operating bandwidth. The total volume of the antenna system is not compact, precisely the height of the planned MIMO antenna is 22.5 mm, which is not compatible with certain wireless applications.

Yong-Ling Ban et al. [69] proposed a hybrid MIMO antenna which for 4G and 5G

applications. Array of two antenna elements works on 2G, 3G and4G frequencies such as 850/900/1800/1900 MHz, 2100 MHz and 2300/2500 MHz While array of 8 elements operates at 3.5 GHz band which could be possibly used for future 5G wireless communication. ECC and isolation characteristics are well below acceptable values for mobile communication. For 8x8 MIMO system the channel capacity obtained from 5G antenna array is just 6 bps/Hz less than the limit.

Byungje Lee et al. [71] proposed a compact LTE band MIMO antenna. The antenna has two similar structure PIFAs which work along with a common T-shaped patch. No additional coupling elements are employed to improve isolation, even then low ECC value and high isolation are obtained. The value of ECC is low which is because of optimized locations of feeds and antenna elements which results in diagonally orthogonal radiation patterns. Mutual coupling is low by having a common T-shaped patch which results in high isolation between the elements.

Zachary Miers et al. [76] designed an LTE dual band MIMO antenna and analyzed with the help of TCM. Current characteristics and field modes can be analyzed and correlated to enhance the performance of MIMO antennas even if they work below 1GHz. TCM also helps in achieving multiband operation and improving impedance matching of excited modes of operation. ECC value is also well below 0.1 but overall antenna size is not compact.

Jung-Nam Lee et al. [77] proposed a MIMO antenna with dual band operation for WLAN bands having high isolation characteristics for both the bands. There are four antenna elements in the structure for which isolation is improved by modifying the ground plane with introduction of slots. High isolation level of 35 dB is achieved in both the bands between the antenna elements. SAR analysis is also presented with human head and hand phantom models. Proposed antenna shows excellent MIMO characteristics such as ECC and isolation values.

Zhongjie Qin et al. [78] designed a compact printed 8 element MIMO antenna. Printed PIFA structure is used which operates at GSM 1900, LTE 2300 and 2500 bands. Pattern diversity is used to achieve good isolation and envelope correlation coefficients. The antenna is fabricated on low cost FR4 substrate with dimensions 136 mm x 68.8 mm which is suitable for future handheld devices.

Osama M. Haraz [79] proposed two broadband and dual band antennas for 5G mobile networks. The frequency of operation of these antennas is 28 GHz and 38 GHz for 5G communications. An extra wide band from 20 GHz to slightly beyond 40 GHz is covered by the proposed antenna. Gain values of the proposed antenna at resonant frequencies is low that can be enhanced as per requirement of future 5G communication.

Wang Han et al. [80] designed a MIMO antenna with tri port structure for Micro or Pico cell applications. The antenna has X shaped printed elements which are oriented at 900, 1200, and 2400 to each other. The arms are connected to each other which forms a self-decoupled structure which results in good isolation below -15 dB between elements. ECC is well below 0.1 in desired band of operation and efficiency is also above 50% in most of the frequency band. Gain value is moderate which can be further worked upon to improve.

J Duan et al. [81] proposed a folded monopole MIMO antenna with four antenna elements. The antenna operates in sub-6 GHz bands such as 1.6 GHz, 3.5 GHz, 4.4 GHz, and 5.7 GHz. The isolation enhancement mechanism used is ground slots and metal rim stub. But even then, the minimum isolation achieved is -12 dB and the peak gain values are also lower than 1.5 dBi.

Malviya et al. [82] presented a four element MIMO patch antenna covering the frequency bands in sub-6 GHz range. The bands supported by the antenna have resonance at 2.38 GHz and 3.5 GHz. Although the size of the radiating element is compact i.e. 6.7 mm x 6.7 mm but the isolation level between the elements is not good enough. The minimum isolation level achieved is -12.5 dB even after employing isolation enhancement technique of partially extended ground plane. The peak gain values are below 4 dBi.

Asim Ghalib et al. [83] proposed a MIMO antenna with four annular ring slot elements. The antenna uses a tuning mechanism for covering the bands between 1.8 GHz and 2.45 GHz. No isolation enhancement technique is used which resulted in poor isolation. The minimum level of isolation is -8.6 dB while the peak gain achieved is 4.71 dBi. The MIMO system performance is not good because of higher coupling between the antenna elements.

Debdeep Sarkar [84] proposed a MIMO antenna based on four element Inverted-L antenna structure. The frequency of operation is 2.7 GHz and the peak gain value is 4 dBi. Few thin strips are connected to the ground to improve the isolation level. But even then, the

isolation is -11 dB which is not that good for MIMO antenna system.

Hasan Tariq Chattha [85] proposed a two element MIMO antenna based on PIFA structure. The resonant frequencies are 2.2 GHz and 3.4 GHz but the antenna element size is not compact i.e. 20 mm x 27 mm. Open ended slots are introduced on the ground plane and a strip is suspended between the elements to enhance the isolation level due to which the minimum isolation level achieved is -19 dB.

Saif et al. [86] presented a 2 x 2 MIMO antenna based on printed monopole geometry. The antenna covers a wideband from 2 to 12 GHz covering several 5G bands. The antenna element size is 3.5 mm x 4.9 mm with the peak gain of 4.8 dB. The isolation level between the elements is below -20 dB which is excellent considering the lower frequency of operation is 2 GHz. To achieve this isolation level, the antenna element separation is kept to at least half the operating wavelength and also the ground plane is defected.

Arumita Biswas et al. [87] proposed an L-shaped monopole MIMO antenna with four elements. The frequency bands supported by the antenna are 3.8 GHz and 4.6 GHz. The radiating element size is 10 mm x 8 mm with the peak gain of 4.71 dBi. The isolation level is improved by using a defected ground plane which resulted in the minimum isolation level of -18.8 dB.

2.5 Summary

Antennas for 5G Communication devices are being developed as the 5G network is deployed in various countries. In this chapter, the research on 5G antennas for single element, MIMO single band and MIMO multi-band antennas is presented and discussed. One of the requirements for 5G devices is to support multiple bands considering the space constraint in devices along with MIMO functionality. Various types of antennas developed by researchers in the last few years are presented in this chapter which showed us the advantages and disadvantages of several types of antennas and techniques to enhance the antenna performance. In the next three chapters, the systematic design of antenna radiating element, design and analysis of novel metamaterial unit cell to achieve high isolation, MIMO antenna for sub-6 GHz band, and MIMO antenna for sub-6 GHz and mmWave bands are presented.

Chapter 3 TCM Analysis of Radiating Element and Design of Metamaterial Unit Cell

3.1 Introduction

In this chapter the systematic design of antenna radiating element is presented and analyzed using TCM. The starting point is the conventional rectangular radiating element shape analysis to find out the characteristic modes and then to modify the shape to achieve desired significant modes. It is shown that modification of shape results in change in modal behaviour of the radiating element, bringing the modes towards the desired resonance i.e. 3.5 GHz band. The design of modified metamaterial unit cell is presented and the properties showing the metamaterial behaviour are also presented.

3.2 TCM Analysis of Radiating Element

Conventionally, the radiating element of PIFA structure is a metallic rectangular plate as shown in Figure 3.1(a). In order to better understand the behavior of the modes, we first obtained the characteristic modes of the rectangular plate with dimensions of 18 mm x 14 mm. These are the modes inherent in the structure by description of TCM, simply as a function of its form and size. If the eigen value of a mode crosses ’0’ level then it is a resonant mode, similarly, in the case of modal significance a mode is resonant if the value of model significance reached to the level ’1’. The CMA results are presented in Figure 3.1 (a) where it can be observed that there are first two modes for which eigen value approaches zero that too above 4.5 GHz. There is no resonance observed below 6 GHz as it is clearly seen in Figure 3.1 (b). This means that to excite the radiating element at 3.5 GHz, a suitable feeding technique with tuning/matching network will be required resulting in low efficiency and low gain.

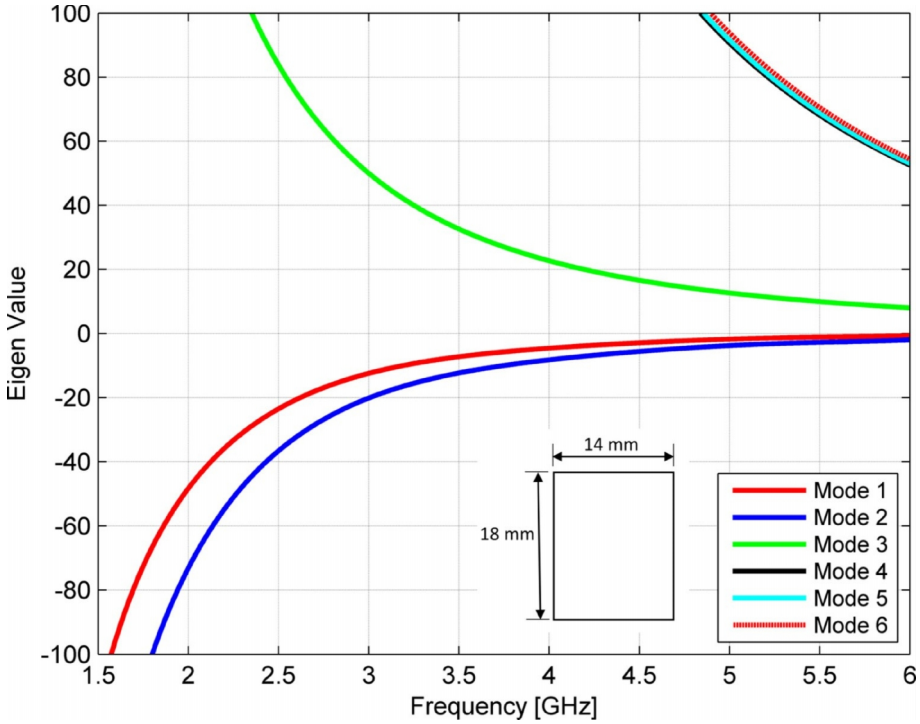

(a)

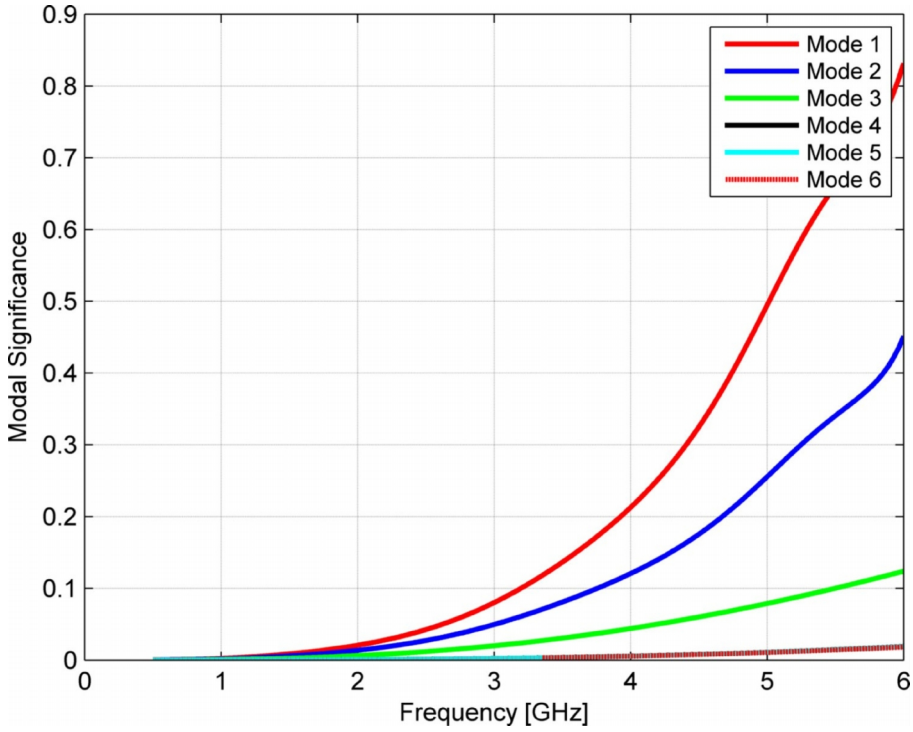

(b)

Figure 3.1: Characteristic Mode Analysis of Basic Rectangular Plate (a) Eigen Value Vs. Frequency Plot (b) Modal Significance Vs. Frequency Plot

In order to improve the behaviour of the plate below 6 GHz, one of the edges is truncated which resulted in an L-shaped element as shown in Figure 3.2 (a). Figure 3.2 presents the CMA results for L-shaped modified geometry of the rectangular plate. It can be observed that the modes are quite the same as we observed in the case of rectangular plate with mode 1 having higher modal significance as shown in Figure 3.2 (b) and the eigen value is very much near to value '0' at 3.5 GHz making it possible to excite the PIFA structure easily to obtain the resonance at 3.5 GHz.

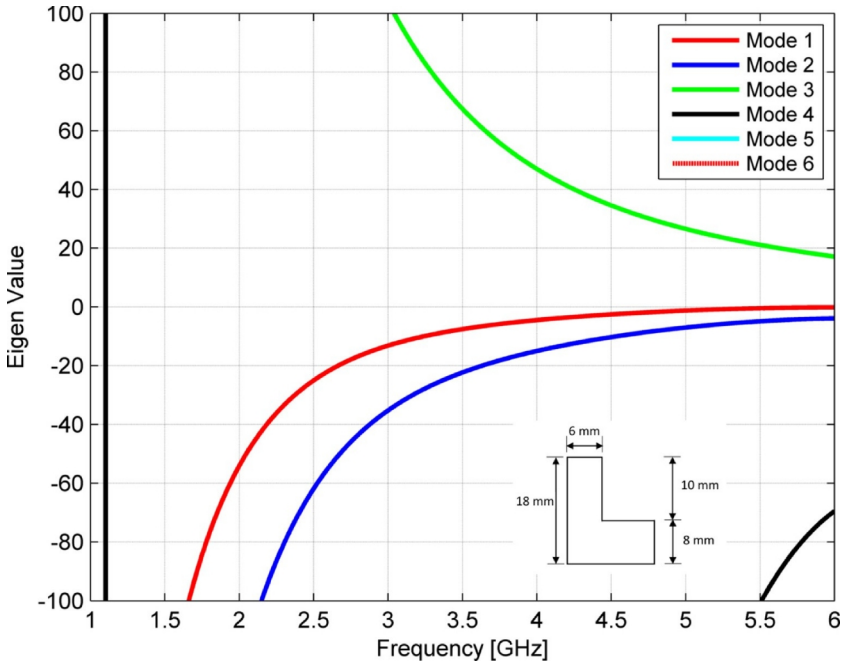

(a)

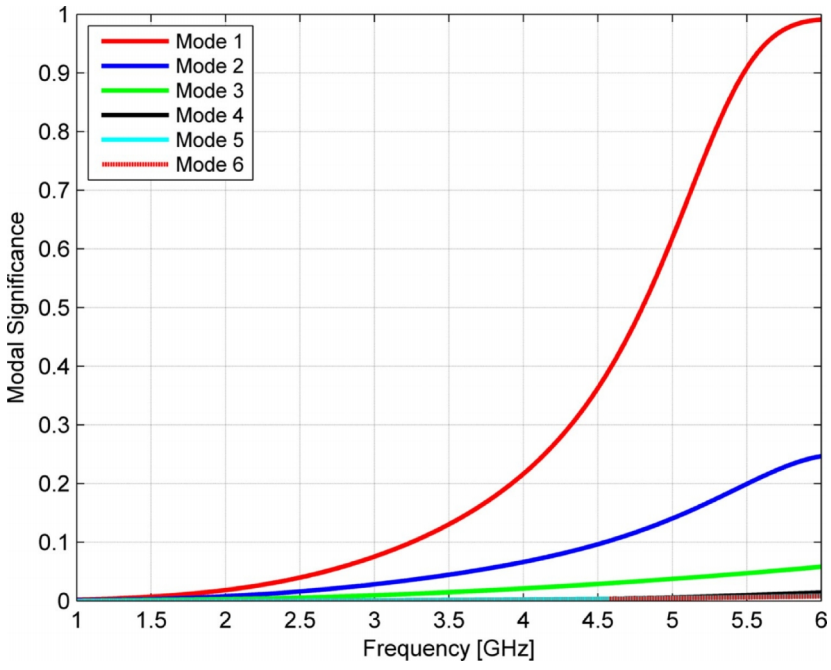

(b)

Figure 3.2: Characteristic Mode Analysis of L-shaped Plate (a) Eigen Value Vs. Frequency Plot (b) Modal Significance Vs. Frequency Plot

As shown in Figure 3.3 (a) the L-shaped element is further modified by introducing an L-slot to achieve the resonance behavior near 3.5 GHz. It can also be observed from Figure 3.3 (b) that the modal significance of mode 1 is highest which reaches to the value '1' near 4 GHz. With proper excitation of mode 1, a resonance at 3.5 GHz band can be obtained.

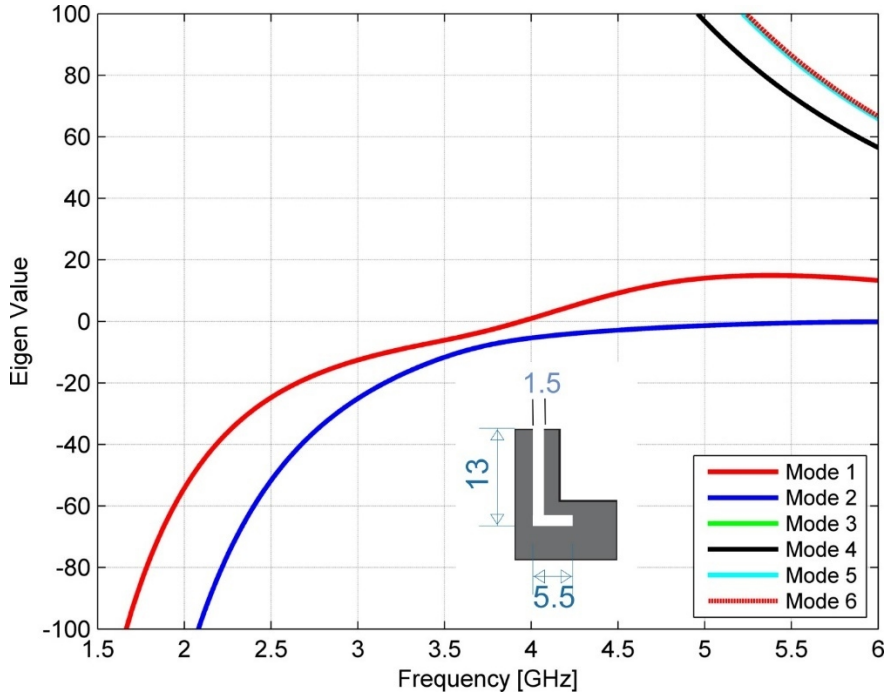

(a)

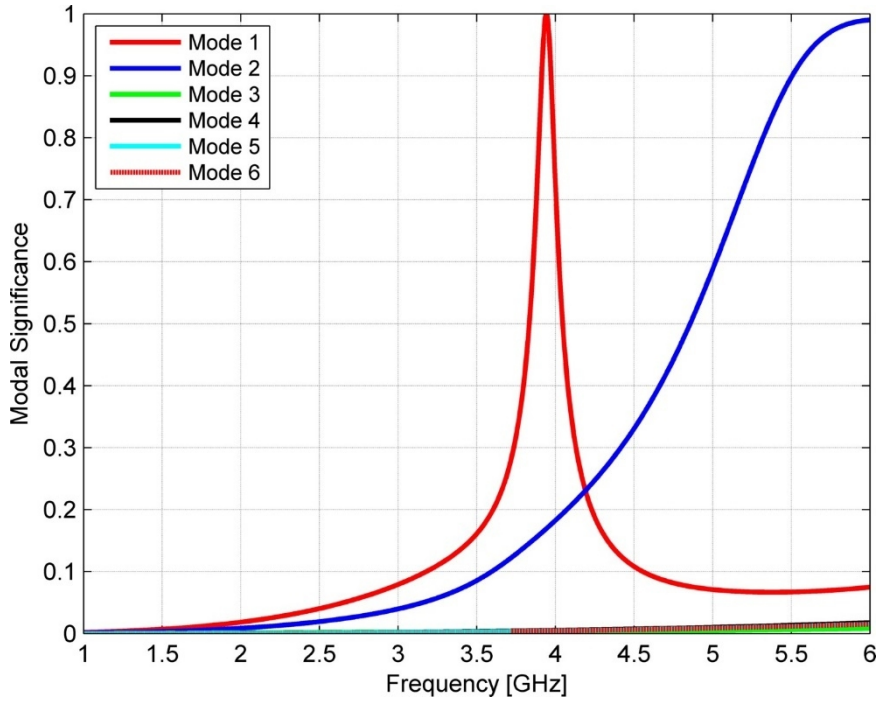

(b)

Figure 3.3: Characteristic Mode Analysis of L-shaped L-slot Plate (a) Eigen Value Vs. Frequency Plot (b) Modal Significance Vs. Frequency Plot

After identifying the significant modes from modal analysis, the current distribution is studied as presented in Figure 3.4. For the first three modes the current distribution remains the same for modified L-shaped element and L-shaped L-slot element. Next section presents CMA of complete PIFA structure helping us understand the modal behaviour as well as decision on exciting a desired mode can be made.

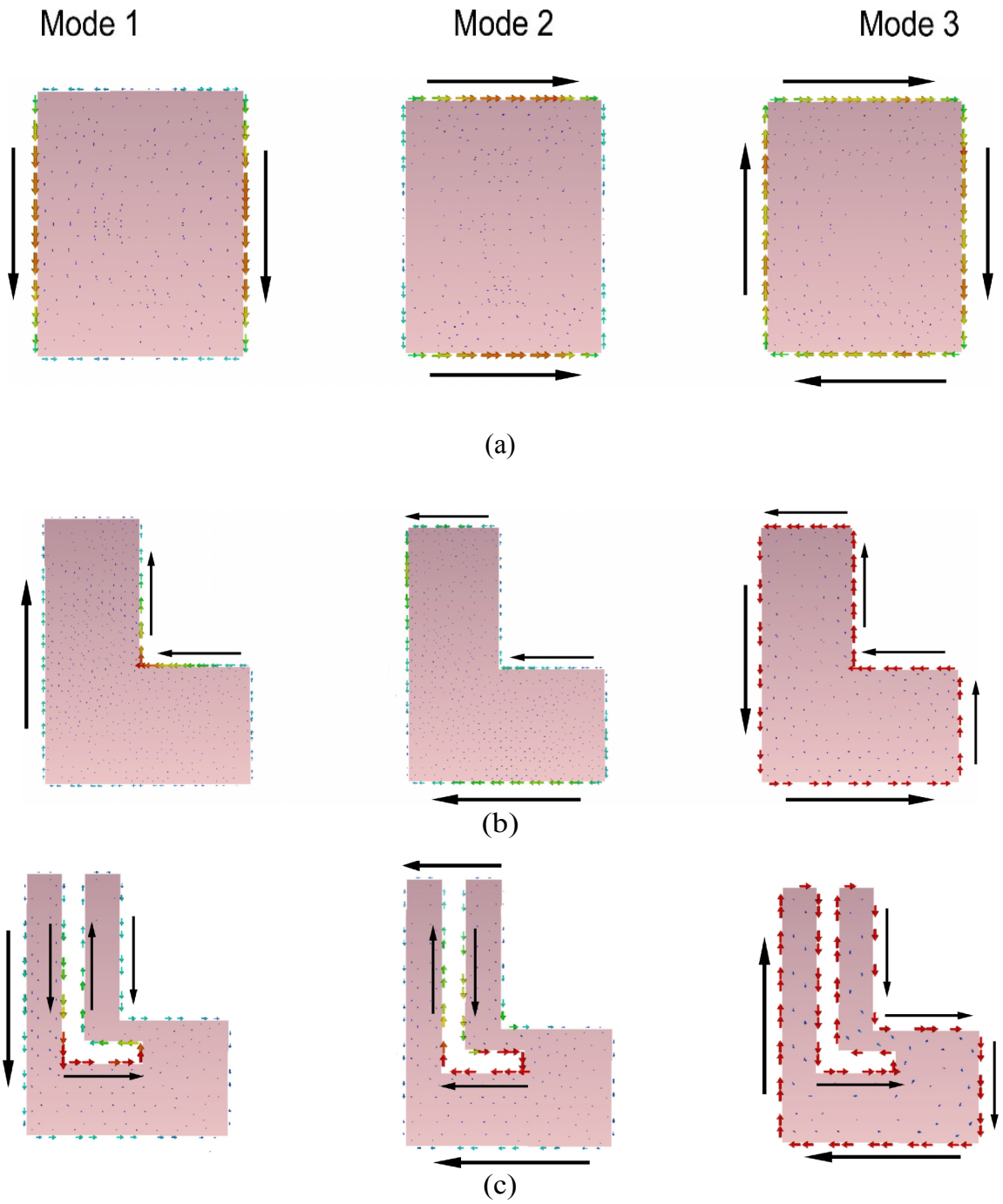

Figure 3.4: Modal Current Distribution (a) Basic Rectangular Plate (b) L-shaped Plate (c) L-shaped L-slot Plate

3.3 TCM Analysis of Complete PIFA Structure

This section presents the CMA of complete PIFA structure comprising of the substrate, ground plane, L-shaped radiating element, a shorting plate, and a feed plate. This help us to understand which modes are present in the proposed antenna structure and what is the significance of each mode. As presented and discussed in [88] that the PIFA structure exhibit localized current resulting in narrow-band operation. The chassis/ground plane shows maximum electric field at the edges/corners, this means that the radiator can be efficiently excited at the edge or corner of the chassis. Also, the current distribution is maximum on the shorting plate [89] which indicates that the feed location needs to be close to shorting plate.

It can be observed from Figure 3.5 (a) that out of the six modes of the final PIFA structure, mode 1 is the most significant mode at 3.5 GHz. So, mode 1 can be excited to get a resonance at 3.5 GHz with wideband coverage. All the modes exhibit wideband behaviour and have different resonant frequencies as shown in Figure 3.5 (b). The feed plate can be placed on the long edge of the ground plane as mode 1 shows maximum electric field on the corners of long edge. This will result in efficient excitation of mode 1 resulting in desired resonant behaviour.

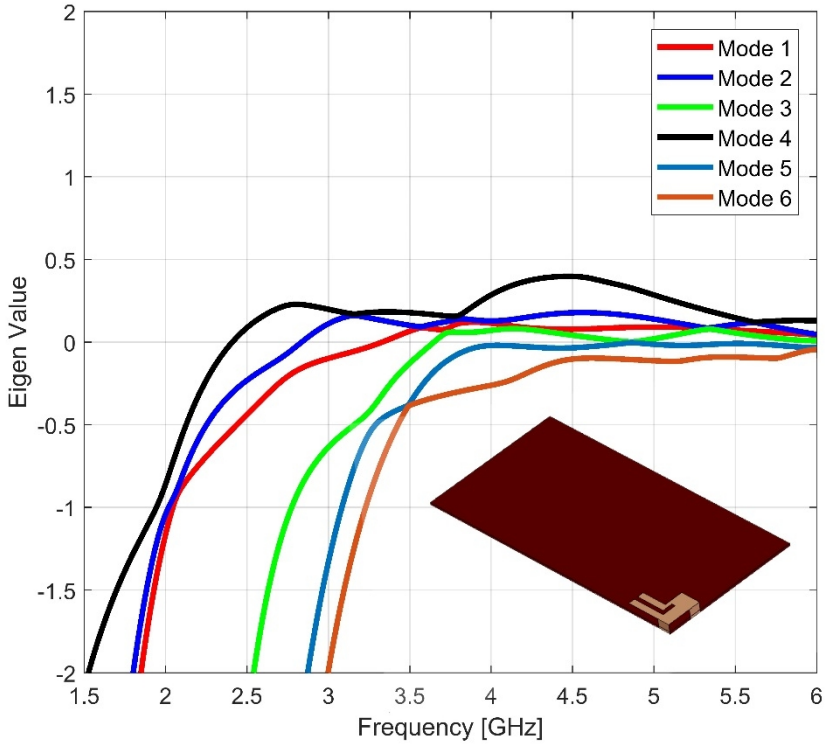

(a)

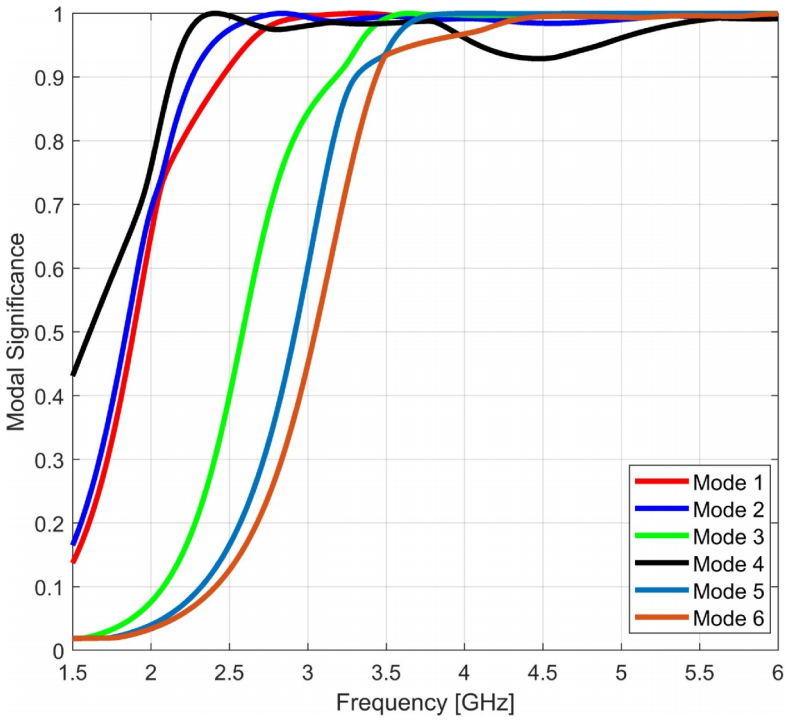

(b)

Figure 3.5: Characteristic Mode Analysis of proposed PIFA antenna Structure (a) Eigen Value Vs. Frequency Plot (b) Modal Significance Vs. Frequency Plot

3.4 Metamaterial Unit Cell Design

A complimentary metamaterial unit cell is placed on the ground plane side of the substrate. The design of CMSRR is done for the frequency range in which the antenna elements resonates and the isolation needs to be the highest. As shown in Figure 3.6 (a), the detailed dimensions of CMSRR designed for 3.5 GHz. Figure 3.6 (b) to (e) shows the metamaterial properties such as permittivity (ε), permeability (μ), refractive index (n) and impedance(z) in the desired frequency range.

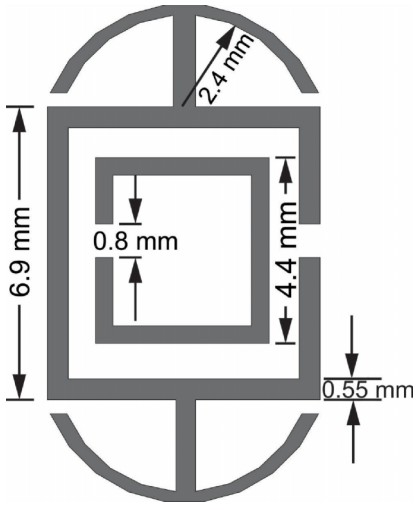

(a)

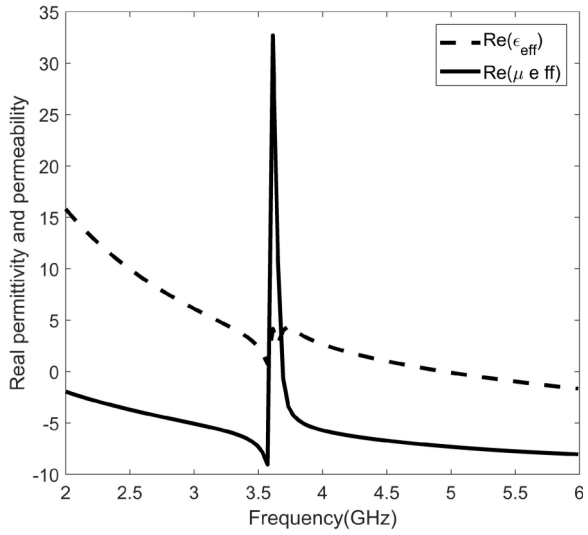
Re(ϵ_{eff})
Re(μ e ff)
Real permittivity and permeability
Frequency(GHz)

(b)

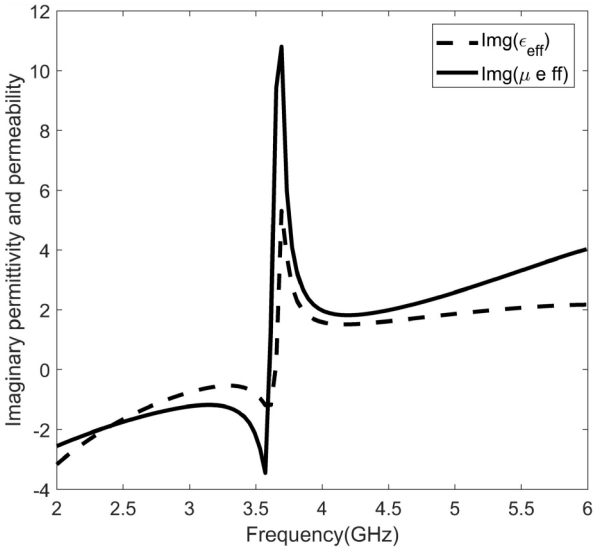
Img(ϵ_{eff})
Img(μ e ff)
Imaginary permittivity and permeability
Frequency(GHz)

(c)

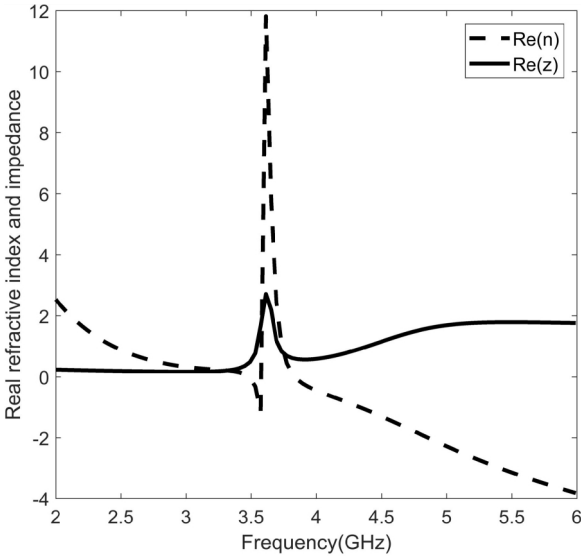
Re(n)
Re(z)
Real refractive index and impedance
Frequency(GHz)

(d)

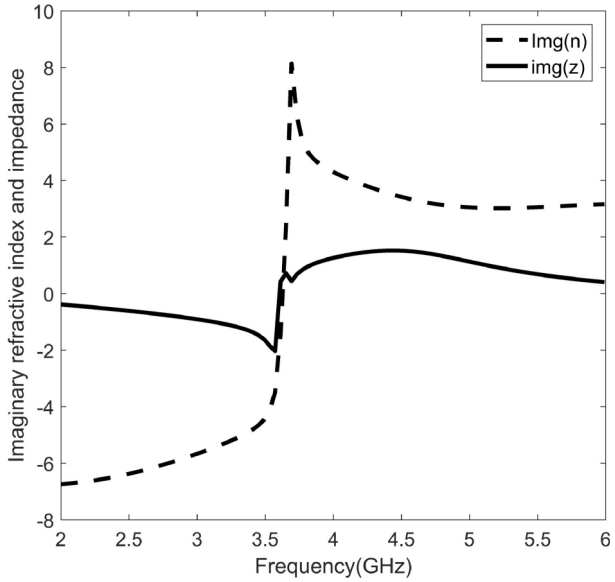

(e)

Figure 3.6: (a) Modified Split Ring Resonator Metamaterial Unit Cell Structure (b) Real permittivity and permeability (c) Imaginary permittivity and permeability (d) Real refractive index and impedance (e) Imaginary refractive index and impedance

It can be observed that ε, μ, and n are negative at 3.5 GHz which shows that the modified CMSRR exhibits double negative (DNG) metamaterial or Left-Handed Material (LHM) properties. The material properties are extracted by using S-parameters and the methodology is explained in [90]. The effect of using LHM complimentary Split Ring Resonator (SRR) in MIMO antenna design for isolation enhancement is not to allow the current from one antenna element to affect other MIMO antenna elements. In the frequency range where SRR shows LHM behavior, the mutual coupling reduces. The complimentary SRR exhibits filtering (band rejection) capability and suppresses the surface waves [91].

1.5 Summary

In this chapter the systematic design of the antenna radiating element is presented. The systematic design is performed by using TCM analysis to find out the modal behavior of the radiating element and then to modify the shape of the element to achieve desired modal behavior. Firstly, the conventional rectangular shaped element is analyzed using TCM and it has been observed that the modes shows significance after 5 GHz. There is no mode which can be excited near 3.5 GHz frequency which is the target frequency band. Therefore, the radiating element is modified into L-shaped element which shifted mode 1 towards 3.5 GHz band but still the excitation of this mode is not easy. So, finally an L-slot is introduced in the

L-shaped radiating element which resulted in mode 1to be significant near 3.5 GHz and can be excited efficiently. Then the TCM analysis of the complete PIFA structure is presented showing the significant modes and it is observed that mode 1 is nearest to 3.5 GHz and can be excited to achieve desired resonance behavior.

In section 3.4, the design and analysis of modified metamaterial unit cell is presented. It can be observed that the proposed unit cell exhibits negative epsilon and negative mu properties which makes a Left-Handed Material (LHM) or Metamaterial. The refractive index is also negative at 3.5 GHz which means that the proposed metamaterial unit cell can be used in complimentary form to enhance the isolation in MIMO system.

Chapter 4 Design of Planar Antenna for sub-6 GHz and Satellite Bands

4.1 Introduction

Various types of devices will be connected to each other via internet forming a large heterogeneous network which will require a communication network supporting such a huge number of devices. This emerging area is known as Internet of Things (IoT) where large number of sensors, appliances, and devices are interconnected and communicates with each other. A potential unlicensed frequency band at 17 GHz is also being explored to support IoT services creating a wireless local area network with wider bandwidth support termed as High-Performance Radio Local Area Network (HIPERLAN) [92] [93]. To fulfill the demand for high data rate, compact devices with a greater number of antenna elements needs to be developed. It requires extensive research to improve several MIMO antennas parameters like isolation, ECC, DG, MEG, TARC, CCL etc.

In most of the MIMO designs the mutual coupling is just near acceptable value [14]. To improve these MIMO parameters, several techniques have been proposed which are discussed in section 1.3. Most of the today's smart phones consists of two MIMO antenna elements for 4G/4G LTE and WLAN services. But future wireless devices supporting much higher data rates require a greater number of antenna elements. Recent works presented 2 elements/ports [27] [85] [72], 4 elements/ports [34] [94] [95] [96] [97] MIMO antenna designs for smart phones supporting 5G frequency bands. In this chapter, a four element MIMO antenna is proposed working on 3.5 GHz band for 5G applications, 12.5 GHz and 17 GHz band for IoT applications. The MIMO system performance is enhanced by using CMSRR proposed in chapter 3.

4.2 Antenna Design and Structure

This section presents the proposed antenna designs starting from single element PIFA to four element MIMO structure. The inclusion of CMSRR on the ground plane of the MIMO antenna is also presented and discussed.

4.2.1 Single Element PIFA

The basic design equation for PIFA is given below:

$$Lp + Wp - Ws = \lambda/4 \tag{4.1}$$

where Lp is length of radiating patch, Wp is width of radiating patch, Ws is Width of Shorting Plate, λ is the wavelength of desired resonant frequency.

However, the equation above does not result in accurate dimensions of the radiating element. So, an empirical equation proposed in [98] is used to calculate the length and width of radiating element with more accuracy.

$$f_0 = \frac{c}{3W\ +3.7h+5.6L\ -3.7W_S-3W_f-2.5L_S-4.3L_b} \tag{4.2}$$

where f_0 is the desired resonant frequency, c is the speed of light, h is the height of the radiating patch, W_s is the width of shorting plate, W_f is the width of feed plate, L_s is the length of shorting plate, L_b is the horizontal distance between feed and shorting plate.

For the proposed design, the radiating element dimensions chosen are Lp = 18 mm, Wp =14 mm, W_s = 8 mm, W_f= 4 mm, L_b= 6 mm and h= 3 mm as shown in Figure 4.1. The desired frequency response and other antenna parameters are achieved by modifying the conventional geometry of PIFA and also by using edge feeding mechanism, controlling the resonance by changing the dimensions of shorting plate etc. The resonance obtained after designing the whole PIFA structure gets affected by few other factors such as position and dimensions of feed plate, introduction of dielectric substrate etc. The resonant frequency and bandwidth can be controlled by changing the shorting plate width, dimensions of the radiating element, height of the radiating element etc. [12].

4.2.2 4 Element MIMO System

Figure 4.1 shows the detailed dimensions of the proposed MIMO antenna system. Single element structure is modified by introducing PIFA elements on all the four corners of the substrate. This section presents the result of 4 element MIMO system with no isolation enhancement technique, MIMO antenna with isolation enhancement using defected ground

structure, and MIMO antenna with isolation enhancement using a complimentary Metamaterial unit cell to achieve high isolation.

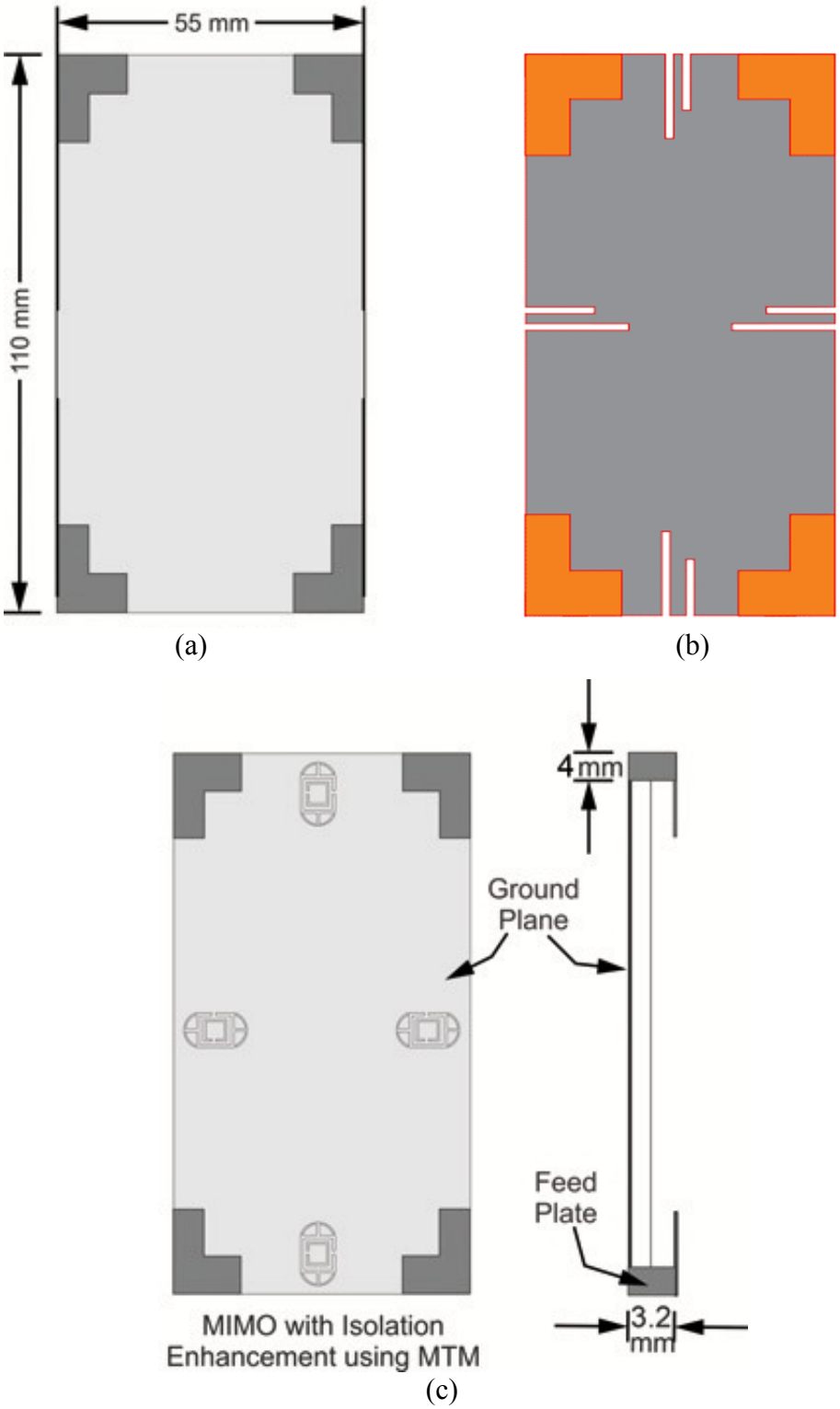

Figure 4.1: Detailed dimensions of Proposed MIMO Antenna System (a) MIMO antenna without isolation enhancement (b) Isolation enhancement using defected ground structure (c) Isolation enhancement using CMSRR

The two isolation enhancement techniques: defected ground structure and CMSRR are implemented to observe and compare the effect on isolation levels. The results are presented in the next sections.

4.3 Results and Discussion

This section presents the simulated and measured results of proposed single element PIFA structure and 4 element MIMO antenna system. The measurement is performed using Vector Network Analyzer (VNA) from Agilent model number E5063A and an anechoic chamber is used for radiation pattern measurement.

4.3.1 Single Element PIFA

1.3.1.1 Return Loss

Figure 4.2 shows the measured and simulated return loss curves of single element PIFA structure. It is observed from the plot in Figure 4.2 (a) that the single element PIFA's resonant frequency is 3.5 GHz and 3.52 GHz with return loss value of -22.41 dB and -19.82 dB for simulated and measured results respectively. The bandwidth covered by the proposed antenna is 421 MHz for simulation and 460 MHz for measured results. As per ITU release 15 document, 5G NR bands covered by the proposed antenna are n77 and n78. At upper frequency bands, the resonances observed are at 11.94 GHz, 17.19 GHz and 12.38 GHz, 17.3 GHz for simulated and measured results respectively as shown in Figure 4.2 (b).

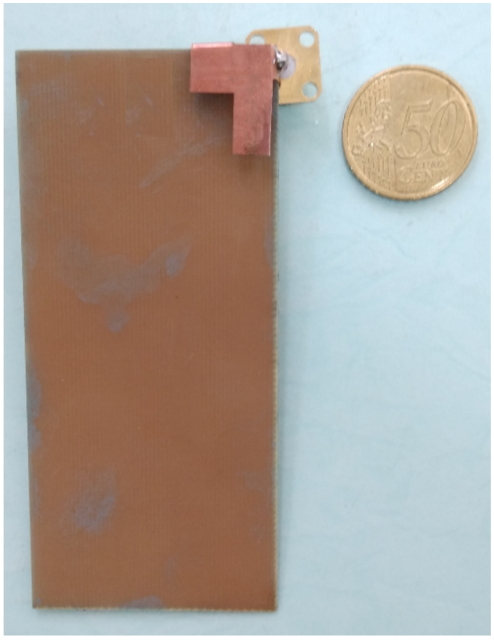

(a)

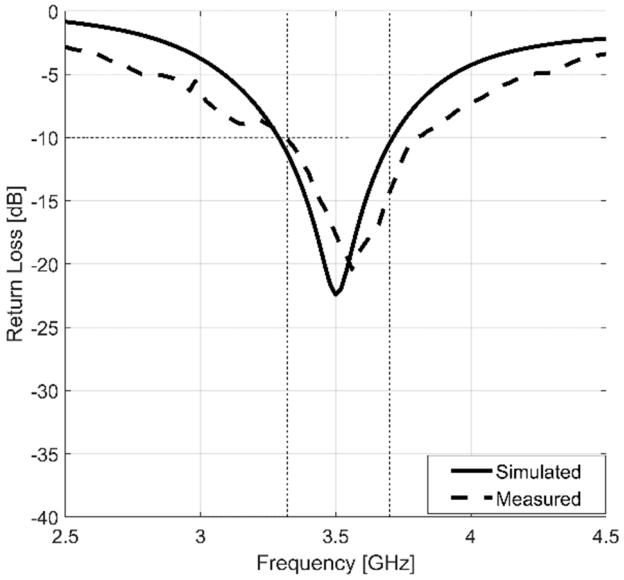

(b)

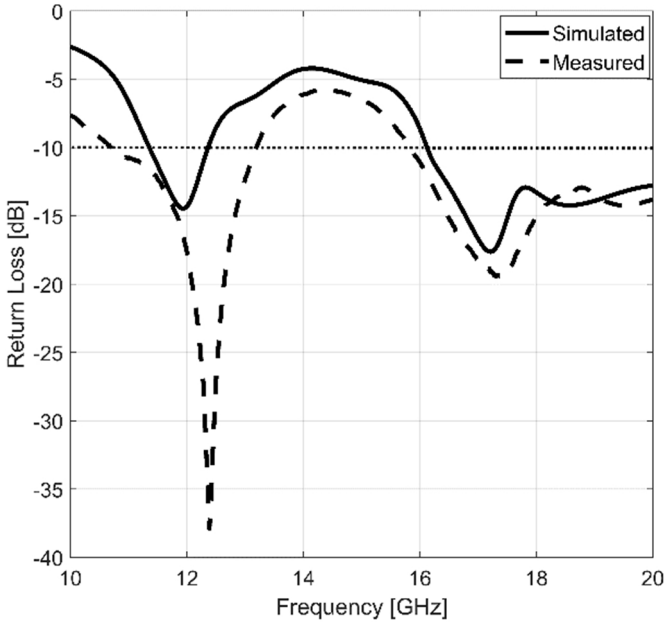

(c)

Figure 4.2: Proposed Single Element L-shaped PIFA (a) Antenna Prototype (b) Return Loss Plot of Lower band (c) Return Loss Plot of Upper band

1.3.1.2 Radiation Pattern and Gain Plot

The measured and simulated E-plane and H Plane radiation patterns of the proposed PIFA structure are shown in Figure 4.3. It is observed from Figure 4.3 (a)and (b) that the PIFA element is directional in E-plane while it exhibits omni-directional radiation pattern in H-plane. From Figure 4.3 (c) to (f), it can be observed that in both E and H planes the proposed PIFA exhibits omni-directional radiation characteristics.

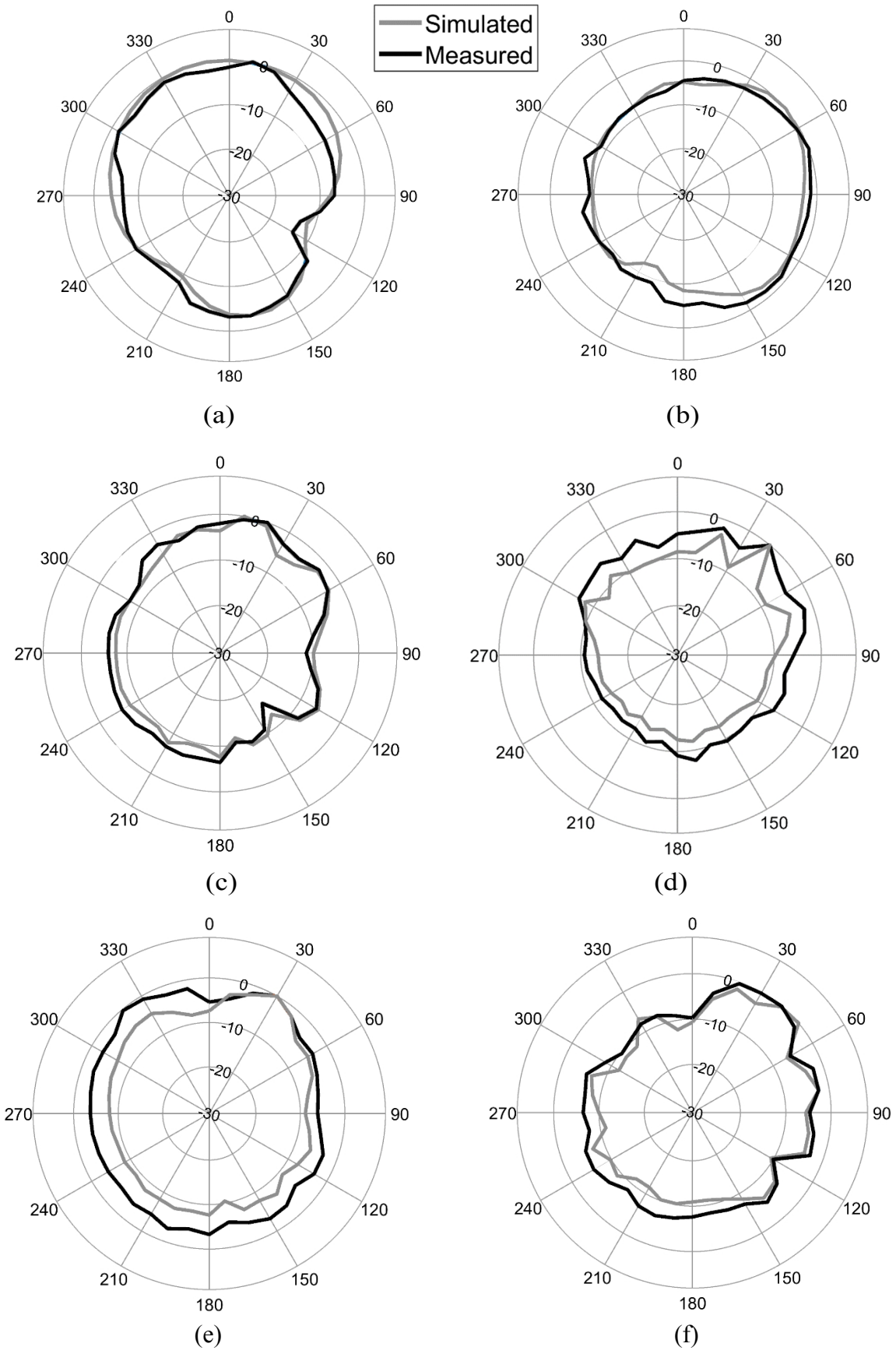

Figure 4.3: 2D Radiation Pattern Plots of Proposed Single Element PIFA (a) E-Plane at 3.52 GHz (b) H- Plane at 3.52 GHz (c) E-Plane at 12.38 GHz (d) H- Plane at 12.38 GHz(e) E-Plane at 17.3 GHz (f) H- Plane at 17.3 GHz

The simulated and measured radiation efficiency is presented in Table 4.1. The proposed antenna shows the measured radiation efficiency above 80% in the operating bands.

Table 4.1: Simulated and Measured radiation efficiency of Single L-shaped Element PIFA

Frequency (GHz)	3.5	11.94	17.3
Simulated Efficiency (%)	93	95	98
Measured Efficiency (%)	81	84	87

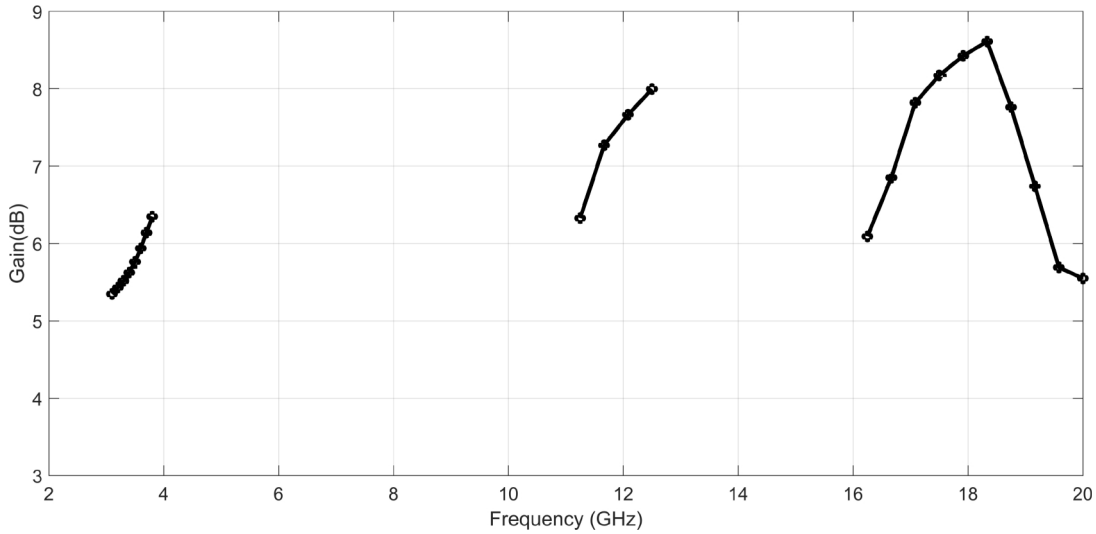

Figure 4.4: Simulated 2D Gain Plot of Proposed Single L-shaped Element PIFA

The proposed single element PIFA gives simulated peak gain of 6.34 dB, 7.99 dB and 8.61 dB in the covered bands as shown in Figure 4.4.

4.3.2 4 Element MIMO antenna system

The single element design is extended to a MIMO system by introducing three more L-shaped elements on the ground plane. These three elements are placed on the remaining three corners of the substrate so as to use edge feeding mechanism and to give space to other circuits and components of a mobile device.

4.3.2.1 MIMO Antenna without Isolation Enhancement Technique

Return Loss and Isolation Curves

The return loss plot is shown in Figure 4.5 (a) and (c) in which it can be observed that all the

four PIFA elements resonates almost at the same frequency in lower as well as upper bands. The isolation level between the antenna elements is shown in Figure 4.5 (b) and (d) where the few of the curves shows same values, therefore, we have shown S12, S13, S14 as S12=S21=S34=S43, S13=S31=S24=S42, and S14=S41=S23=S32. The isolation between all the antenna elements is below -15 dB level except for S13, which is above -15 dB at resonance.

(a)

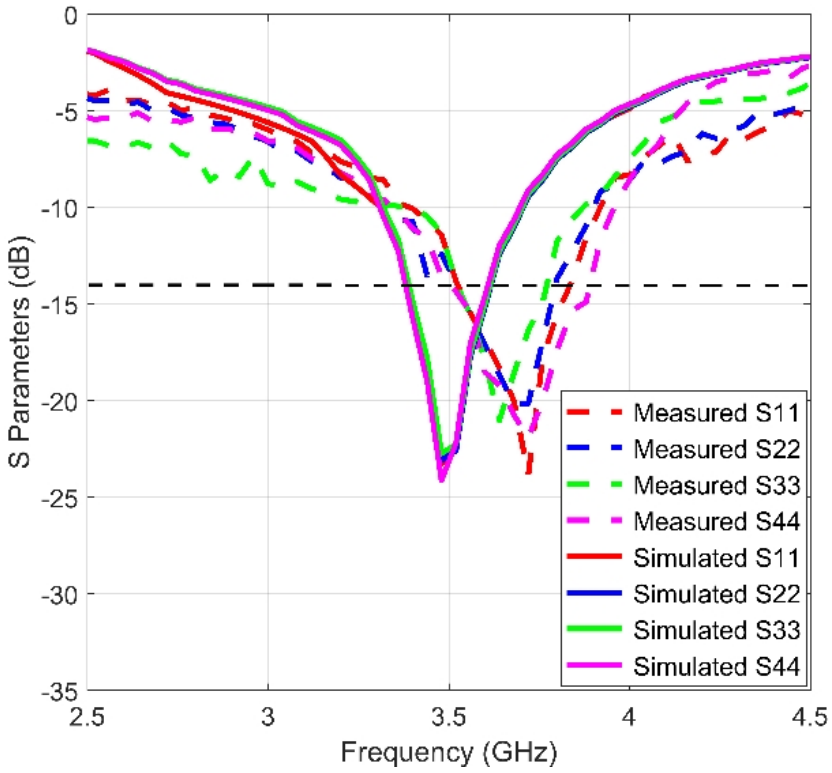

(b)

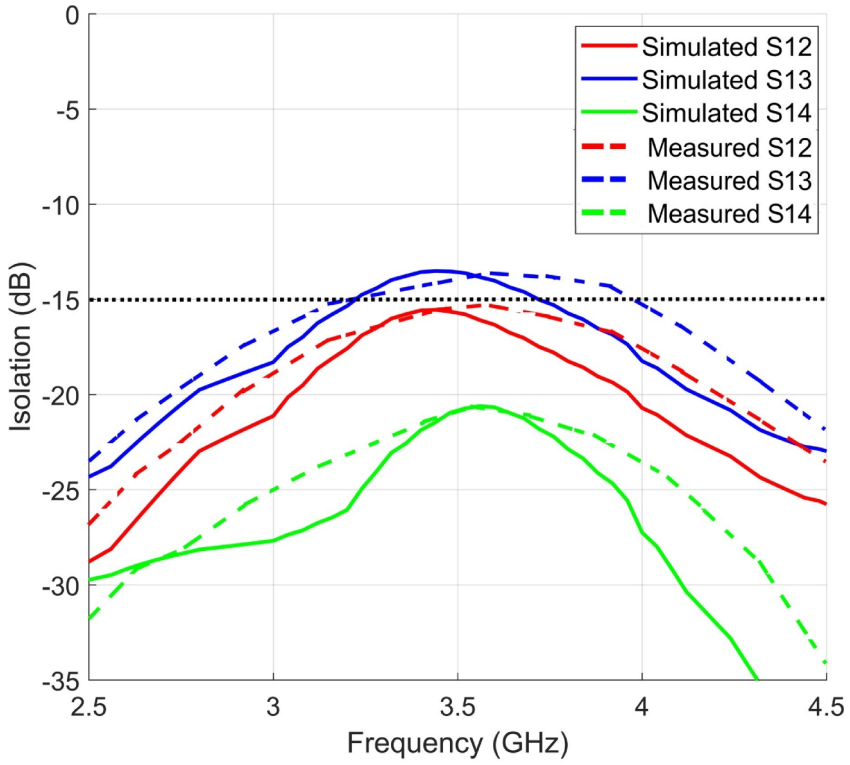
Simulated S12
Simulated S13
Simulated S14
Measured S12
Measured S13
Measured S14
Isolation (dB)
Frequency (GHz)
0
-5
-10
-15
-20
-25
-30
-35
2.5
3
3.5
4
4.5

(c)

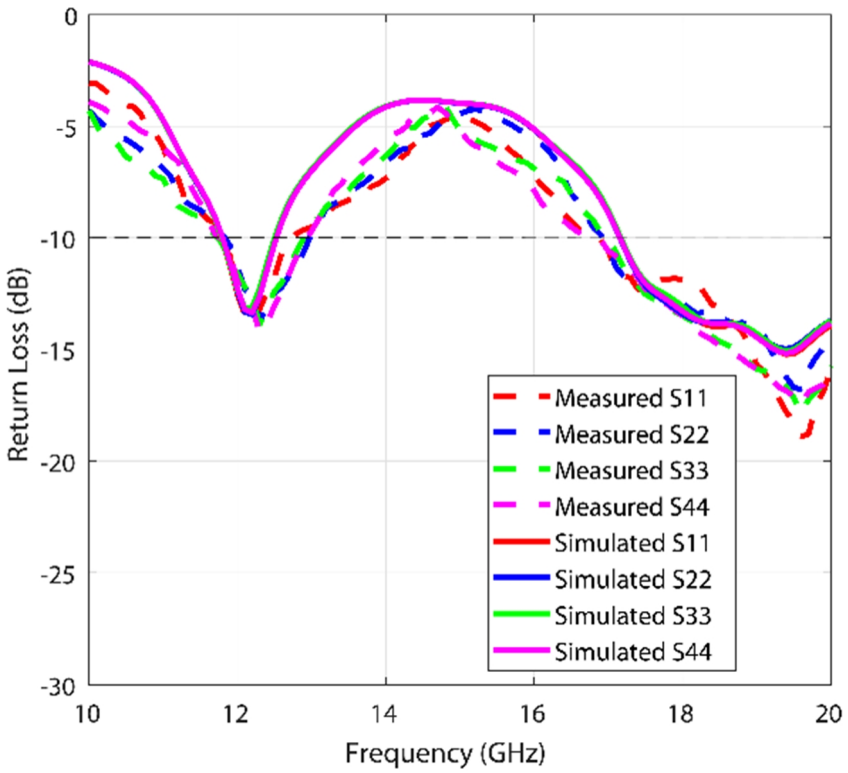
Measured S11
Measured S22
Measured S33
Measured S44
Simulated S11
Simulated S22
Simulated S33
Simulated S44
Return Loss (dB)
Frequency (GHz)
0
-5
-10
-15
-20
-25
-30
10
12
14
16
18
20

(d)

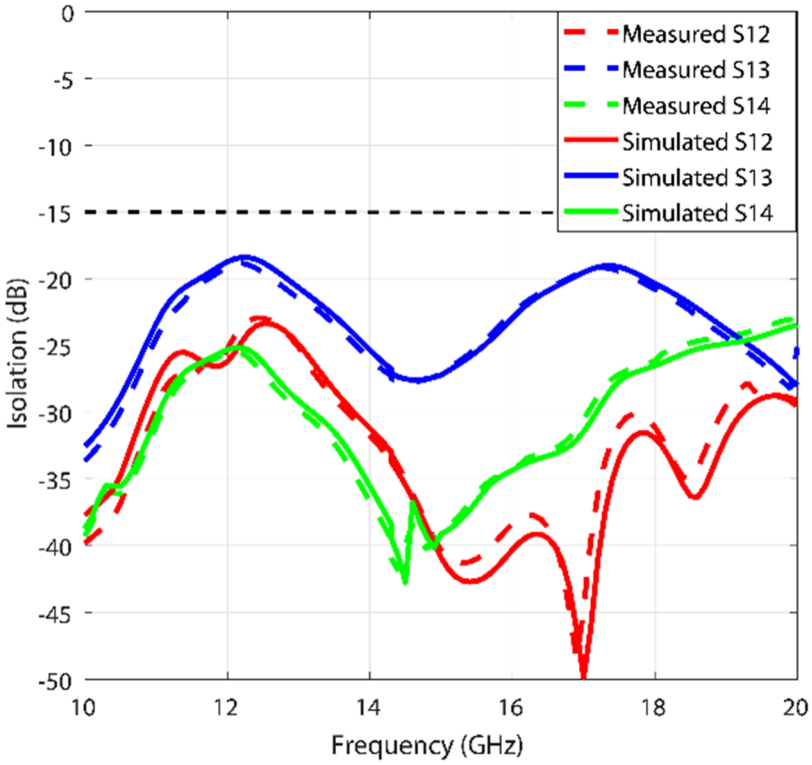

(e)

Figure 4.5: Proposed 4 L-shaped element MIMO antenna without isolation enhancement (a) Antenna Prototype (b) Return loss curves for lower band (c) Isolation curves for lower band (d) Return loss curves for upper band (e) Isolation curves for upper band

For the bands above 10 GHz the resonant frequencies are at 12.16 GHz and 19.41 GHz for simulated results while for measured results the resonant frequencies are 12.21 GHz and 19.62 GHz. The isolation level between the elements is below -18 dB for the bands above 10 GHz.

Envelope Correlation Coefficient and Diversity Gain

As presented in equation 1.3, for a 4 element MIMO antenna system, the value of N=4, i, j= 1,2,3 or 4 are replaced in equation 1.3 which gives us $\rho_e(1,\ 2,\ 4)$ and $\rho_e(1,\ 3,\ 4)$:

$$\rho_e(1,2,4) = \frac{|S_1^*\ S_1\ +S_2^*\ S_2\ +S_1^*\ S_3\ +S_1^*\ S_4\ |^2}{(1-|S_1\ |^2-|S_2\ |^2-|S_3\ |^2-|S_4\ |^2)(1-|S_1\ |^2-|S_2\ |^2-|S_3\ |^2-|S_4\ |^2)\eta_{1r}\eta_{2r}\eta_{4r}} \quad (4.3)$$

$$\rho_e(1,3,4) = \frac{|S_1^*\ S_1\ +S_2^*\ S_2\ +S_1^*\ S_3\ +S_1^*\ S_4\ |^2}{(1-|S_1\ |^2-|S_2\ |^2-|S_3\ |^2-|S_4\ |^2)(1-|S_1\ |^2-|S_2\ |^2-|S_3\ |^2-|S_4\ |^2)\eta_{1r}\eta_{3r}\eta_{4r}} \quad (4.4)$$

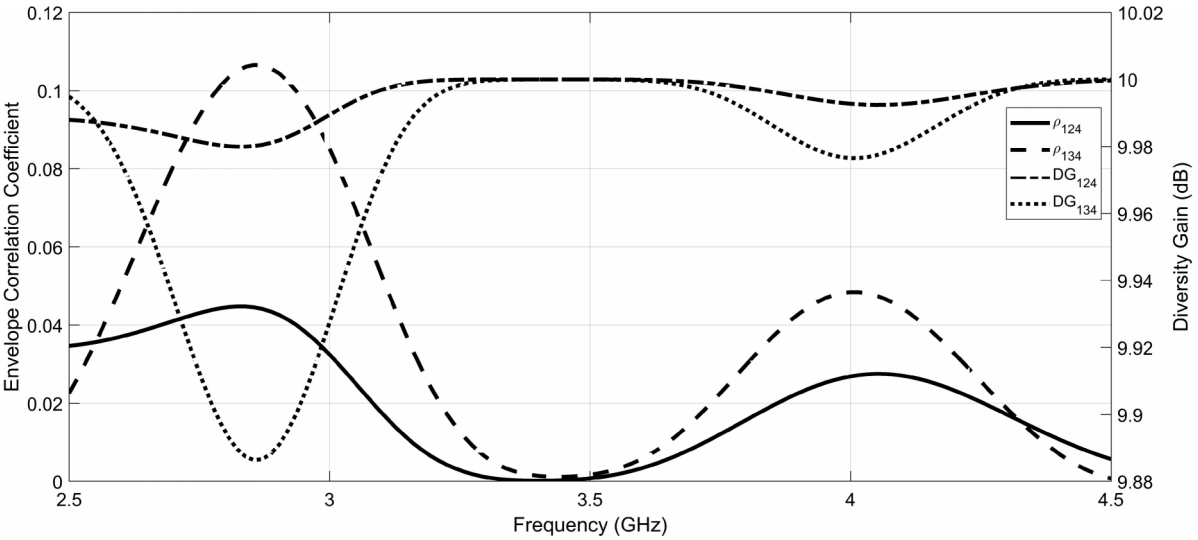

Figure 4.6: Simulated ECC and DG Curves for Proposed L-shaped element MIMO System without isolation enhancement

As shown in Figure 4.6, the value of ECC is below 0.02 in covered band around 3.5 GHz. Also, the value of DG is 10 dB in the band covered by the proposed antenna system. This shows that the proposed MIMO system exhibits good MIMO performance.

Total Active Reflection Coefficient (TARC)

For the proposed 4 element MIMO system, the TARC values were obtained by exciting port 1 with signal having 0^0 phase while the other three ports were fed with different phases. The combination of phases considered in the analysis of TARC are in sequence for Port1, Port2, Port3, and Port4:

Case 1: 0^0, 30^0, 60^0, 90^0;
Case 2: 0^0, 45^0, 90^0, 135^0;
Case 3: 0^0, 60^0, 120^0, 180^0;
Case 4: 0^0, 90^0, 60^0, 120^0.

In this manner the effective bandwidth of the proposed MIMO antenna system can be observed for different phase excitation. As shown in Figure 4.7, the level of TARC is below -6 dB in the desired band coverage around 3.5 GHz for both simulated and measured results.

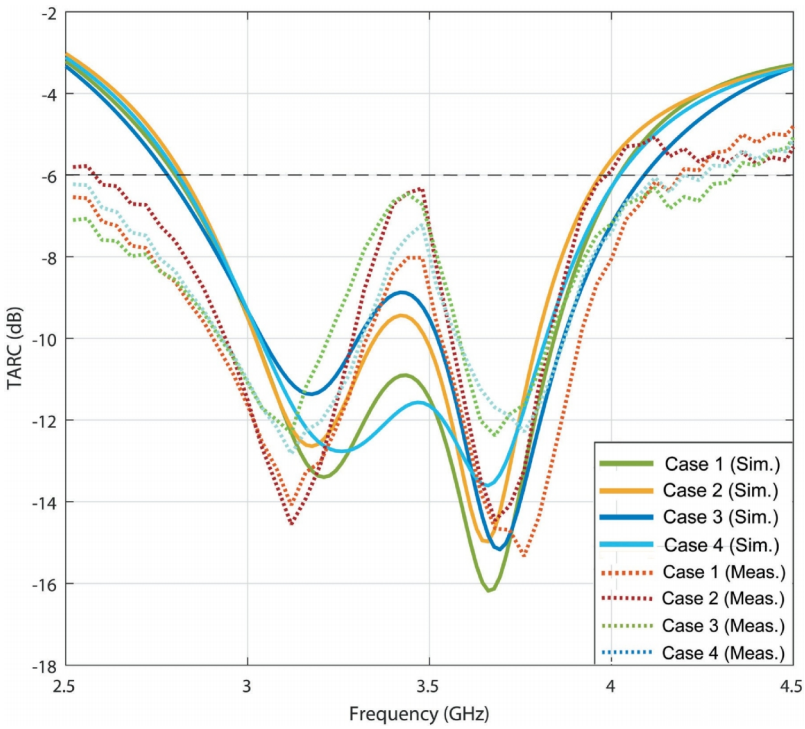

Figure 4.7: TARC Plot for proposed L-shaped element MIMO System without isolation enhancement

Channel Capacity Loss (CCL)

Channel Capacity is influenced by other diversity performance parameters and it grows linearly with increase in no. of antenna elements.

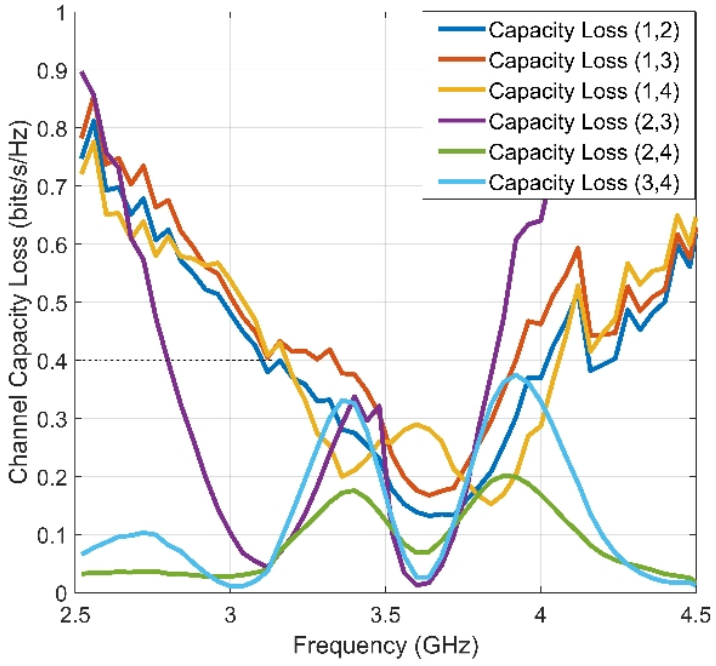

(a)

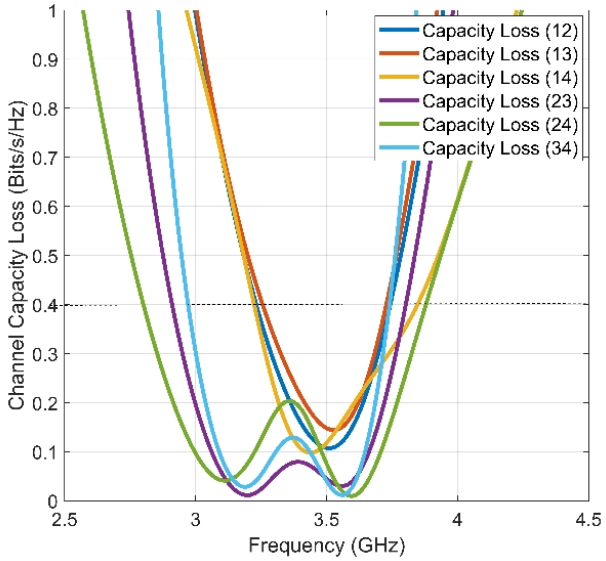

(b)

Figure 4.8: Channel Capacity Loss Plot of Proposed L-shaped element MIMO system without isolation enhancement (a) Simulated (b) Measured

The measure of system degradation can be evaluated in terms of channel capacity loss (CCL). For the proposed MIMO antenna system, CCL is well below 0.4 bits/sec/Hz in the desired band as shown in Figure 4.8 for both simulated and measured results.

Mean Effective Gain

Figure 4.9 shows the simulated and measured MEG ratios for the proposed MIMO antenna system without isolation enhancement. In the covered frequency bands the MEG ratio is near to 1 showing good diversity performance.

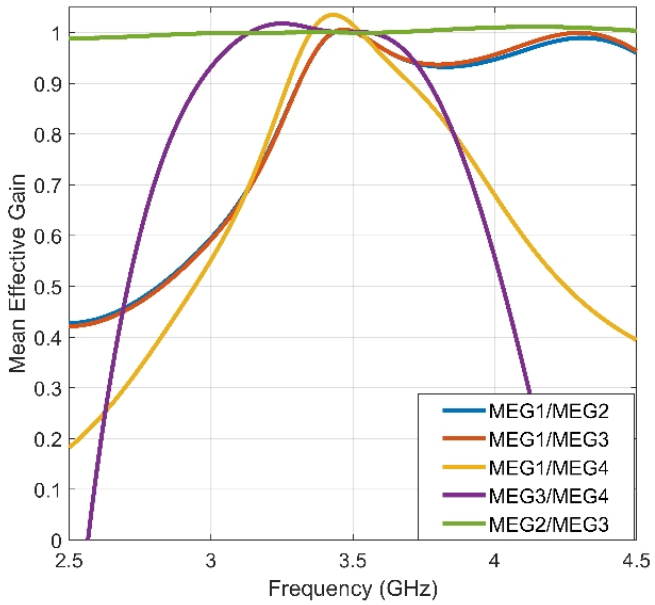

(a)

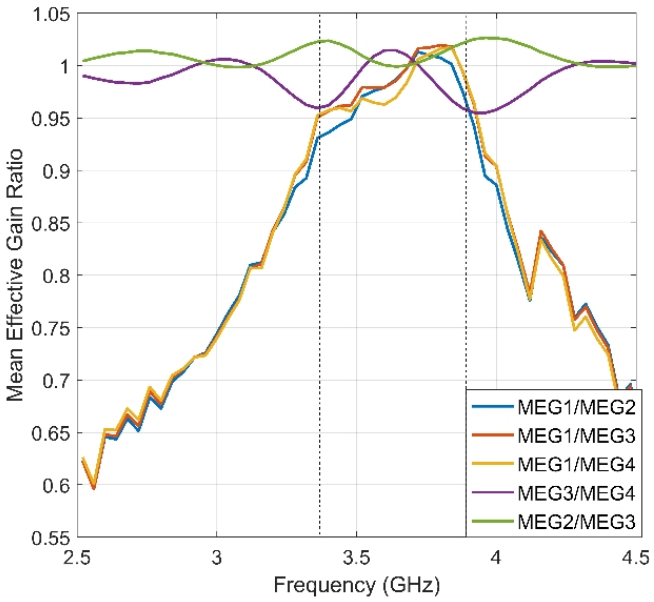

(b)

Figure 4.9: Mean Effective Gain Ratio Plot of Proposed L-shaped element MIMO system (a) Simulated (b) Measured

4.3.2.2 MIMO Antenna with Isolation Enhancement using Defected Ground Structure

Return Loss and Isolation Curves

The simulated S-parameters plot is shown in Figure 4.10 in which it can be observed that all the four PIFA elements resonates almost at the same frequency around 3.75 GHz. But compared to Figure 4.5 (a), the resonant frequency is shifted to the upper side of the spectrum due to the introduction of open-ended slots on the ground plane. This means that the isolation enhancement technique affects the resonance behavior of the MIMO antenna which is not desired.

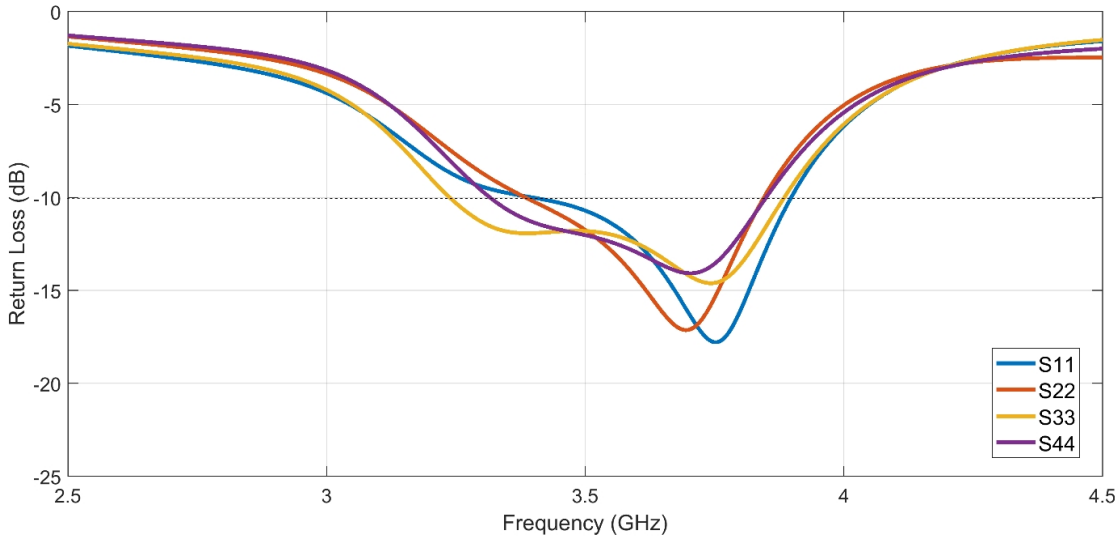

(a)

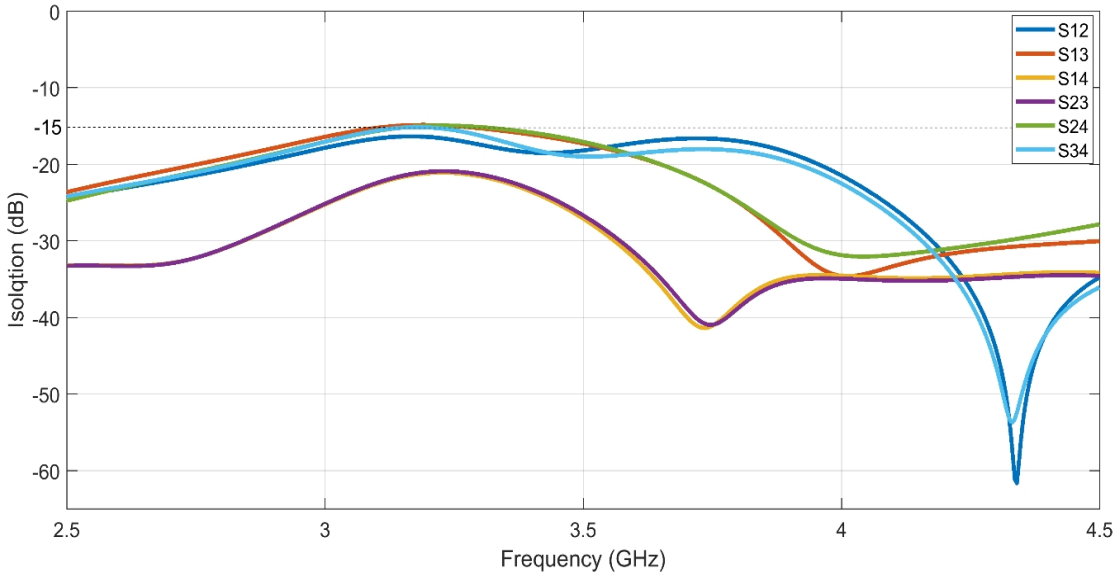

(b)

Figure 4.10: Simulated S-Parameter Plots of Proposed 4 element MIMO antenna with defected ground structure (a) Return loss curves for sub-6 GHz band (b) Isolation curves for sub-6 GHz band

Also, the isolation level enhancement is not good enough as the level is improved just by 1 to 2 dB at the start of the covered band. The isolation level for S13 and S24 is just near the acceptable -15 dB level. The defected ground structure technique using open-ended slots is not much effective in obtaining significant improvement in the isolation levels.

4.3.2.3 MIMO Antenna with Isolation Enhancement using CMSRR

Return Loss and Isolation Curves

The S-parameters plots are shown in Figure 4.11 in which it can be observed that all the four PIFA elements resonates almost at the same frequency around 3.45 GHz for simulation results and at 3.71 GHz for measured results. The resonant frequencies above 6 GHz are at 11.90 GHz and 18.92 GHz while the isolation level is below -18 dB for the entire upper band.

The antenna elements are well isolated for sub 6 GHz band as there is an improvement of more than -8.5 dB in isolation level at resonance. Now, S13 is well below -15 dB level having value -19.10 dB for simulation results while for measured results the value of S13 is -21.73 dB.

(a)

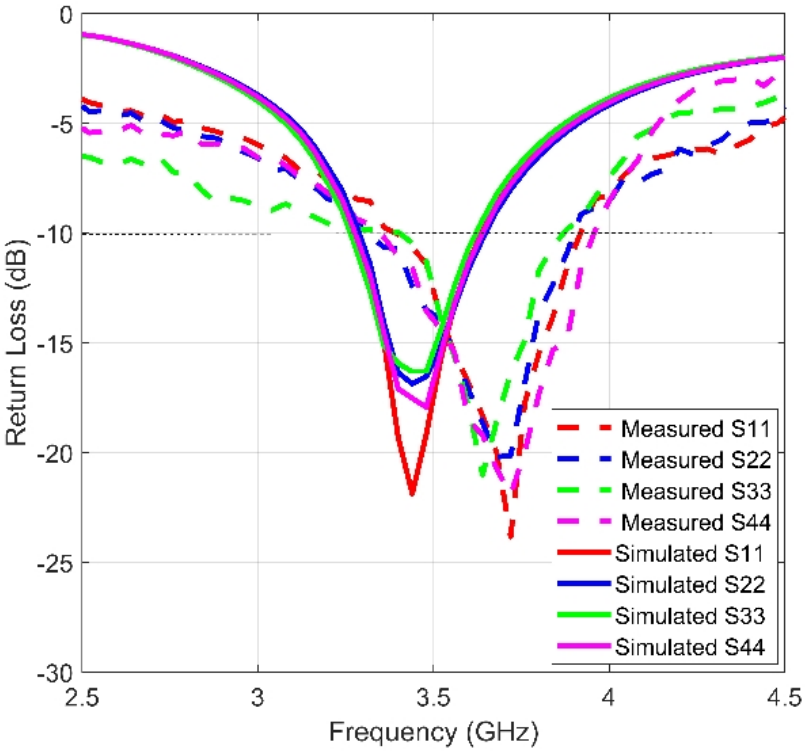
0
-5
-10
-15
-20
-25
-30
Return Loss (dB)
2.5
3
3.5
4
4.5
Frequency (GHz)
Measured S11
Measured S22
Measured S33
Measured S44
Simulated S11
Simulated S22
Simulated S33
Simulated S44

(b)

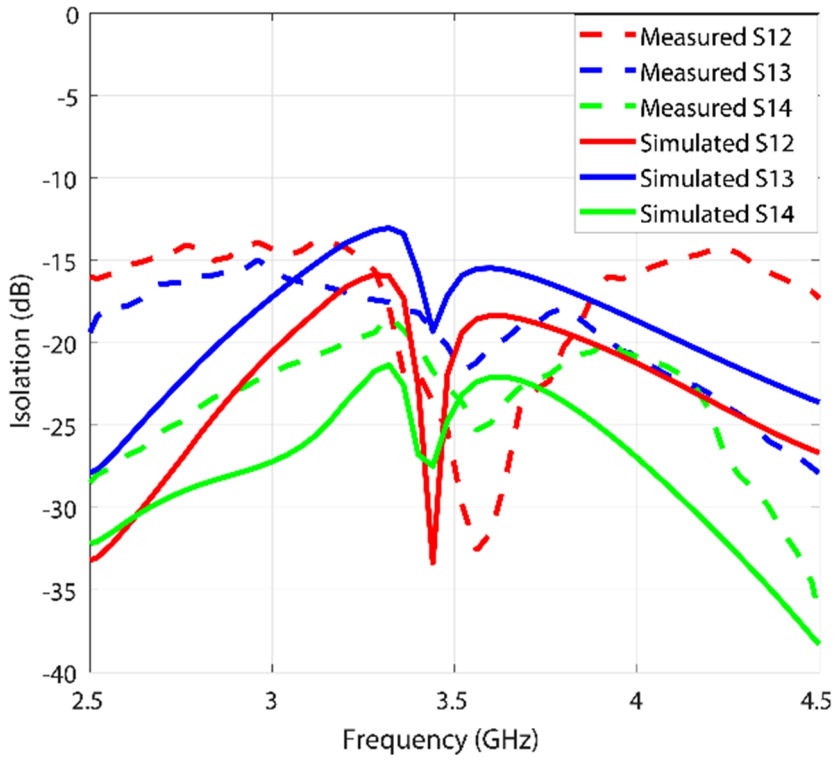
Measured S12
Measured S13
Measured S14
Simulated S12
Simulated S13
Simulated S14
Isolation (dB)
Frequency (GHz)
0
-5
-10
-15
-20
-25
-30
-35
-40
2.5
3
3.5
4
4.5

(c)

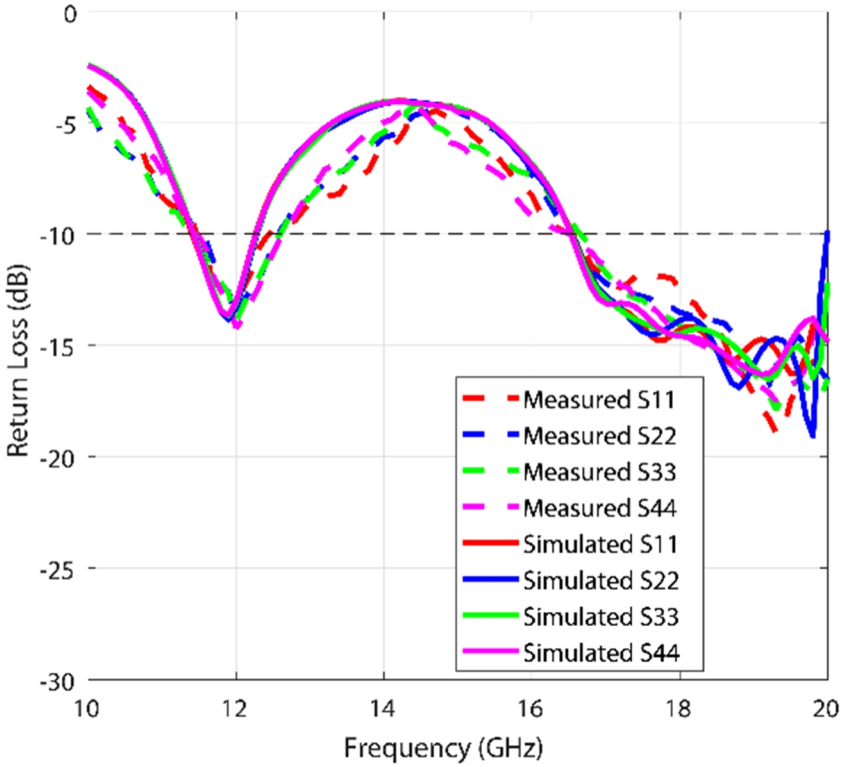
Measured S11
Measured S22
Measured S33
Measured S44
Simulated S11
Simulated S22
Simulated S33
Simulated S44
Return Loss (dB)
Frequency (GHz)
0
-5
-10
-15
-20
-25
-30
10
12
14
16
18
20

(d)

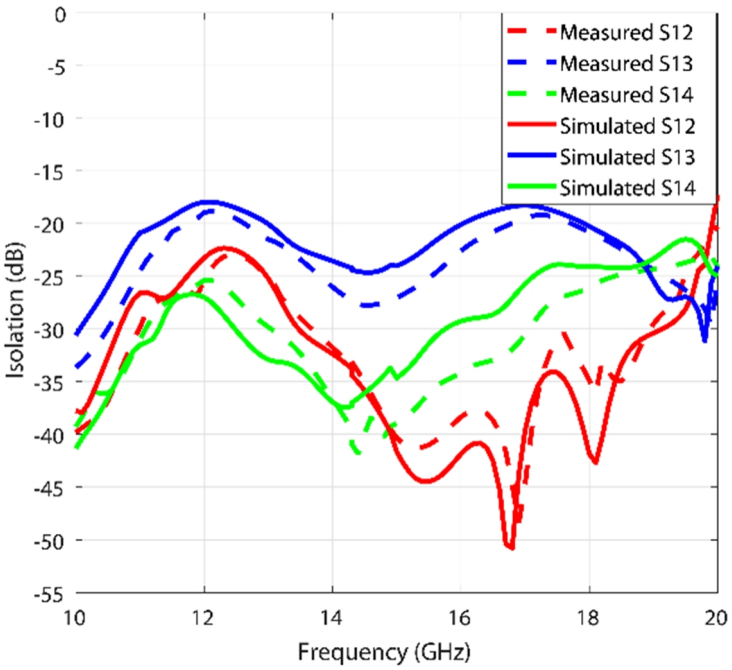

(e)

Figure 4.11: Proposed 4 L-shaped element MIMO antenna with CMSRR (a) Antenna Prototype (b) Return loss curves for lower band (b) Isolation curves for lower band (c) Return loss curves for upper band (d) Isolation curves for upper band

Envelope Correlation Coefficient and Diversity Gain

Figure 4.12 shows the simulated and measured ECC and DG values for 4 element MIMO system with MTM. ECC value should be below 0.5 level for MIMO systems and for the proposed MIMO antenna, ECC value is below 0.08 in the desired frequency band. DG level is above 9.95 dB in the desired frequency band which is considered to be excellent.

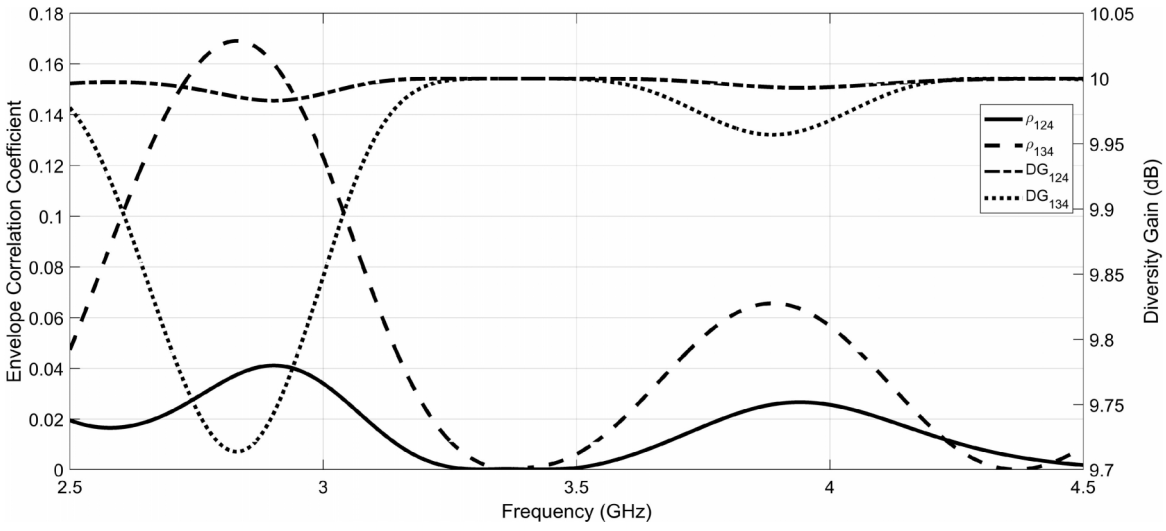

Figure 4.12: Simulated ECC and DG Curves for Proposed four L-shaped element MIMO System with CMSRR

Total Active Reflection Coefficient (TARC)

The ports of the proposed MIMO were excited as per the cases mentioned in section 4.3.2.1. It can be observed from Figure 4.13, the level of TARC is below -6 dB for the entire covered band around 3.5 GHz. This shows that the effective bandwidth of the proposed MIMO antenna doesn't vary much for different phase excitation of ports.

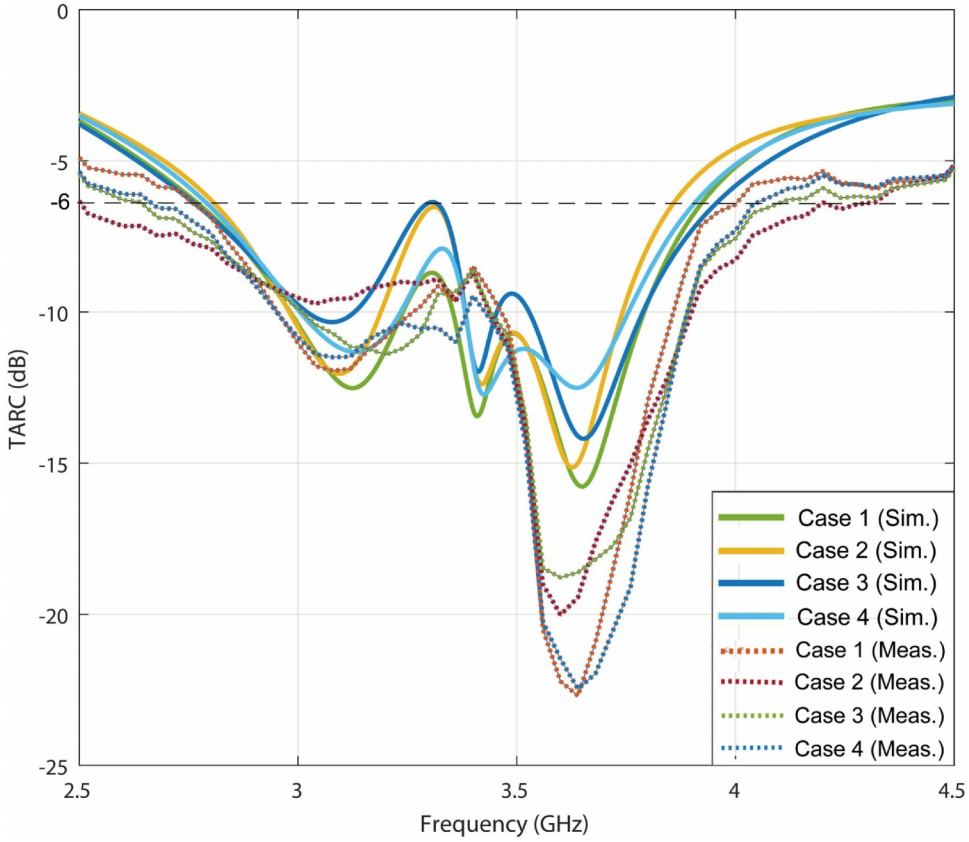

Figure 4.13: TARC Plot for proposed L-shaped element MIMO System with CMSRR

Channel Capacity Loss (CCL)

As shown in Figure 4.14, CCL is calculated for each pair of antenna elements and the level is below 0.4 bits/sec/Hz for the band covered by the proposed antenna. This shows that the degradation in system performance is low resulting in high channel capacity.

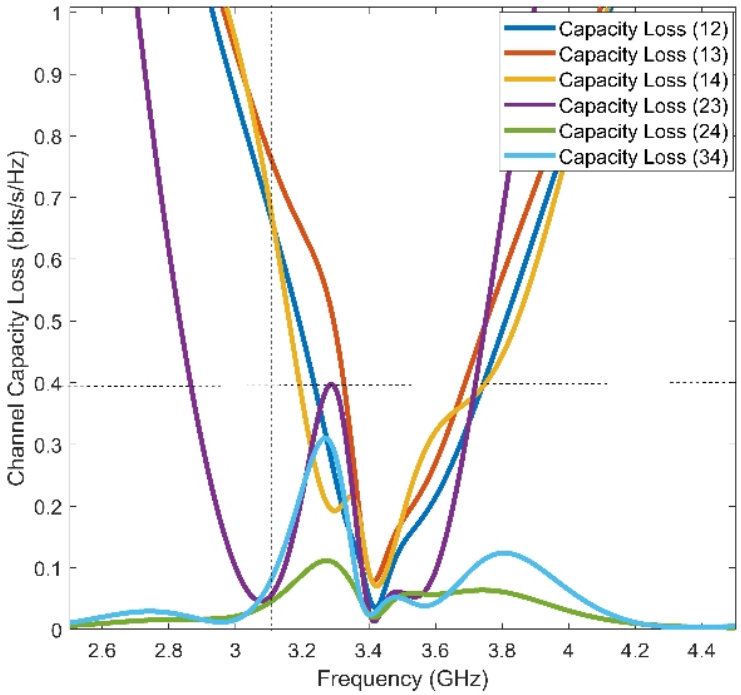

(a)

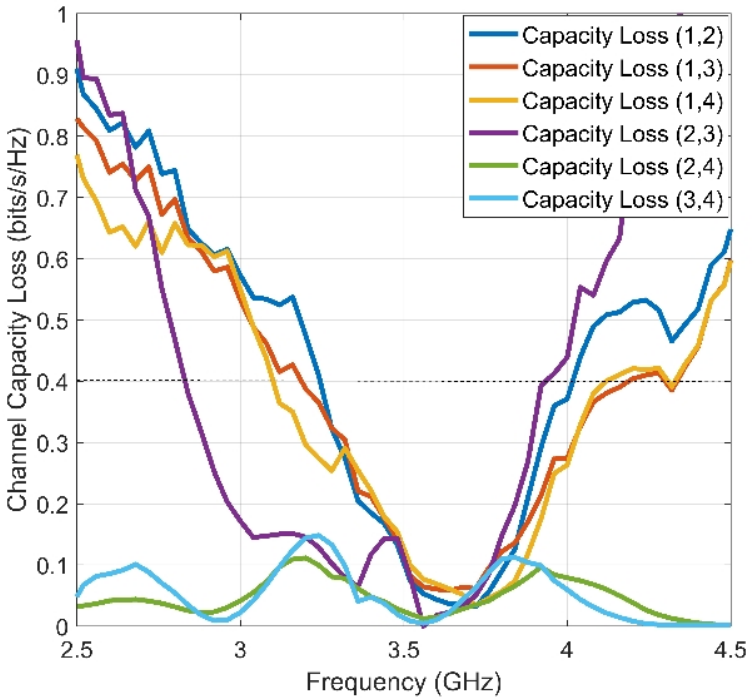

(b)

Figure 4.14: Channel Capacity Loss Plot of Proposed L-shaped element MIMO system with CMSRR (a) Simulated (b) Measured

Mean Effective Gain

Figure 4.15 shows the simulated and measured MEG ratios for the proposed MIMO antenna system with isolation enhancement. As it can be observed that in the covered frequency bands

the MEG ratio is quite near to 1 showing good diversity performance.

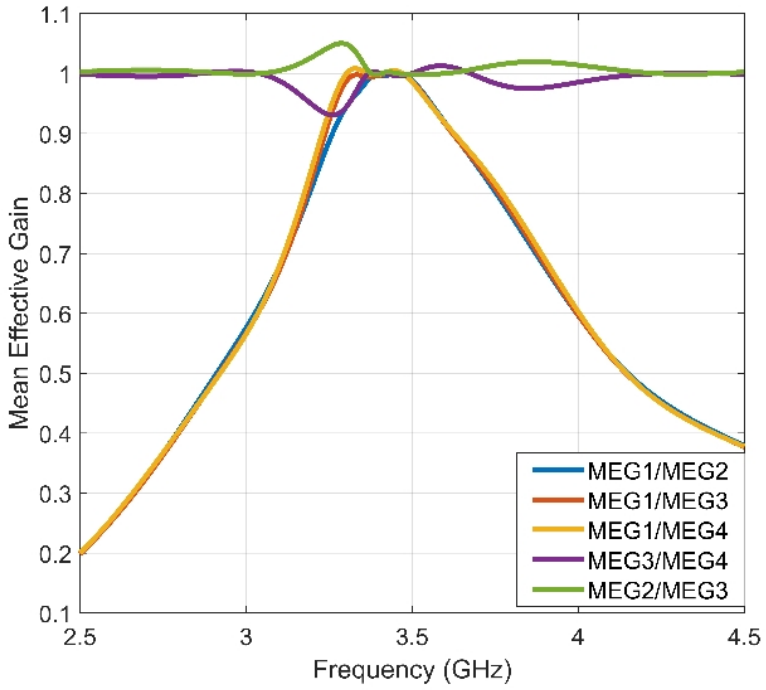

(a)

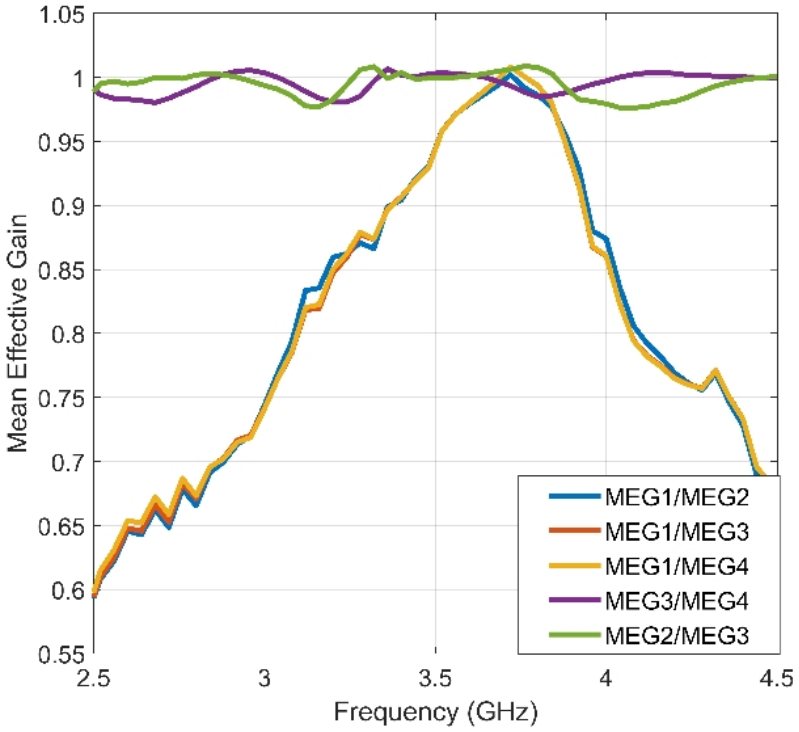

(b)

Figure 4.15: Mean Effective Gain Ratio Plot of Proposed L-shaped element MIMO system with CMSRR (a) Simulated (b) Measured

The performance of the antenna system gets affected due to proximity to human body (hand and head) [99]. Therefore, the performance of the proposed MIMO system is investigated in two cases i.e. SAM head and hand (Talk) mode, two hand (TH) data mode as shown in figure 4.16.

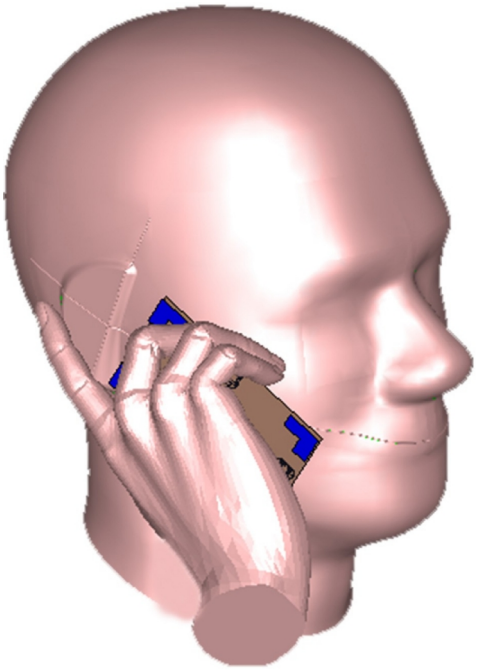

(a)

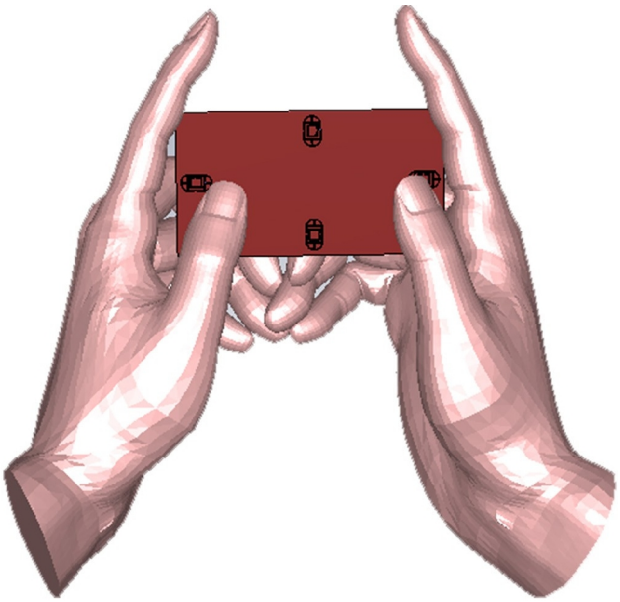

(b)

Figure 4.16: User Scenarios (a) Talk Mode (b) TH data mode

The table 4.2 presents the value of SAR (1g tissue) at resonant frequency of 3.5 GHz. It can

be observed that the SAR values are well below 1.6 W/Kg limit for both free space and talk mode cases.

Table 4.2: Simulated SAR analysis of proposed 4 L-shaped element MIMO Antenna with CMSRR

Frequency (GHz)	**SAR Talk Mode (W/Kg)**	**SAR THM (W/Kg)**
3.5	0.72	0.65

The effect on radiation efficiency of the proposed MIMO antenna is presented in Table 4.3. Due to the symmetrical arrangement of the antenna elements, the radiation efficiency values were calculated for one of the antenna elements. It can be observed that the presence of user's hand reduces the radiation efficiency of the MIMO antenna but still the values are acceptable for smooth operation of the device.

Table 4.3: Simulated and Measured Radiation Efficiency of proposed 4 L-shaped element MIMO Antenna

Frequency (GHz)	3.5	11.94	17.3
Simulated Efficiency in free space (%)	92	95	97
Measured Efficiency in free space (%)	78	81	83
Simulated Efficiency in THM (%)	48	55	58

Table 4.4: Comparison of proposed four L-shaped element MIMO antenna with literature

Ref. No.	**Antenna Type**	**Isolation Technique**	**Resonant Frequency (GHz)**	**Minimum Isolation (dB)**	**Element dimensions L x W x h**	**Peak Gain (dB)**	**No. of Ports**
[19]	PIFA	Decoupling slits and shielding wall	2.65	-17	22.1 x 19.3 x 7	Not given	2
[22]	Loop/IFA hybrid	Offset arrangement and grounding strips	3.5/5.8	-11	10.5 x 3.1 x 1	Not given	8
[25]	Microstrip Patch	Neutralization Line	5.4-5.96	-13	20 x 23.4 x 34.8	8.3	2
[54]	Annular Ring Slot	Nil	1.8-2.45 (Tuned)	-8	10.1 (Radius) x 0.76 (Thickness)	2.43	4

[81]	Folded Monopole	Ground slots and metal rim stub	1.6, 3.5, 4.4, 5.7	-12	23 x 12.5 x 1.6	0.48, 1.49	4
[82]	Patch	Partially extended ground	2.38, 3.5	-12.5	6.7 x 6.7 x 1.52	4, 3.3	4
[84]	ILA	Thin strips connecting ground	2.7	-11	19.4 x 12 x 1.6	4	4
[85]	PIFA	Suspended strip between elements and open slots on ground	2.2, 3.4	-19	20 x 27 x 3.5	Not given	2
[95]	Dendritic meandered micro-strip structure	Slot Lines	3.5, 5.5, 7	-15, -28, -16	19 x 9.1 x 1.6	Not given	4
[96]	Single Element	Ground Slot	3.3-3.7	-14	25.8 x 2.5 x 0.8	Not given	4
[97]	Slot based	DGS	2.1, 2.5, 3.5, 17.2	-4, -10	14 x 1.6 x 0.76, 16.6 x 12.2 x 0.76	3, 8	2 (4G), 2 (5G)
Our Work	PIFA L-shaped element	**CMSRR**	**3.5, 12.5, 17**	**-21.73, -18, -19**	**18 x 14 x 3.2**	**6.34, 7.99, 8.61**	4

1.3 Summary

In this chapter, a PIFA structure is proposed for sub-6 GHz 5G applications and 17 GHz IoT applications. The proposed antenna uses an L-shaped radiating element which is designed systematically using TCM as presented in chapter 3. The bands covered by the proposed antenna are 3.5 GHz, 12.5 GHz and 17 GHz. A four element MIMO antenna is also proposed using the same L-shaped element. Without any isolation enhancement technique, the isolation level between certain antenna element pairs is not below -15 dB. So, to enhance the isolation and other MIMO system performance parameters, two techniques are implemented:

defected ground structure (open-ended slots) and CMSRR. It has been observed that the effect of open-ended slots is not good enough to achieve significant improvement in the isolation levels. Due to the inclusion of CMSRR, the isolation level is enhanced by 8 dB which is way more than defected ground structure (open-ended slots) technique. At the end of the chapter, SAR analysis is also presented for talk mode (human head and hand) and data mode (two-hand). The SAR levels are well below the allowed limits. A comparison table is also presented to show that the proposed antenna is better than the research available in literature. The isolation levels and gain values are much better than most of the work available in literature.

Chapter 5 Design of Planar Antenna for sub-6 GHz and Millimeter Wave (mmWave) bands

5.1 Introduction

Various types of devices will be connected to each other via internet forming a large heterogeneous network which will require a communication network supporting such a huge number of devices. This emerging area is known as Internet of Things (IoT) where large number of sensors, appliances, and devices are interconnected and communicates with each other. To fulfill the demand for high data rate, compact devices with a greater number of antenna elements needs to be developed.

In most of the MIMO designs the mutual coupling is just near acceptable value [14]. To improve these MIMO parameters, several techniques have been proposed which are discussed in section 1.3. Most of the today's smart phones consists of two MIMO antenna elements for 4G/4G LTE and WLAN services. But future wireless devices supporting much higher data rates require a greater number of antenna elements. Recent works presented 2 elements/ports [27] [85] [72], 4 elements/ports [34] [94] [95] [96] [97] MIMO antenna designs for smart phones supporting 5G frequency bands. In this chapter, two element and four element MIMO antennas are proposed working on 3.5 GHz, 4.2 GHz bands, and a wide mmWave band (24 GHz – 36 GHz) for 5G applications. The MIMO system performance is enhanced by using CMSRR proposed in chapter 3.

5.2 Structure of the Proposed Antenna

This section presents the proposed single element PIFA, two element MIMO, and 4 element MIMO antenna design.

5.2.1 Single Element PIFA

The dimensions of the rectangular radiating patch of the proposed antenna are Lp = 18 mm, Wp =14 mm, W_s = 8 mm, W_f = 4 mm, L_b= 6 mm and h= 3 mm. And as already presented in previous section that the modal analysis helps in achieving the desired resonant frequency by modifying the rectangular patch. Also, there is an effect of position and dimensions of feed plate, introduction of dielectric substrate on the resonance of PIFA structure [6].

5.2.2 Two Element MIMO Antenna System

From a single element antenna to form a MIMO antenna system is to have a greater number of antenna elements. For the proposed MIMO antenna system, as shown in Figure 5.2 the two opposite corners (width wise) of the substrate have L-shaped with L-slot antenna elements placed with shorting and feed plate.

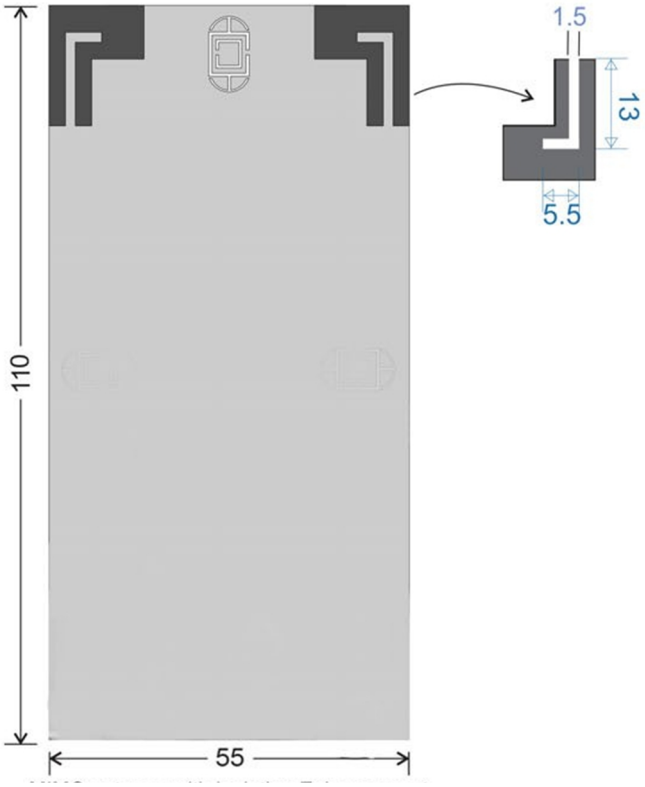

Figure 5.1: Detailed Dimensions of Proposed L-shaped L-slot Multi-band two element MIMO Antenna System (in mm)

5.2.3 Four Element MIMO Antenna System

For the proposed MIMO antenna system, as shown in Figure 5.2 the four corners of the substrate have L-shaped with L-slot antenna elements placed with shorting and feed plate. Figure's left side shows the MIMO system with no isolation enhancement structure and on the right side the MIMO antenna system with complimentary modified split ring resonator (CMSRR) on the ground plane is presented. The proposed CMSRR exhibits metamaterial properties at 3.5 GHz band.

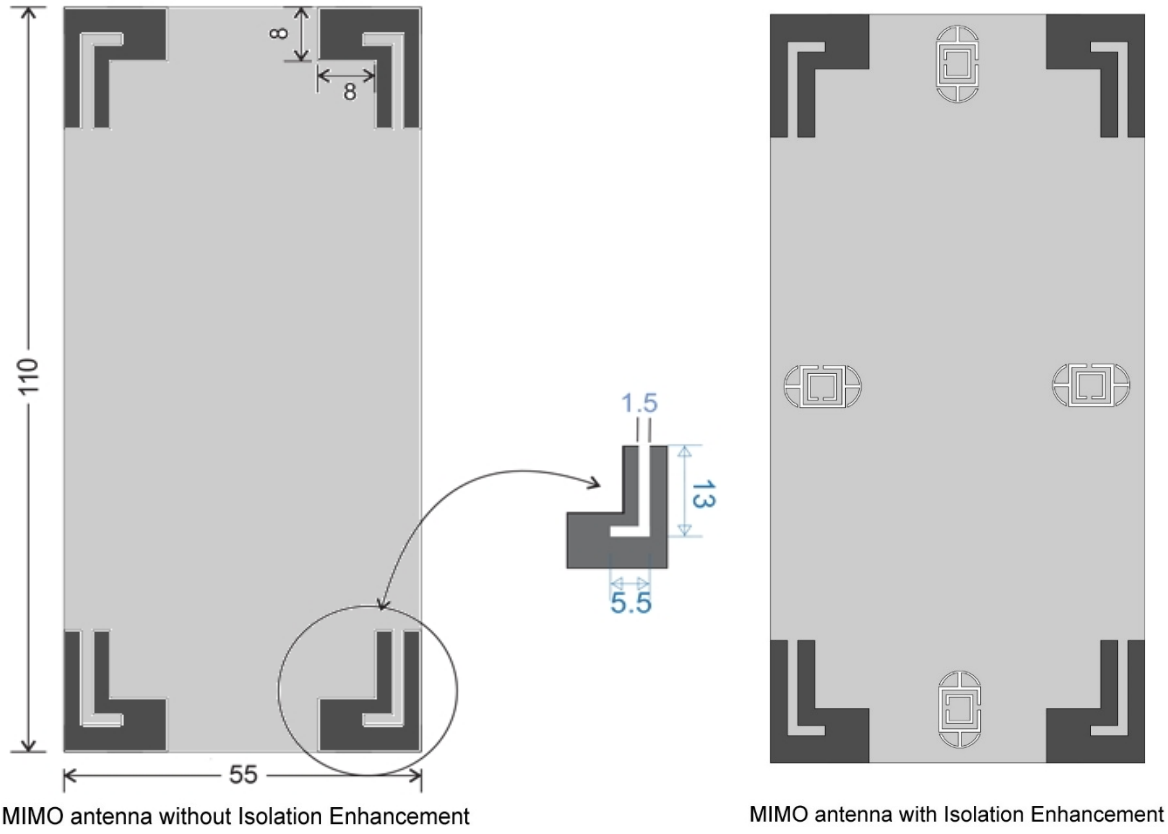

Figure 5.2: Detailed Dimensions of Proposed L-shaped L-slot Multi-band MIMO Antenna System (in mm)

5.3 Results and Discussion

This section presents various antenna parameters both simulated and measured of single element PIFA and four element MIMO antenna system. For the measurement the Performance Network Analyzer (PNA) model number N5230C (10 MHz to 40 GHz) from Keysight is used and an anechoic chamber is used to measure the radiation pattern (supporting measurements up to 20 GHz). For the mmWave bands, the measured radiation patterns are not presented due to unavailability of testing facilities at those frequency bands.

5.3.1 Single Element L-shaped L-slot PIFA

Return Loss

Figure 5.3 (a) shows the antenna prototype and the simulated and measured return loss plot of single element L-shaped L-slot PIFA structure is shown in Figure 5.3 (b). From Figure 5.3 (b) the resonant frequencies can be observed at 3.59 GHz, 4.24 GHz, 25.5 GHz, and 32.7 GHz with return loss value of -26.3 dB, -10.96 dB, -24.95 dB and -24.22 dB from simulation and at 3.51 GHz, 4.3 GHz, 24.8 GHz, and 30.24 GHz with return loss value of -17.9 dB, -18.1 dB, -18.42 dB, and -17.12 dB from measured results.

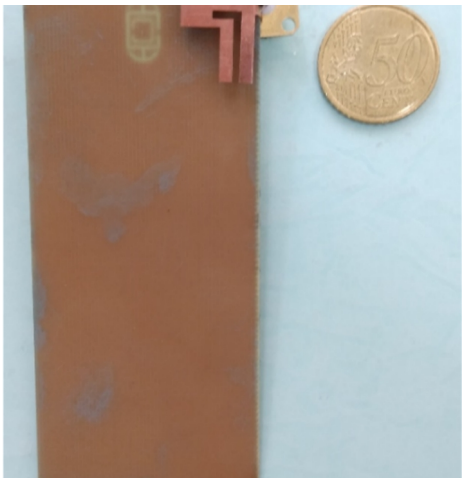

(a)

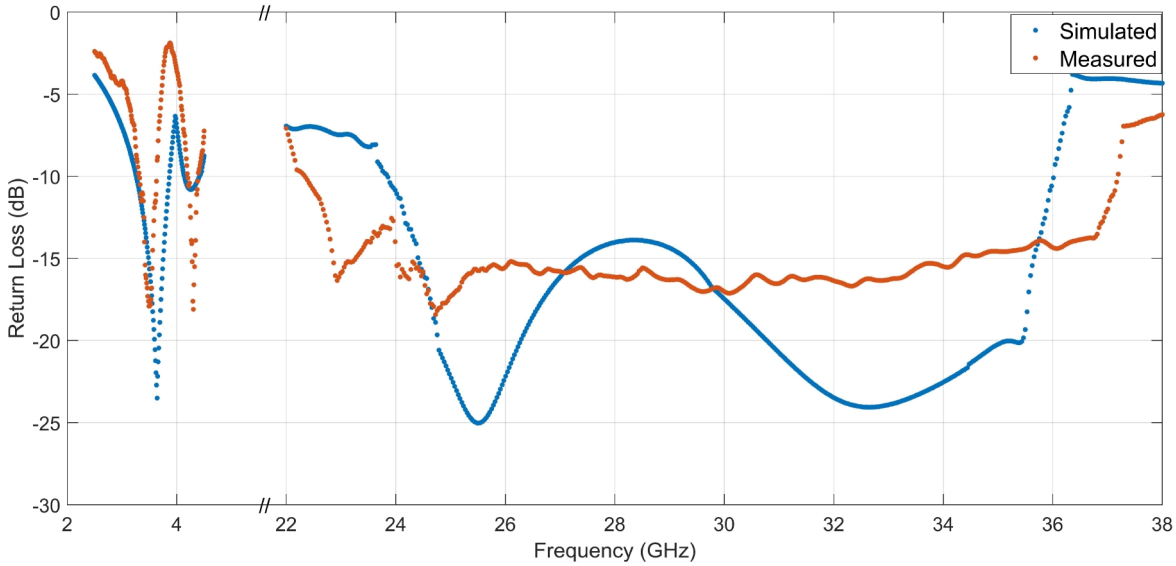

(b)

Figure 5.3: Propose Single Element L-shaped L-slot PIFA (a) Antenna prototype (b) Return Loss Plot

In sub-6 GHz band the proposed antenna exhibits 860 MHz of bandwidth and more than 12 GHz of bandwidth in mmWave band for simulation. From measured results, the bandwidth coverage is 510 MHz in sub 6 GHz band and more than 14 GHz in mmWave band. The proposed antenna covers n77, n78, n257, n258 and n261 5G NR bands as per ITU release 16 document.

Radiation Pattern and Gain Plot

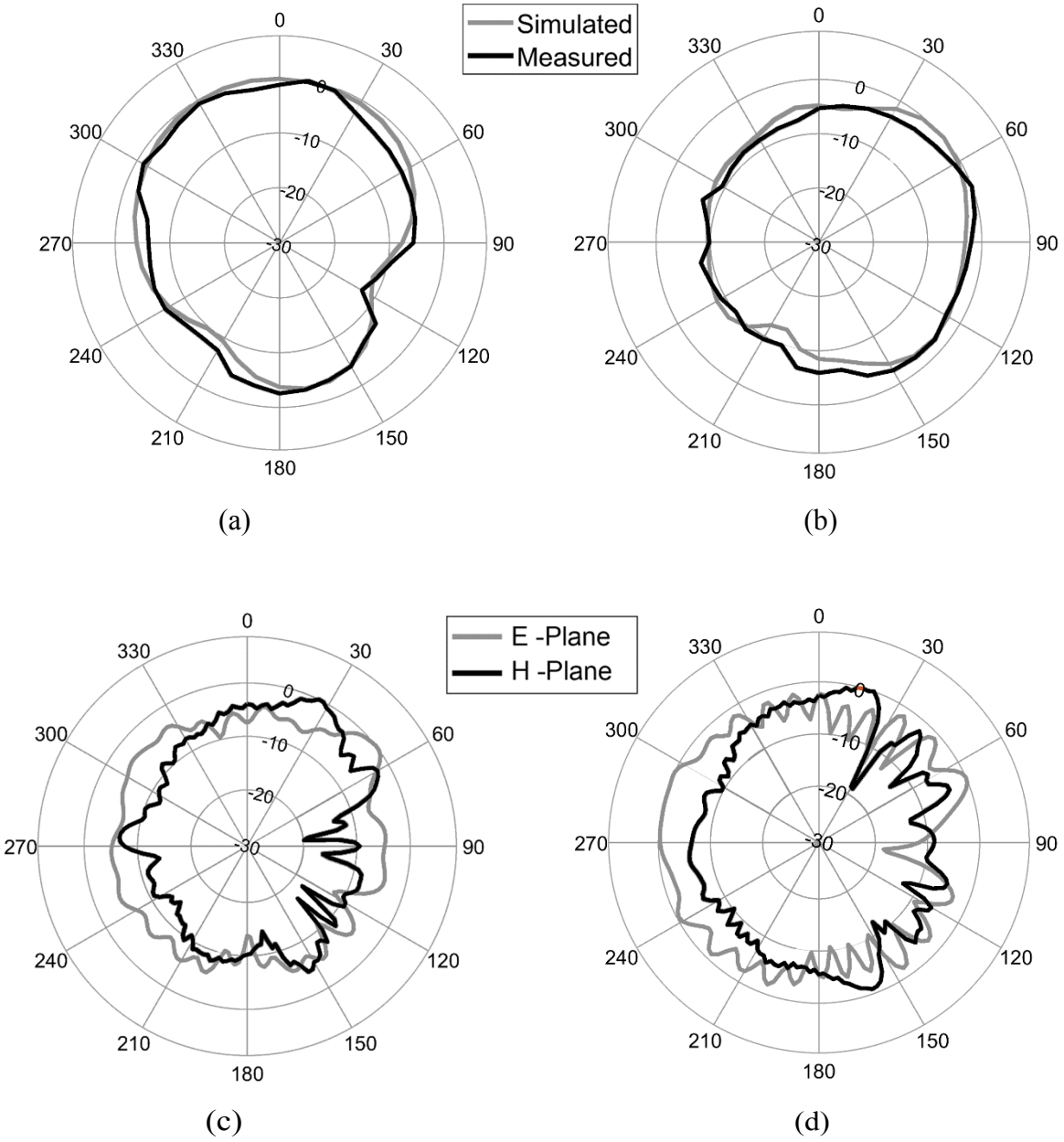

Figure 5.4: 2D Radiation Pattern Plot of Proposed Single L-shaped L-slot Element PIFA (a) E-Plane at 3.52 GHz (b) H- Plane at 3.52 GHz (c) Simulated E and H Plane at 26 GHz (d) Simulated E and H Plane at 32 GHz

Simulated and measured radiation pattern for sub-6 GHz band and simulated radiation

pattern for mmWave bands are presented in Figure 5.4. Figure 5.4 (a) and (b) shows that the proposed PIFA has directional E plane behaviour and omni-directional H-plane behaviour. From Figure 5.4 (c) it can be observed the E plane is omni-directional while H plane is directional. From Figure 5.4 (d) it can be observed both the planes are omni-directional.

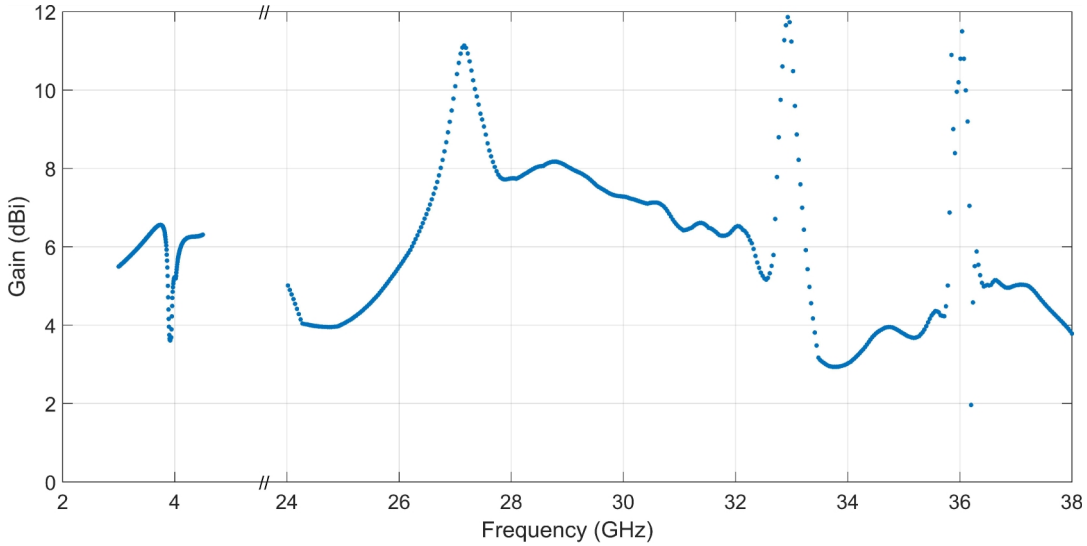

Figure 5.5: Simulated 2D Gain Plot of Proposed Single L-shaped L-slot Element PIFA

The simulated peak gain values of the proposed PIFA are 6.36 dBi at 3.5 GHz, 6.24 dBi at 4.25 GHz, 7.59 dBi at 25.5 GHz and 6.42 dBi at 32.7 GHz in the frequency bands covered by the antenna as shown in Figure 5.5.

5.3.2 Two Element MIMO Antenna with CMSRR

Return Loss and Isolation Curves

Figure 5.6 presents the antenna prototype and S-parameters plots for the proposed two element MIMO antenna system with CSMRR. The resonant frequencies for both the PIFA elements are mostly the same around 3.5, 4.3 GHz, and mmWave bands. The isolation level is below −21 dB throughout the covered frequency bands.

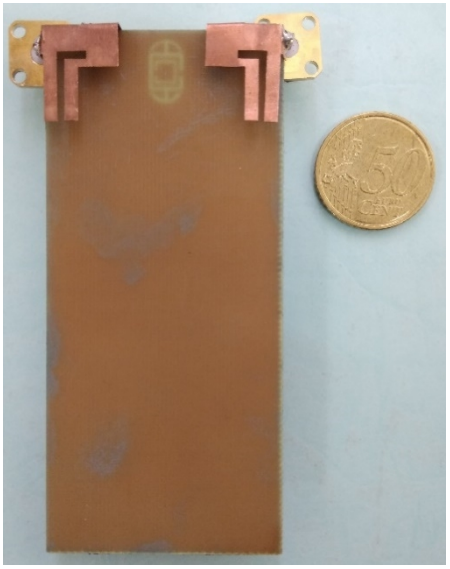

(a)

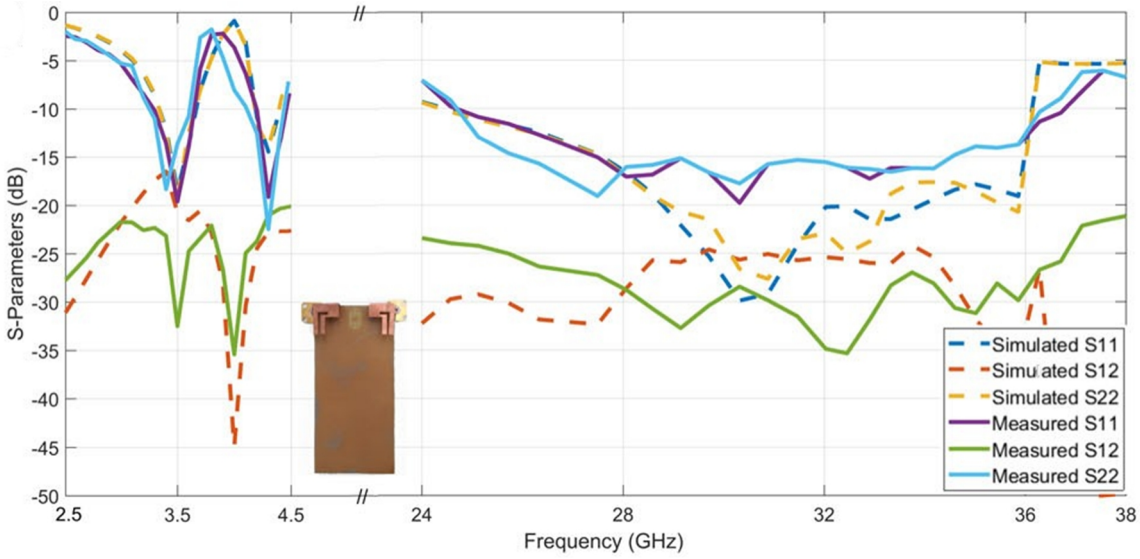

(b)

Figure 5.6 Proposed L-shaped L-slot element two element MIMO antenna with CMSRR (a) Antenna Prototype (b) S-Parameter plots

Envelope Correlation Coefficient (ECC)

The simulated and measured ECC curves are shown in Figure 5.7 for proposed two element MIMO antenna system with CMSRR. In the covered bands the ECC value is below 0.05 level.

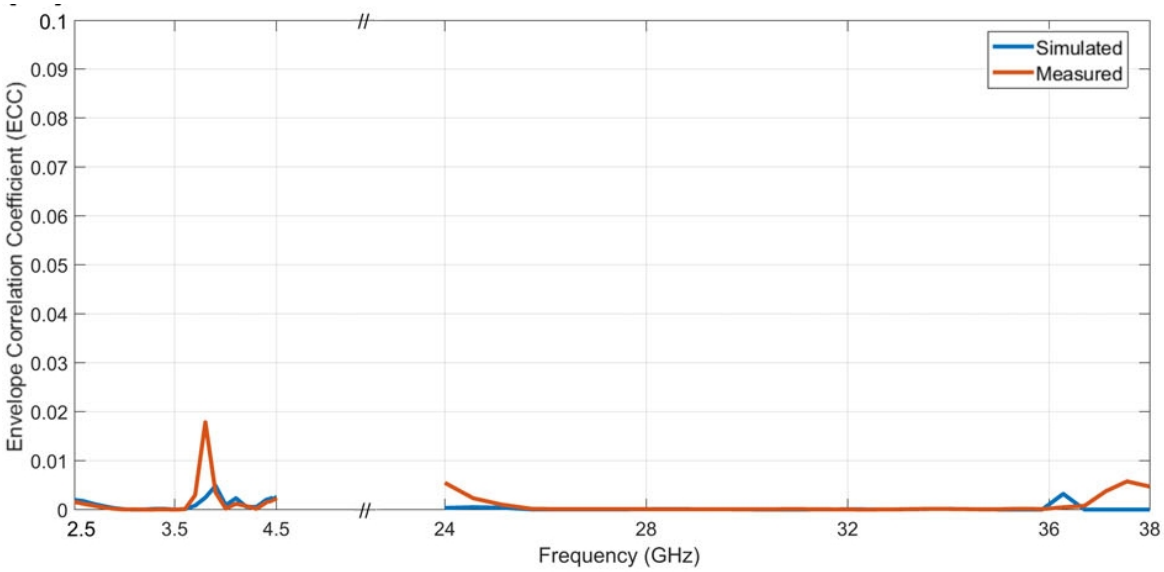

Figure 5.7: Simulated and measured ECC curves of Proposed two L-shaped L-slot element MIMO antenna with CMSRR

Total Active Reflection Coefficient (TARC)

Figure 5.8 shows the simulated and measured TARC level for the covered frequency bands which is below -10 dB for different values of theta.

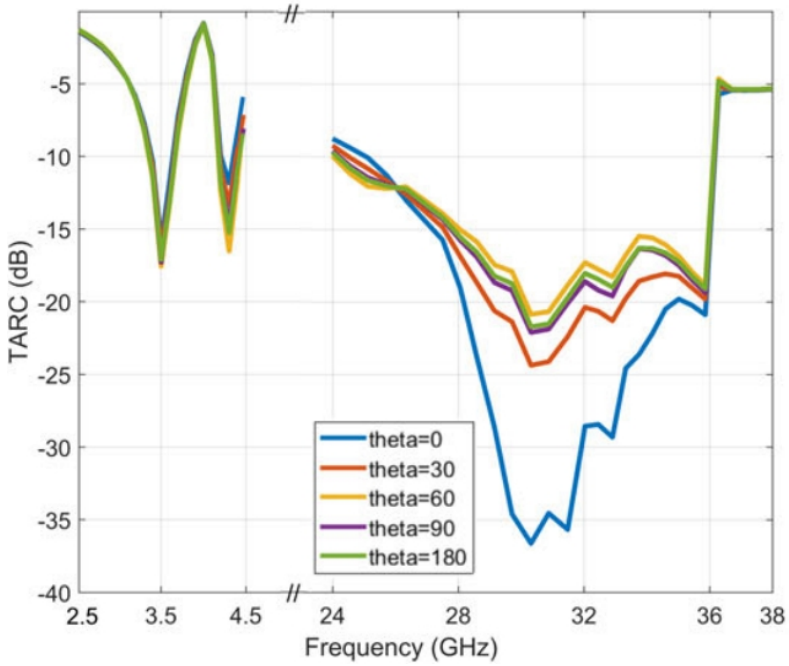

(a)

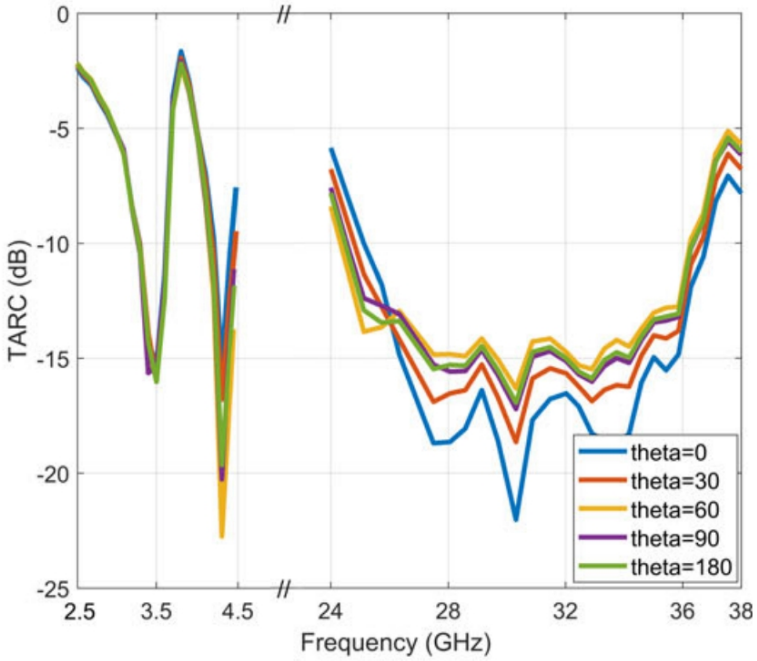

(b)

Figure 5.8: TARC Plots for proposed L-shaped L-slot two element MIMO System with CMSRR (a) Simulated (b) Measured

Channel Capacity Loss

Acceptable value for CCL is 0.4 b/sec/Hz and the proposed two element MIMO antenna system shows lower than 0.4 b/s/Hz in the covered bands as shown in Figure 5.9 for both simulated and measured results.

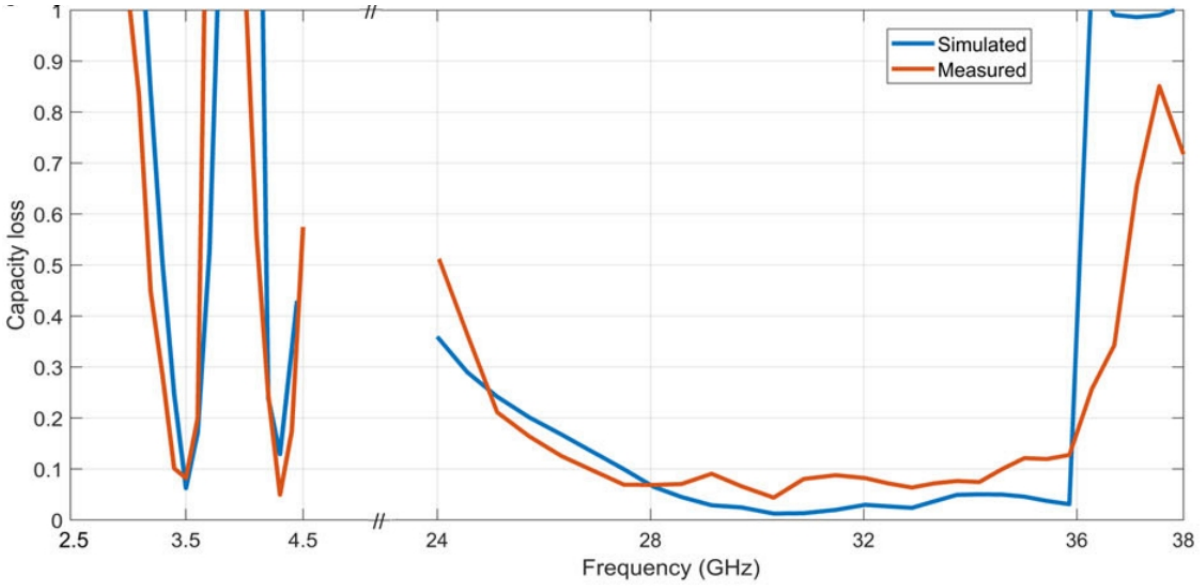

Figure 5.9: Channel Capacity Loss Plot of Proposed L-shaped L-slot two element MIMO Antenna with CMSRR

Mean Effective Gain

The MEG of each element calculated using the equation above can further be taken in ratios between two MEGs which are shown in Figure 5.10. The ratio of MEGs should be '1' or near to '1' for good diversity performance. For the proposed two element MIMO antenna system, the MEG ratios are near to '1' for the covered frequency bands.

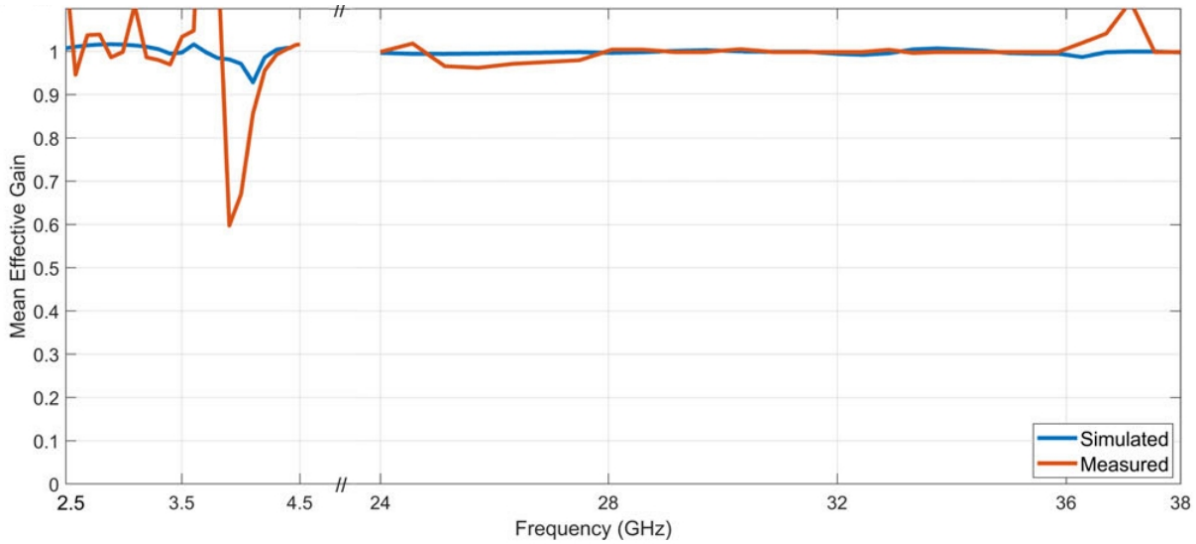

Figure 5.10: Curves for Mean Effective Gain Ratio of Proposed L-shaped L-slot two element MIMO Antenna with CMSRR

5.3.3 Four Element MIMO Antenna with no isolation enhancement mechanism

The MIMO antenna structure is designed by placing the antenna radiating element at each corner of the substrate. The placement on the corners makes it easy to feed the antenna element on the edge and giving more space to other components and circuits of the device.

Return Loss and Isolation Curves

Figure 5.11 (a) presents the fabricated prototype of the antenna. Figure 5.11 (b) presents the return loss plots for all the four ports with almost the same resonant frequency in sub-6 GHz as well as in mmWave band. Figure 5.11 (c) shows the isolation level between the antenna elements where only S12, S13, S14 are presented as S12=S21=S34=S43, S13=S31=S24=S42, and S14=S41=S23=S32. The level of isolation is lower than -15 dB

except for S13 having the isolation a little above -15 dB in lower band. The resonant frequencies for sub-6 GHz bands are 3.5 GHz and 4.2 GHz. For the mmWave bands the resonant frequencies of simulated results are at 28.8 GHz and 30.7 GHz while the resonant frequencies for measured results 24.5 GHz and 30.45 GHz. The isolation level is below -23 dB for mmWave band.

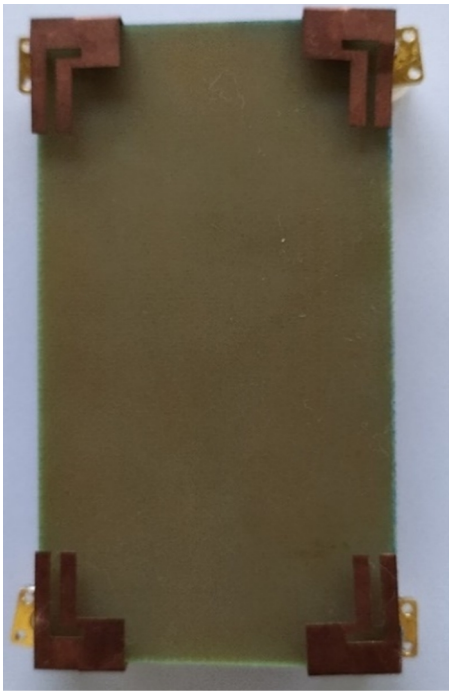

(a)

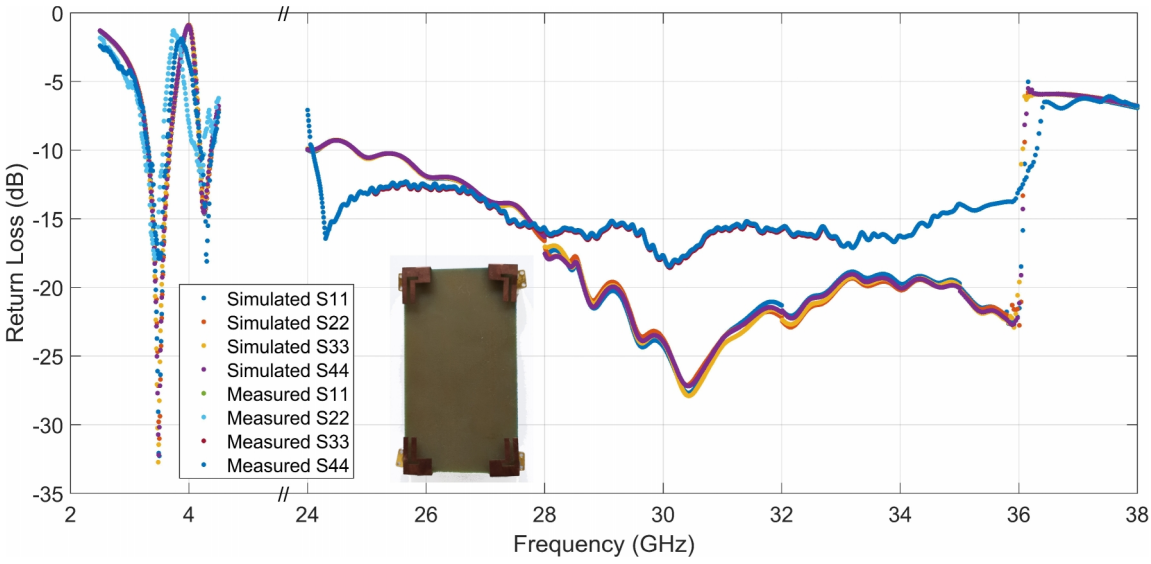

(b)

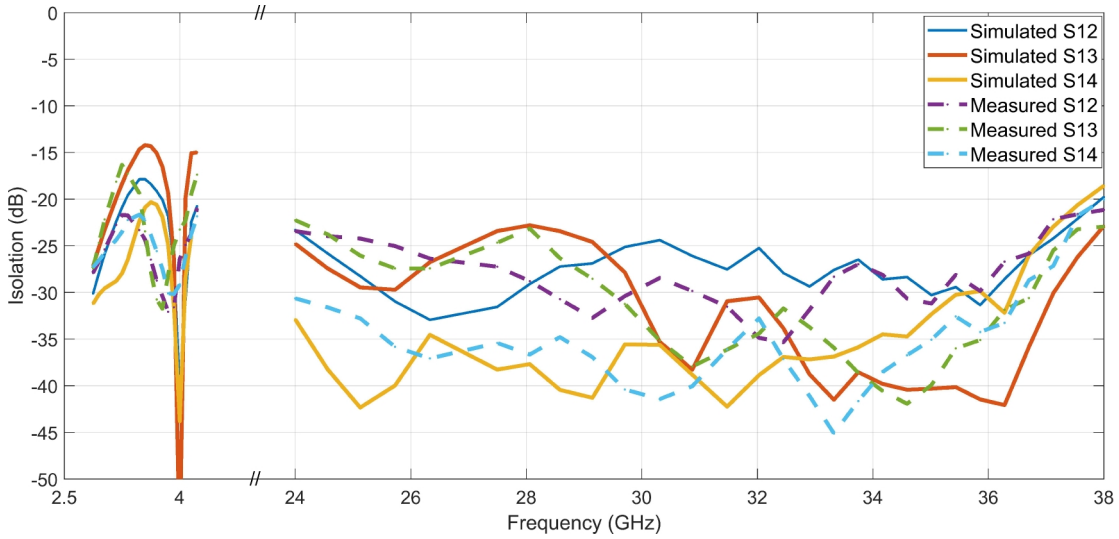

(c)

Figure 5.11: Proposed 4 L-shaped L-slot element MIMO antenna without isolation enhancement (a) Antenna Prototype (a) Return loss curves (b) Isolation curves

Envelope Correlation Coefficient and Diversity Gain

ECC is an important MIMO performance parameter to measure the isolation between the antenna elements. For calculating ECC from antenna parameters equations 4.3 and 4.4 are used. The acceptable value for ECC needs to be below 0.5 level.

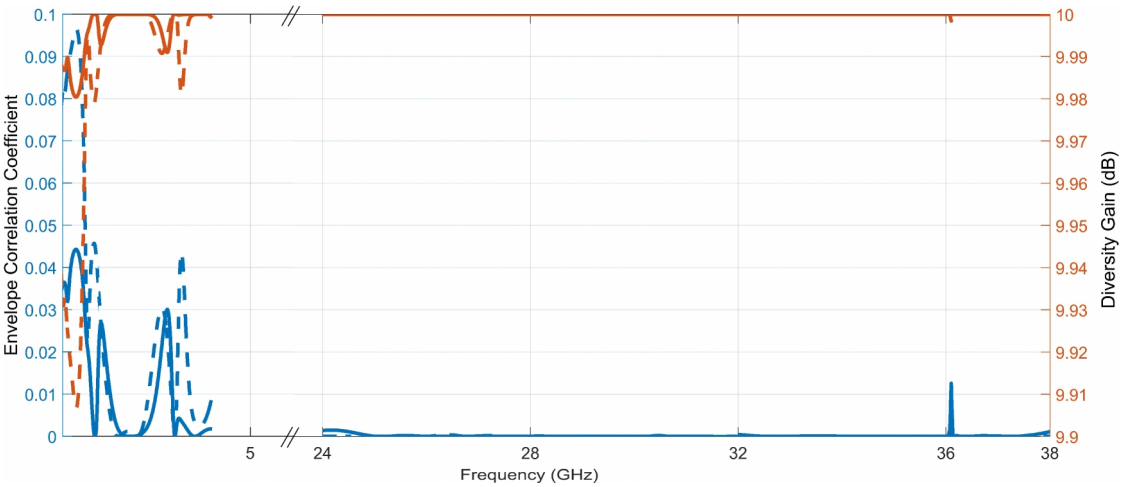

Figure 5.12: Simulated ECC and DG Curves for Proposed L-shaped L-slot MIMO antenna System without isolation enhancement

The curves presented in Figure 5.12 are for ECC and DG for both sub-6 GHz and mmWave bands. As it can be observed from the blue color curves the value for ECC in the covered bands is below 0.01. From the orange color curves, it can be observed that the value of DG is above 9.98 for the covered bands.

Total Active Reflection Coefficient (TARC)

Figure 5.13 shows that the proposed MIMO system performs well with variation in elevation angle as TARC is below -10 dB level for both simulation and measured results.

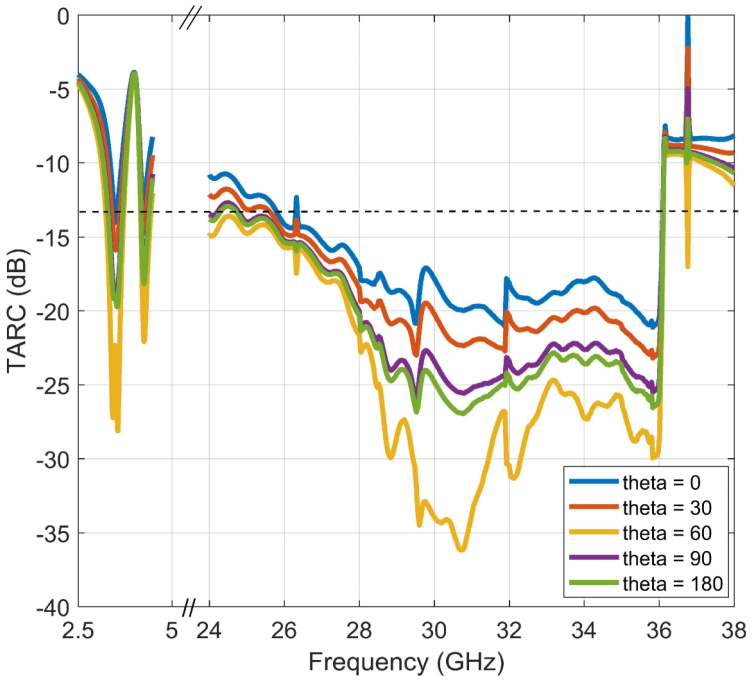

(a)

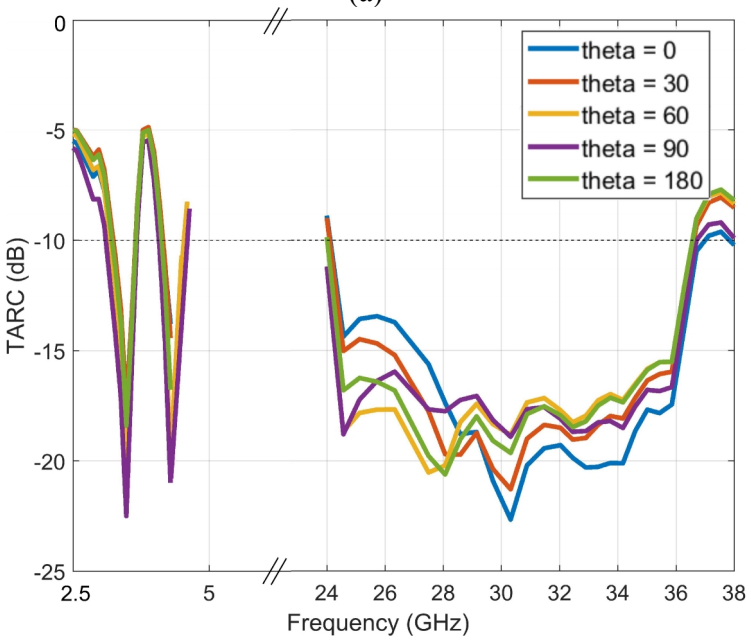

(b)

Figure 5.13: TARC Plot for proposed L-shaped L-slot MIMO System without isolation enhancement (a) Simulated (b) Measured

Channel Capacity Loss

The system performance degradation can be measured in terms of channel capacity loss (CCL). Acceptable value for CCL is 0.4 bits/sec/Hz and the proposed MIMO antenna system shows lower than 0.4 b/s/Hz in the covered bands of operation as shown in Figure 5.14 for both simulated and measured results.

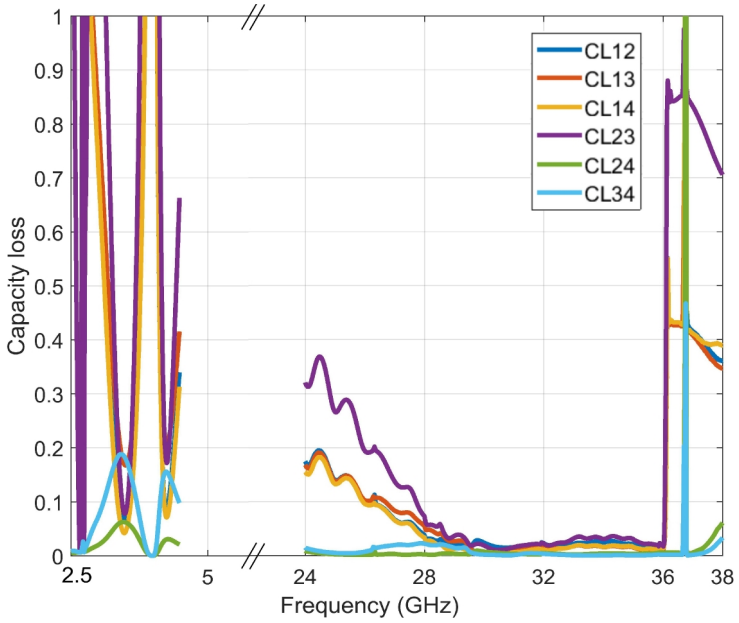

(a)

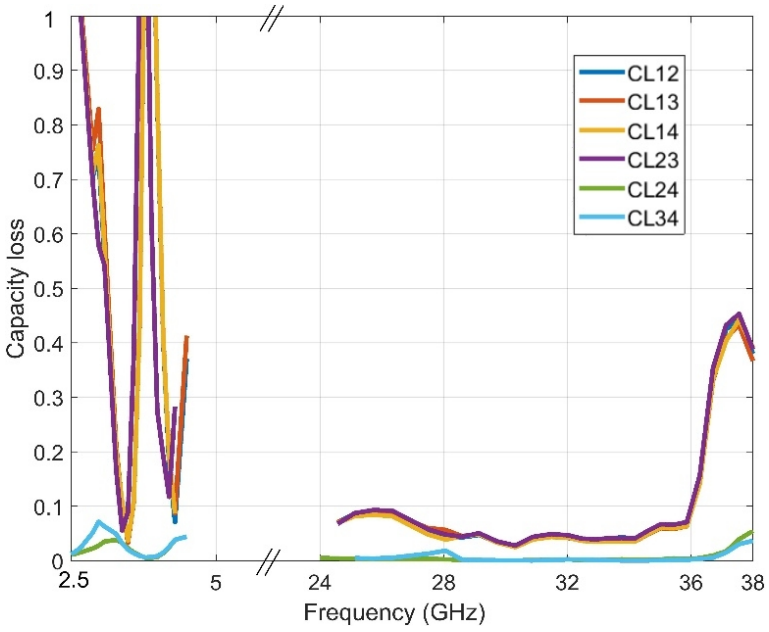

(b)

Figure 5.14: Channel Capacity Loss Plot of Proposed L-shaped L-slot MIMO Antenna without isolation enhancement (a) Simulated (b) Measured

Mean Effective Gain

The MEG of each element calculated using the equation above can further be taken in ratios between two MEGs and the plots for different ratios are shown in Figure 5.15. The ratio of MEGs should be '1' or near to '1' for good diversity performance. For the proposed MIMO antenna system, the MEG ratios are near to '1' for the covered frequency bands.

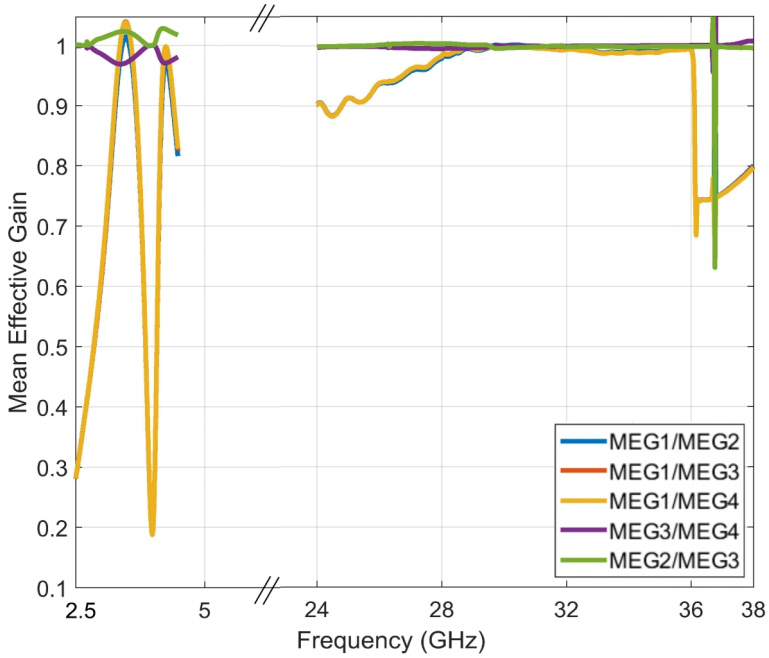

(a)

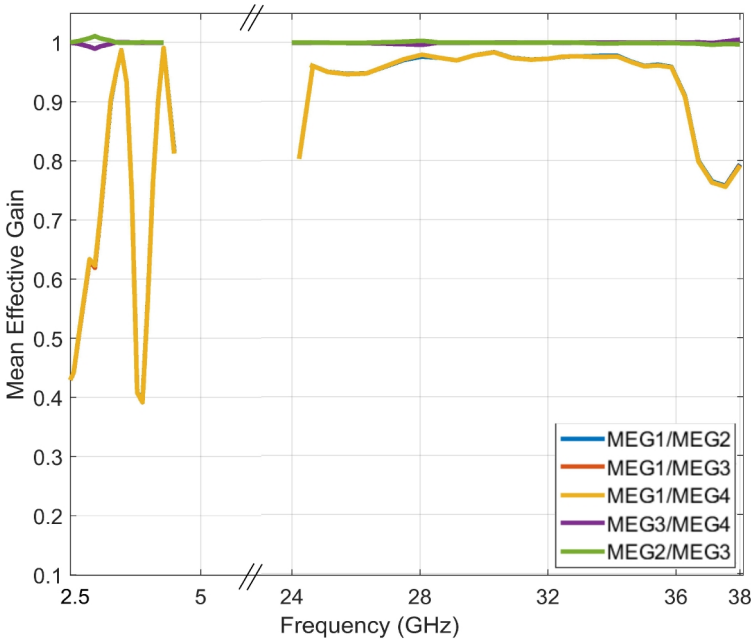

(b)

Figure 5.15: Curves for Mean Effective Gain Ratio of Proposed L-shaped L-slot MIMO Antenna without isolation enhancement (a) Simulated (b) Measured

5.3.4 Four Element MIMO Antenna with Isolation Enhancement using CMSRR

Return Loss and Isolation Curves

Figure 5.16 presents the antenna prototype and S-parameters plots for the proposed MIMO antenna system with isolation enhancement. The resonant frequencies for all the four PIFA elements are mostly the same around 3.5 GHz, 4.2 GHz and mmWave band as presented in Figure 5.16 (b). The isolation level between the antenna elements are shown in Figure 5.16 (c) and it can be observed that the CMSRR improved the isolation level for 3.5 GHz band by -8 dB at least. The isolation level for mmWave band is well below -23 dB throughout.

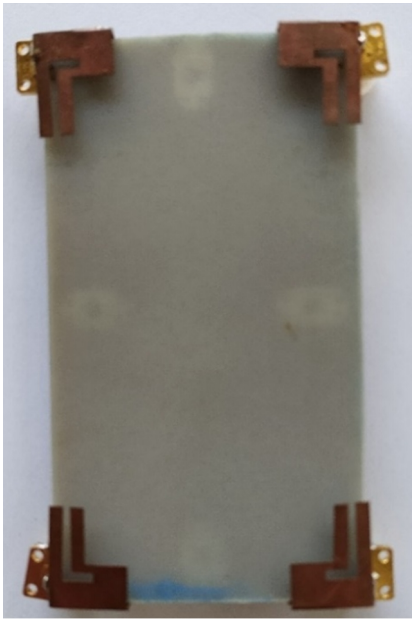

(a)

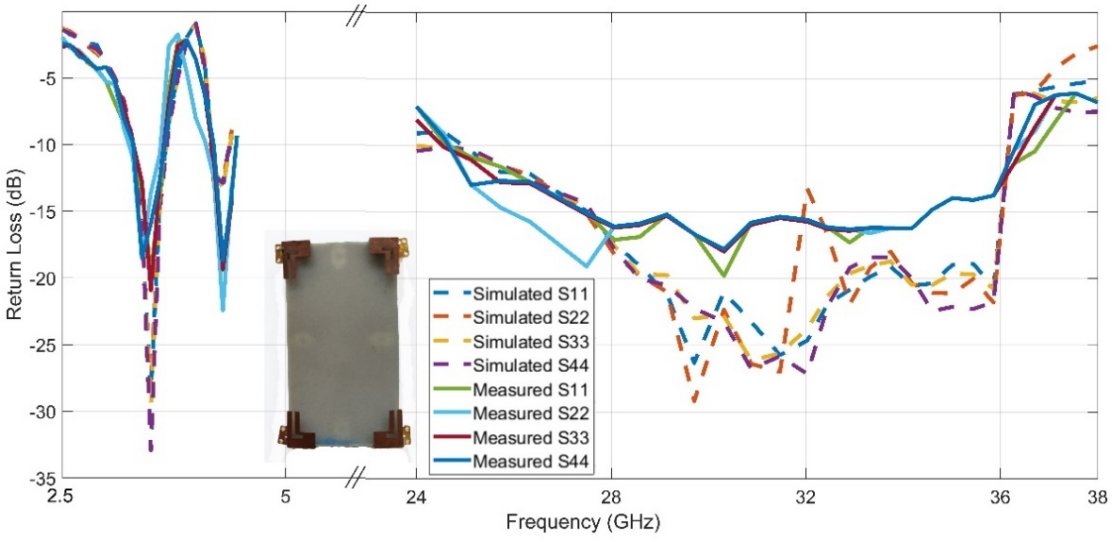

(b)

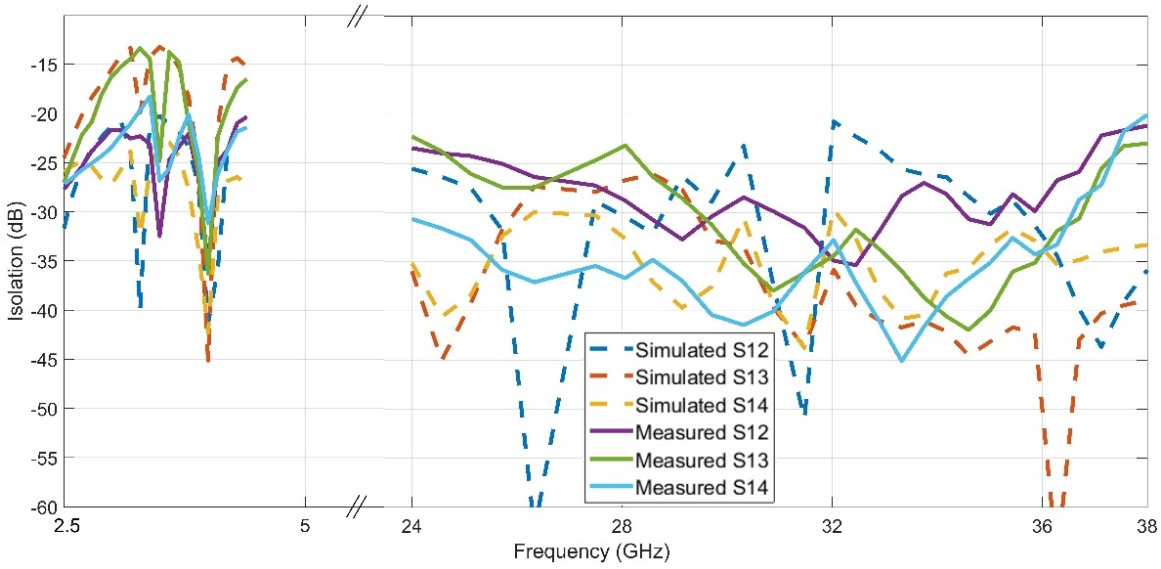

(c)

Figure 5.16: Proposed 4 L-shaped L-slot element MIMO antenna with CMSRR (a) Antenna Prototype (b) Return loss curves (c) Isolation curves

Envelope Correlation Coefficient and Diversity Gain

The simulated ECC and DG curves are shown in Figure 5.17 for proposed MIMO antenna system with CMSRR. In the covered bands the ECC value is below 0.05 level. The value of DG is also near to '10' level throughout the covered bands of operation. These performance parameter values for the proposed MIMO system is considered to be excellent.

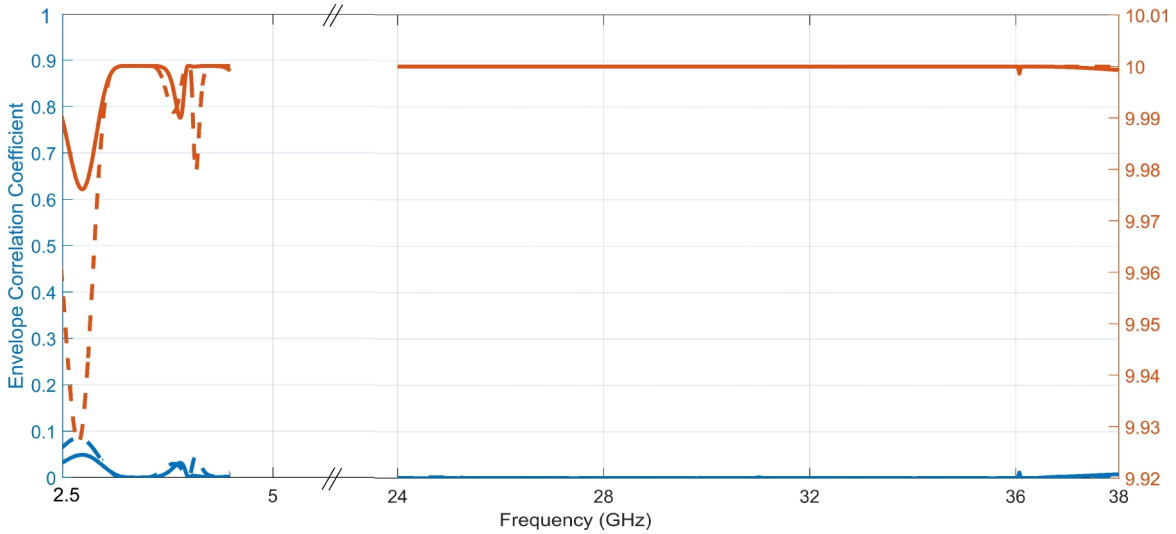

Figure 5.17: Simulated ECC and DG Curves for Proposed L-shaped L-slot MIMO System with CMSRR

Total Active Reflection Coefficient (TARC)

Figure 5.18 shows the TARC level for the covered frequency bands which is below -10 dB for different values of theta.

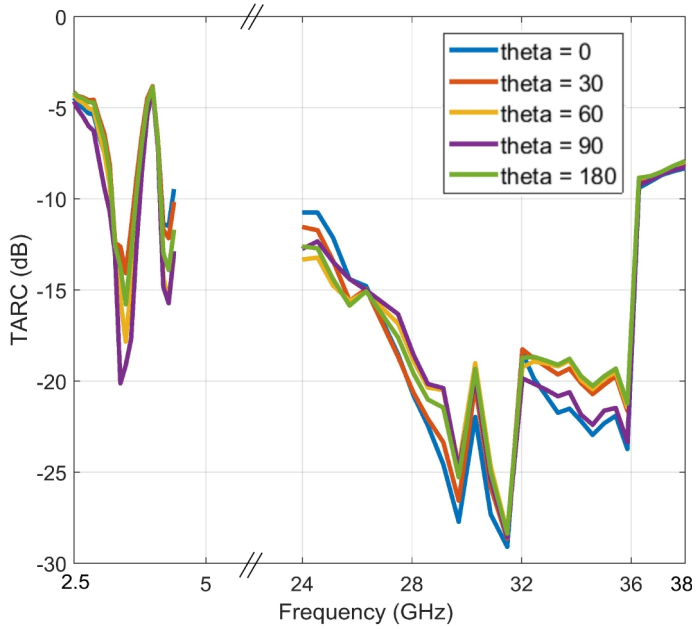

(a)

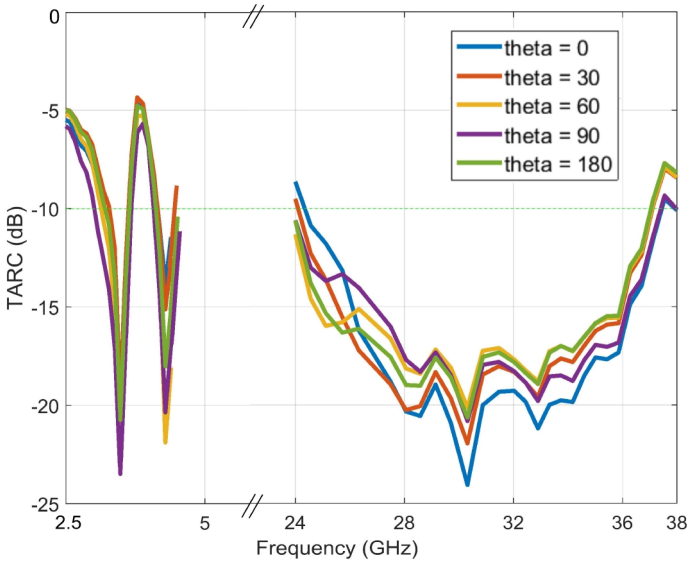

(b)

Figure 5.18: TARC Plot for proposed L-shaped L-slot MIMO System with CMSRR (a) Simulated (b) Measured

Channel Capacity Loss (CCL)

CCL is calculated for different pairs of antenna elements and the curves are presented in Figure 5.19. The value of CCL for all the element pairs is well below 0.4 b/s/Hz showing that

the system performance degradation is low resulting in high channel capacity.

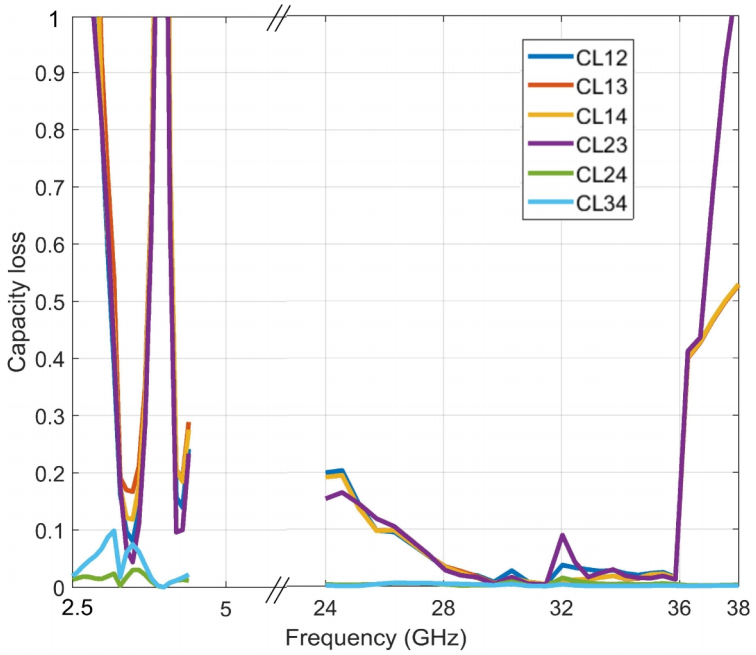

(a)

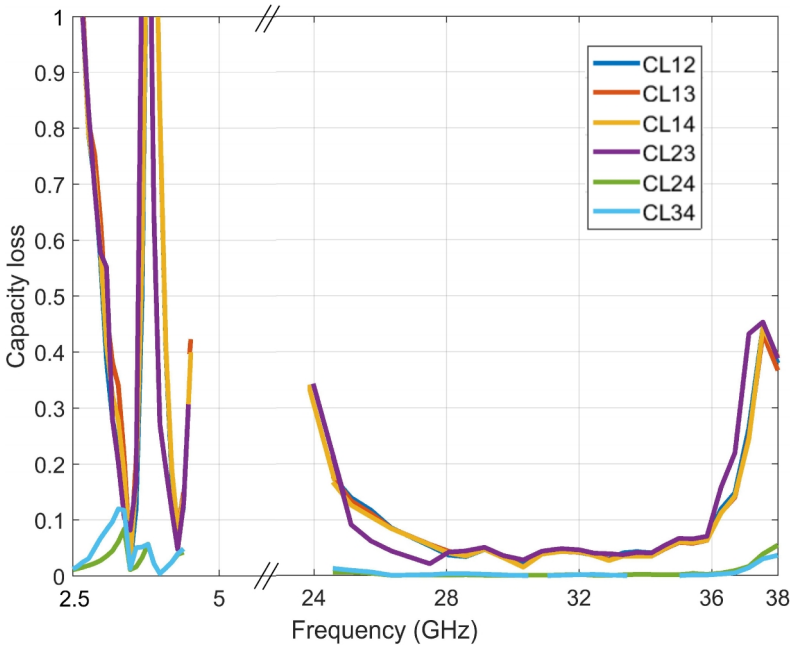

(b)

Figure 5.19: Channel Capacity Loss Plot of Proposed L-shaped L-slot MIMO Antenna with CMSRR (a) Simulated (b) Measured

Mean Effective Gain

The simulated and measured MEG ratio curves are shown in Figure 5.20. The value of MEG ratio curves is quite near to ’1’ level for the covered bands exhibiting good diversity

performance.

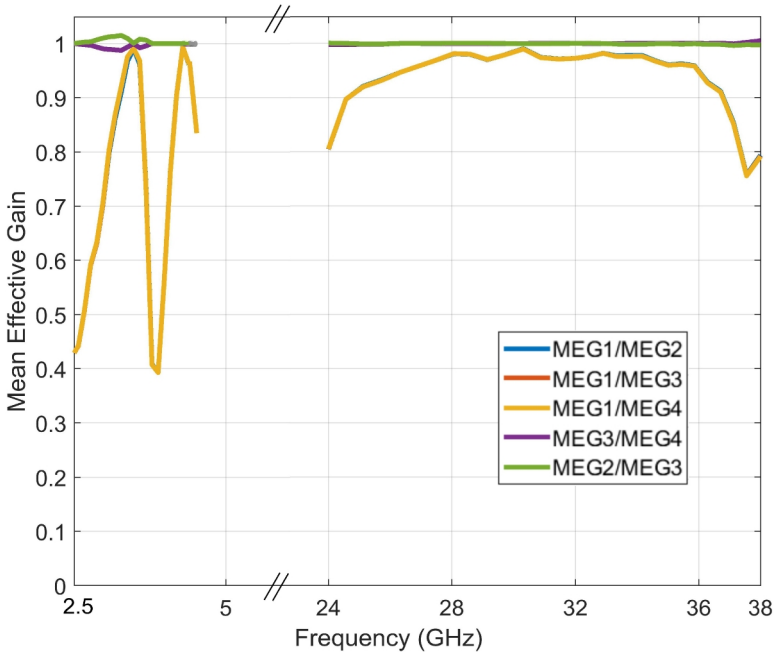

(a)

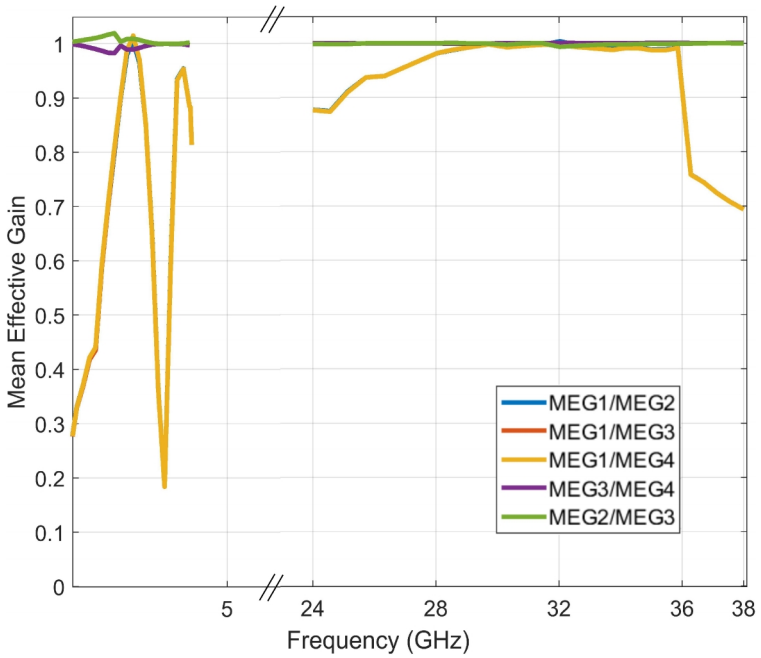

(b)

Figure 5.20: Mean Effective Gain Ratio Plot of Proposed L-shaped L-slot MIMO Antenna with CMSRR (a) Simulated (b) Measured

Specific Absorption Rate (SAR) Analysis and User's hand effects

The performance of the antenna system gets affected due to close proximity of human body (hand and head) [99]. Therefore, the performance of the proposed MIMO system is

investigated in two cases i.e. SAM head and hand (Talk) mode, two hand (TH) data mode as shown in figure 5.21.

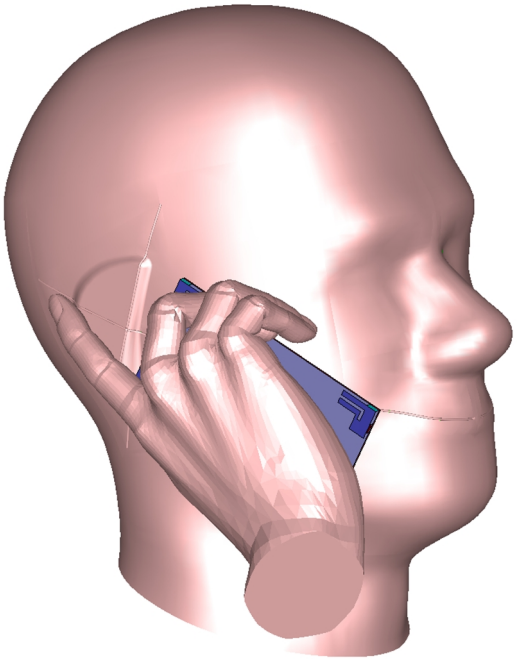

(a)

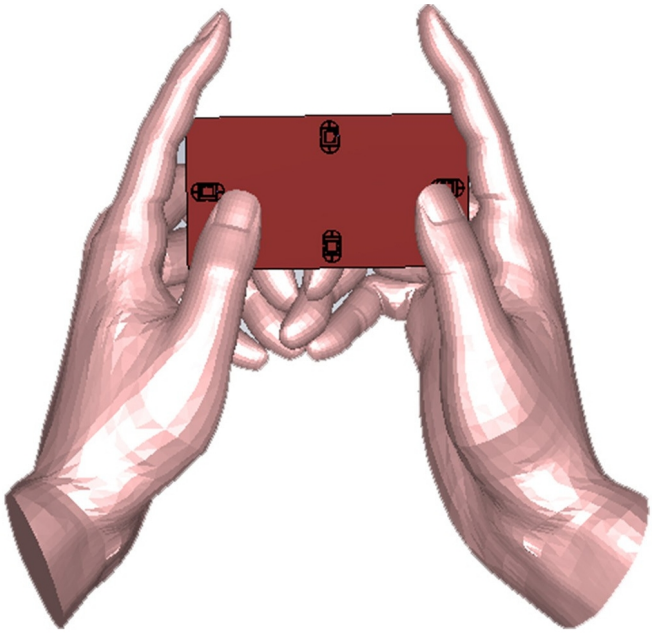

(b)

Figure 5.21: User Scenarios for four L-shaped L-slot MIMO antenna (a) Talk Mode (b) TH data mode

The table 5.1 presents the value of SAR (1g tissue) at resonant frequency of 3.5 GHz. It can be observed that the SAR values are well below 1.6 W/Kg limit for both free space and talk mode cases.

Table 5.1: Simulated SAR analysis of proposed four L-shaped L-slot element MIMO Antenna with CMSRR

Frequency (GHz)	**SAR Talk Mode (W/Kg)**	**SAR THM (W/Kg)**
3.5	0.76	0.69

The effect on radiation efficiency of the proposed MIMO antenna is presented in Table 5.2 Due to the symmetrical arrangement of the antenna elements, the radiation efficiency values were calculated for one of the antenna elements. It can be observed that the presence of user's hand reduces the radiation efficiency of the MIMO antenna but still the values are acceptable for smooth operation of the device.

Table 5.2: Simulated and Measured Radiation Efficiency of proposed four L-shaped L-slot element MIMO Antenna

Frequency (GHz)	3.5	4.2	30
Simulated Efficiency in free space (%)	94	92	87
Measured Efficiency in free space (%)	78	76	--
Simulated Efficiency in THM (%)	46	54	61

Table 5.3: Comparison of proposed four L-shaped L-slot element MIMO antenna with literature

Ref. No.	**Antenna Type**	**Isolation Technique**	**Resonant Frequency (GHz)**	**Minimum Isolation (dB)**	**Element dimensions L x W x h**	**Peak Gain (dB)**	**No. of Ports**
[19]	PIFA	Decoupling slits and shielding wall	2.65	-17	22.1 x 19.3 x 7	Not given	2
[22]	Loop/IFA hybrid	Offset arrangement and grounding strips	3.5/5.8	-11	10.5 x 3.1 x 1	Not given	8
[25]	Microstrip Patch	Neutralization Line	5.4-5.96	-13	20 x 23.4 x 34.8	8.3	2
[87]	L-shaped Monopole	Defected Ground Structure	3.8, 4.6	-18.8	10 x 8	4.71	4

[54]	Annular Ring Slot	Nil	1.8-2.45 (Tuned)	-8	10.1 (Radius) x 0.76 (Thickness)	2.43	4
[96]	Single Element	Ground Slot	3.3-3.7	-14	25.8 x 2.5 x 0.8	Not given	4
Our Work	PIFA L-shaped L-slot	**CMSRR**	**3.5, 4.2, 24-36**	**-24.9, -32.2, -23**	**18 x 14 x 3.2**	**6.36, 6.24, 11.9**	**4**

1.3 Summary

In this chapter, a PIFA structure is proposed for sub-6 GHz and mmWave bands for 5G applications. The proposed antenna uses an L-shaped L-slot radiating element which is designed systematically using TCM as presented in chapter 3. The bands covered by the proposed antenna are 3.5 GHz, 4.2 GHz, and a wideband from 24 GHz to 36 GHz. A four element MIMO antenna is also proposed using the same L-shaped L-slot element. Without any isolation enhancement technique, the isolation level between certain antenna element pairs is not below -15 dB. So, to enhance the isolation and other MIMO system performance parameters, CMSRR is introduced on the ground plane. CMSRR design is presented in chapter 3. Due to the inclusion of CMSRR, the isolation level is enhanced by 8 dB.

A comparison table is also presented to show that the proposed antenna is better than the research available in literature. The isolation levels and gain values are much better than most of the work available in literature. And as per our knowledge, this is for the first an antenna is proposed covering both sub-6 GHz and mmWave bands using the same radiating element. At the end of the chapter, SAR analysis is also presented for talk mode (human head and hand) and data mode (two-hand). The SAR levels are well below the allowed limits.

Chapter 6 Conclusion and Future Scope

6.1 Conclusion

In this thesis, planar antennas for 5G and IoT applications have been designed, analyzed, and developed. The research work presented in the thesis is motivated by the need of innovative antenna solutions for 5G communication devices.

In this thesis two antenna designs are proposed working in sub-6 GHz and mmWave bands for 5G and IoT applications. In the first design, covered under objectives 1 to 4, a compact multi-band MIMO antenna system covering 3.5 GHz band for 5G applications, 12.5 GHz, and 17 GHz band for IoT applications is proposed. As per the objectives, firstly a single element PIFA is designed systematically using TCM analysis. A four element PIFA MIMO system is proposed with high isolation (>21 dB) in lower band between the elements using complimentary Metamaterial structure on the ground plane as per objectives 2 and 3. Finally, the antenna is fabricated and measurements are performed using network analyzer and anechoic chamber.

In the second design, covered under objectives 1 to 4, a four element multi-band MIMO antenna system covering sub-6 GHz and mmWave bands is proposed. The resonant frequencies are 3.5 GHz, 4.2 GHz, and 26 GHz, and 35 GHz. CMSRR is employed to enhance the isolation between the antenna elements with minimum isolation level of -23 dB in sub-6 GHz and mmWave bands.

In this thesis work, the objectives to design, analyze, simulate, optimize, fabricate, and measure the multi-band planar MIMO antenna for 5G applications has been accomplished. In the next section, few ideas for the future work are suggested.

6.2 Future Scope

MIMO antennas for 5G wireless devices will be one of the most important component as high data rate can be achieved through large bandwidth and higher number of antenna elements both at transmitter and receiver. In this research work, the analysis and design of antenna is done systematically using TCM analysis and CMSRR is used to enhance the isolation level, which helped us to achieve the research objectives. The results obtained are encouraging as four element MIMO antennas showed excellent MIMO performance as can be seen from MIMO parameters.

Some of the suggestions for future work are:

- The radiation pattern measurements at mmWave bands can be performed if the facility is available in near future.
- SAR analysis can be performed experimentally using the test setup (if available) which will give us the practical SAR values.
- The MIMO functionality can also be checked properly by using a MIMO test setup which needs arbitrary waveform generator, four port network analyzer, reverberation chamber etc.
- The number of MIMO antenna elements can be increased to design 8-element, 10-element or 12-element MIMO system.

References

[1] G. Wen, Q. Rao, S. Ali and D. Wang, "Handset antenna design: practice and theory," *Progress In Electromagnetics Research,* vol. 80, p. 123–160, 2008.

[2] Shanzhi Chen and Jian Zhao, "The requirements, challenges, and technologies for 5G of terrestrial mobile telecommunication," *IEEE Communications Magazine,* vol. 52, p. 36–43, 5 2014.

[3] T. S. Rappaport, S. Sun, R. Mayzus, H. Zhao, Y. Azar, K. Wang, G. N. Wong, J. K. Schulz, M. Samimi and F. Gutierrez, "Millimeter wave mobile communications for 5G cellular: It will work!," *IEEE access,* vol. 1, p. 335–349, 2013.

[4] H. Wong, K. Luk, C. H. Chan, Q. Xue, K. K. So and H. W. Lai, "Small antennas in wireless communications," *Proceedings of the IEEE,* vol. 100, p. 2109–2121, 7 2012.

[5] Samsung, 2015. [Online]. Available: http://www.samsung.com/global/business-images/insights/2015/Samsung-5GVision-0.pdf. [Accessed 10 01 2021].

[6] W. Lei, A. C. Soong, L. Jianghua, W. Yong, B. Classon, Xiao, Weimin, D. Mazzarese, Z. Yang and T. Saboorian, 5G system design, Springer Nature Switzerland AG, 2020.

[7] N. Kumar, A Multiband PIFA antenna for handheld devices, LAP LAMBERT Academic Publishing, 2018.

[8] K. Sohraby, D. Minoli, B. Occhiogrosso and W. Wang, "A review of wireless and satellite-based m2m/iot services in support of smart grids," *Mobile Networks and Applications,* vol. 23, no. 4, pp. 881-895, 2018.

[9] A. Jaiswal, R. K. Sarin, B. Raj and S. Sukhija, "A novel circular slotted microstrip-fed patch antenna with three triangle shape defected ground structure for multiband applications," *Advanced Electromagnetics,* vol. 7, no. 3, pp. 56-63, 2018.

[10] A. A. Ayubi, S. Sukhija and R. K. & Sarin, "Slotted Implantable Patch Antenna for ISM Band Application and Its Usage in WiMAX with an I-Shaped Defected Ground Structure," *Transactions on Electrical and Electronic Materials,* vol. 18, no. 6, p. 359–363, 2017.

[11] S. Sukhija and R. K. Sarin, "Low-profile patch antennas for biomedical and wireless applications," *Journal of Computational Electronics,* vol. 16, no. 2, pp. 354-368, 2017.

[12] K.-L. Wong, “Planar Antennas for Wireless Communication, John Wiley and Sons, Inc., 2003.

[13] N. Kumar, A. Thakur and J. Sharma, "Study of Planar Inverted-F Antenna (PIFA) for Mobile Devices”," *International Journal of Electronics and Communication Technology,* vol. 4, no. 3, pp. 83-85, 2013.

[14] M. S. Sharawi, "Printed multi-band mimo antenna systems and their performance metrics [wireless corner]," *IEEE Antennas and Propagation Magazine,* vol. 55, p. 218–232, 10 2013.

[15] L. Malviya, R. K. Panigrahi and M. V. Kartikeyan, "MIMO antennas with diversity and mutual coupling reduction techniques: a review," *International Journal of Microwave and Wireless Technologies,* vol. 9, no. 8, pp. 1763-1780, 2017.

[16] J. Malik, A. Patnaik and M. Kartikeyan, "Printed Antennas for MIMO: Exploitation of Polarization Diversity," in *Compact Antennas for High Data Rate Communication*, Springer, Cham., 2018, pp. 81-90.

[17] H. Zhai, Z. Ma, Z. Li and C. Liang, "Reduction of mutual coupling between pifa antennas for dual-band wimax operations," *Microwave and Optical Technology Letters,* vol. 55, p. 2321–2324, 10 2013.

[18] L. Malviya, R. K. Panigrahi and M. V. Kartikeyan, "Four element planar MIMO antenna design for long-term evolution operation," *IETE Journal of Research,* vol. 64, no. 3, pp. 367-373, 2018.

[19] H. Li, B. K. Lau and S. He, "Design of closely packed pattern reconfigurable antenna array for mimo terminals," *IEEE Transactions on Antennas and Propagation,* vol. 65, p. 4891–4896, 9 2017.

[20] A. Chauhan, S. Sharma and C. C. Tripathi, "Design and Fabrication of Ultra Wide-Band Antenna with Band Notching Property for WLAN using Defected Ground Structure," *International Journal on Communication,* vol. 5, no. 1, pp. 42-49, 2014.

[21] S. Zhang, B. K. Lau, Y. Tan, Z. Ying and S. He, "Mutual coupling reduction of two pifas with a t-shape slot impedance transformer for mimo mobile terminals," *IEEE Transactions on Antennas and Propagation,* vol. 60, p. 1521–1531, 3 2012.

[22] K.-L. Wong, B.-W. Lin and B. W.-Y. Li, "Dual-band dual inverted-F/loop antennas as a compact decoupled building block for forming eight 3.5/5.8-GHz MIMO antennas in the future smartphone," *Microwave and Optical Technology Letters,* vol. 59, p. 2715–2721, 11 2017.

[23] Q. Liu and K. Qian, "MIMO Antenna Decoupled with a resonator decoupling network applied for WLAN Applications," in *AIP Conference Proceedings 1967*, 2018.

[24] M. Wang, Y. Li, H. Zou, M. Peng and G. Yang, "Compact mimo antenna for 5g portable device using simple neutralization line structures," in *2018 IEEE International Symposium on Antennas and Propagation & USNC/URSI National Radio Science Meeting*, Boston, 2018.

[25] S. Luo, Y. Li, Y. Xia and L. Zhang, "Low Mutual Coupling Antennaca Array with Gain Enhancement Using Metamaterial Loading and Neutralization Line Structure," *Applied Computational Electromagnetics Society Journal,* vol. 34, no. 3, pp. 411-418, 2019.

[26] C. Yang, J. Kim, H. Kim, J. Wee, B. Kim and C. Jung, "Quad-band antenna with high isolation mimo and broadband scs for broadcasting and telecommunication services," *IEEE Antennas and Wireless Propagation Letters,* vol. 9, p. 584–587, 2010.

[27] S. Padmanathan, A. A. Al-Hadi, P. J. Soh and M. F. Jamlos, "Dual port MIMO Half-Shaped Cubical Parasitic PIFA design for pattern and frequency reconfiguration applied in mobile

terminals," in *2016 IEEE Asia-Pacific Conference on Applied Electromagnetics (APACE)*, Langkawi, 2016.

[28] J. B. Pendry, A. J. Holden, D. J. Robbins and W. J. Stewart, "Magnetism from conductors and enhanced nonlinear phenomena," *IEEE transactions on microwave theory and techniques,* vol. 47, p. 2075–2084, 1999.

[29] Y. Lee, D. Ga and J. Choi, "Design of a MIMO antenna with improved isolation using MNG metamaterial," *International Journal of Antennas and Propagation,* vol. 2012, 2012.

[30] M. H. Rabah, D. Seetharamdoo and M. Berbineau, "Analysis of miniature metamaterial and magnetodielectric arbitrary-shaped patch antennas using characteristic modes: Evaluation of the Q factor," *IEEE Transactions on Antennas and Propagation,* vol. 64, p. 2719–2731, 2016.

[31] M. H. Rabah, D. Seetharamdoo, A. de Lustrac and M. Berbineau, "Analysis of metamaterial inclusions for association with radiating elements using the theory of characteristic modes," in *The 8th European Conference on Antennas and Propagation (EuCAP 2014)*, The, 2014.

[32] R. HafeziFard, M. Naser-Moghadasi, J. Rashed-Mohassel and R.-A. Sadeghzadeh Sheikhan, "Mutual coupling reduction for two closely-space meander line antennas using metamaterial substrate," *IEEE Antennas and Wireless Propagation Letters,* p. 1–1, 2015.

[33] Y. Dong and T. Itoh, "Metamaterial-based antennas," *Proceedings of the IEEE,* vol. 100, p. 2271–2285, 7 2012.

[34] G. Zhai, Z. N. Chen and X. Qing, "Enhanced isolation of a closely spaced four-element mimo antenna system using metamaterial mushroom," *IEEE Transactions on Antennas and Propagation,* vol. 63, p. 3362–3370, 8 2015.

[35] H. Jiang, L.-M. Si, W. Hu and X. Lv, "A symmetrical dual-beam bowtie antenna with gain enhancement using metamaterial for 5g mimo applications," *IEEE Photonics Journal,* vol. 11, p. 1–9, 2 2019.

[36] L. Nama, S. Bhattacharya and P. K. Jain, "An Ultra-thin Wideband Linear to Circular Polarization Converter using Metasurface," in *IEEE International Symposium on Antennas and Propagation & USNC/URSI National Radio Science Meeting*, Boston, MA, 2018.

[37] J. R. Reis, M. Vala, T. R. Fernandes and R. F. S. Caldeirinha, "Metamaterial-inspired Flat-Antenna Design for 5G Small-cell Base-Stations Operating at 3.6 GHz," in *12th International Symposium on Communication Systems, Networks and Digital Signal Processing (CSNDSP)*, Porto, 2020.

[38] L. Nama, S. Bhattacharyya and P. K. Jain, " A Metasurface-Based, Ultrathin, Dual-Band, Linear-to-Circular, Reflective Polarization Converter: Easing Uplinking and Downlinking for Wireless Communication," *IEEE Antennas and Propagation Magazine,* 2021.

[39] R. Selvaraju, M. H. Jamaluddin, M. R. Kamarudin, J. Nasir and M. H. Dahri, "Complementary split ring resonator for isolation enhancement in 5G communication antenna array," *rogress In*

Electromagnetics Research C, vol. 83, pp. 217-228, 2018.

[40] R. Selvaraju, M. H. Jamaluddin, M. R. Kamarudin, J. Nasir and M. H. Dahri, "Mutual Coupling Reduction and Pattern Error Correction in a 5G Beamforming Linear Array Using CSRR," *IEEE Access ,* vol. 6, pp. 65922-65934, 2018.

[41] A. Bhattacharya, B. Roy, R. F. Caldeirinha and A. K. Bhattacharjee, "Low-profile, extremely wideband, dual-band-notched MIMO antenna for UWB applications," *International Journal of Microwave and Wireless Technologies,* vol. 11, no. 7, pp. 719-728, 2019.

[42] M. Cabedo-Fabres, E. Antonino-Daviu, A. Valero-Nogueira and M. F. Bataller, "The theory of characteristic modes revisited: A contribution to the design of antennas for modern applications," *IEEE Antennas and Propagation Magazine,* vol. 49, p. 52–68, 2007.

[43] Y. Chen and C.-F. Wang, Characteristic modes: theory and applications in antenna engineering, Hoboken, NJ: John Wiley & Sons, Inc, 2015.

[44] D. Manteuffel and R. Martens, "Systematic design method of a mobile multiple antenna system using the theory of characteristic modes," *IET Microwaves, Antennas & Propagation,* vol. 8, p. 887–893, 9 2014.

[45] R. Garbacz and R. Turpin, "A generalized expansion for radiated and scattered fields," *IEEE Transactions on Antennas and Propagation,* vol. 19, p. 348–358, 5 1971.

[46] R. Harrington and J. Mautz, "Theory of characteristic modes for conducting bodies," *IEEE Transactions on Antennas and Propagation,* vol. 19, p. 622–628, 9 1971.

[47] J. J. Adams and J. T. Bernhard, "A modal approach to tuning and bandwidth enhancement of an electrically small antenna," *IEEE Transactions on Antennas and Propagation,* vol. 59, p. 1085–1092, 4 2011.

[48] C. Wang, Y. Chen and S. Yang, "Bandwidth enhancement of a dual-polarized slot antenna using characteristic modes," *IEEE Antennas and Wireless Propagation Letters,* vol. 17, p. 988–992, 6 2018.

[49] M. M. Elsewe and D. Chatterjee, "Characteristic mode analysis of excitation feed probes in microstrip patch antennas," in *2016 IEEE International Symposium on Antennas and Propagation (APSURSI)*, Fajardo, 2016.

[50] D. Manteuffel and R. Martens, "Compact multimode multielement antenna for indoor uwb massive mimo," *IEEE Transactions on Antennas and Propagation,* vol. 64, p. 2689–2697, 7 2016.

[51] Q. Zhang, R. Ma, W. Su and Y. Gao, "Design of a multimode uwb antenna using characteristic mode analysis," *IEEE Transactions on Antennas and Propagation,* vol. 66, p. 3712–3717, 7 2018.

[52] A. Ghalib, R. Hussain and M. S. Sharawi, "Characteristic modes of circular slot antennas etched on a finite ground plane," in *2017 IEEE International Symposium on Antennas and Propagation*

& USNC/URSI National Radio Science Meeting, San Diego, CA, USA, 2017.

[53] H. Li, Y. Tan, B. K. Lau, Z. Ying and S. He, "Characteristic mode based tradeoff analysis of antenna-chassis interactions for multiple antenna terminals," *IEEE Transactions on Antennas and Propagation,* vol. 60, p. 490–502, 2 2012.

[54] A. Ghalib, R. Hussain and M. S. Sharawi, "Analysis of slot-based radiators using TCM and its application in MIMO antennas," *International Journal of RF and Microwave Computer-Aided Engineering,* vol. 29, p. e21544, 2 2019.

[55] R. G. Vaughan and J. B. Andersen, "Antenna diversity in mobile communications," *IEEE Transactions on Vehicular Technology,* vol. 36, p. 149–172, 11 1987.

[56] S. Blanch, J. Romeu and I. Corbella, "Exact representation of antenna system diversity performance from input parameter description," *Electronics Letters,* vol. 39, p. 705, 2003.

[57] P. Hallbjorner, "The significance of radiation efficiencies when using S-parameters to calculate the received signal correlation from two antennas," *IEEE Antennas and Wireless Propagation Letters,* vol. 4, p. 97–99, 2005.

[58] M. Manteghi and Y. Rahmat-Samii, "Multiport characteristics of a wide-band cavity backed annular patch antenna for multipolarization operations," *IEEE Transactions on Antennas and Propagation,* vol. 53, p. 466–474, 2005.

[59] Ka Ming Mak and Hau Wah Lai and Kwai Man Luk and Chi Hou Chan, "Circularly polarized patch antenna for future 5g mobile phones," *IEEE Access,* vol. 2, p. 1521–1529, 2014.

[60] N. M. Nor, M. H. Jamaluddin, M. R. Kamarudin and M. Khalily, "Rectangular Dielectric Resonator Antenna Array for 28 GHz Applications," *Progress In Electromagnetics Research C,* vol. 63, pp. 53-61, 2016.

[61] H. W. Lai and H. Wong, "Substrate integrated magneto-electric dipole antenna for 5G Wi-Fi," *IEEETransactionsonAntennasandPropagation,* vol. 63, no. 2, pp. 870-874, 2014.

[62] A. Neto, M. d. M. Dantas, J. d. S. Silva and H. Fernandes, "Antenna for Fifth Generation (5G) Using a EBG Structure," in *New Contributions in Information Systems and Technologies*, Springer International Publishing, 2015, pp. 33-38.

[63] O. M. Haraz, M. M. Ashraf and S. Alshebili, "8x8 Patch antenna array with polarization and space diversity for future 5G cellular applications," in *International Conference on Information and Communication Technology Research*, 2015.

[64] L. H. Trinh, F. Ferrero, L. Lizzi, R. Staraj and J. Ribero, "“Reconfigurable antenna for future spectrum reallocations in 5G communications," *IEEE Antennas and Wireless Propagation Letters,* vol. 15, pp. 1297-1300, 2015.

[65] S. Sharma, C. C. Tripathi and R. Rishi, "Two Port Integrated Reconfigurable Microstrip Patch Antenna," *Progress In Electromagnetics Research,* vol. 89, pp. 39-50, 2019.

[66] X.-X. Yang, G.-N. Tan, B. Han and H.-G. Xue, "Millimeter Wave Fabry-Perot Resonator

Antenna Fed by CPW with High Gain and Broadband," *International Journal of Antennas and Propagation,* vol. 2016, 2016.

[67] P. N. Choubey, W. Hong, Z. Hao, P. Chen, T. Duong and J. Mei, "A wide band dual-mode SIW cavity-backed triangular- complimentary split-ring-slot (TCSRS) antenna," *IEEE Transactions on Antennas and propagation,* vol. 64, no. 6, pp. 2541-2545, 2016.

[68] I. A. Silva, L. J. Matos, P. A. Pinna, V. P. Magri, J. A. Souza and F. P. Campos, "A 10-GHz SIWG slot array antenna prototype on FR-4 substrate," *Microwave Optical Technology Letters,* vol. 58, no. 5, pp. 1059-1065, 2016.

[69] Y.-L. B. e. al., "4G/5G multiple antennas for future multi-mode smartphone applications," *IEEE access,* vol. 4, pp. 2981-2988, 2016.

[70] J. Malik, A. Patnaik and M. V. Kartikeyan, "Novel Printed MIMO Antenna With Pattern and Polarization Diversity," *IEEE Antennas and Wireless Propagation Letters,* vol. 14, pp. 739-742, 2015.

[71] B. Lee, F. J. Harackiewicz and H. Wi, "Closely mounted mobile handset MIMO antenna for LTE 13 band application," *IEEE Antennas and Wireless Propagation Letters,* vol. 13, pp. 411-414, 2014.

[72] K. J. Babu, R. W. Aldhaheri, M. Younus Talha and I. S. Alruhaili, "Design of a compact two element mimo antenna system with improved isolation," *Progress In Electromagnetics Research Letters,* vol. 48, p. 27–32, 2014.

[73] H. Chattha, I. Hameed, M. Nasir, Y. Huang and S. Alja'afreh, "Single element two port Planar Inverted-F diversity antenna for wireless applications," in *Loughborough Antennas and Propagation Conference*, Loughborough, 2013.

[74] N. Ojaroudiparchin, M. Shen and G. F. Pedersen, "Investigation on the performance of low profile insensitive antenna with improved radiation characteristics for the future 5G applications," *Microwave and Optical Technology Letters,* vol. 58, no. 9, pp. 2148-2151, 2016.

[75] O. M. Haraz, M. Ashraf and S. Alshebeili, "Single-band PIFA MIMO antenna system design for future 5G wireless communication applications," in *IEEE11th International Conference on Wireless and Mobile Computing, Networking and Communications*, 2015.

[76] Z. Miers, H. Li and B. K. Lau, "Design of bandwidth-enhanced and multiband mimo antennas using characteristic modes," *IEEE Antennas and Wireless Propagation Letters,* vol. 12, p. 1696–1699, 2013.

[77] J.-N. L. e. al., "Design of Dual-Band MIMO Antenna with High Isolation for WLAN Mobile Terminal," *ETRI Journal,* vol. 35, no. 2, pp. 177-187, 2013.

[78] Z. Q. e. al., "Printed eight-element MIMO systemfor compact and thin 5G mobile handset," *Electronics Letters,* vol. 52, no. 6, pp. 416-418, 2016.

[79] O. M. Haraz, "Broadband and 28/38-GHz dual-band printed monopole/elliptical slot ring

antennas for the future 5G cellular communications," *Journal of Infrared, Millimeter, and Terahertz Waves,* vol. 37, no. 4, pp. 308-317, 2016.

[80] W. Han, L. Longsheng and Z. Zhijun, "A tri-port MIMO antenna designed for Micro/Pico Cell applications with self-decoupled structure," *China Communications,* vol. 11, no. 11, pp. 1-6, 2014.

[81] J. Duan, K. Xu, X. Li, S. Chen, P. Zhao and G. Wang, "Dual-band and enhanced-isolation MIMO antenna with L-shaped meta-rim extended ground stubs for 5G mobile handsets," *International Journal of RF and Microwave Computer-Aided Engineering,* vol. 29, 8 2019.

[82] L. Malviya, M. V. Kartikeyan and R. K. Panigrahi, "Multi-standard, multi-band planar multiple input multiple output antenna with diversity effects for wireless applications," *International Journal of RF and Microwave Computer-Aided Engineering,* vol. 29, p. e21551, 2 2019.

[83] A. Ghalib, R. Hussain and M. S. Sharawi, "Low profile frequency agile MIMO slot antenna with TCM characterization," in *2017 11th European Conference on Antennas and Propagation (EUCAP)*, Paris, 2017.

[84] D. Sarkar and K. V. Srivastava, "A compact four-element mimo/diversity antenna with enhanced bandwidth," *IEEE Antennas and Wireless Propagation Letters,* vol. 16, p. 2469–2472, 2017.

[85] H. T. Chattha, "Compact high isolation wideband 4G and 5G multi-input multi-output antenna system for handheld and internet of things applications," *International Journal of RF and Microwave Computer-Aided Engineering,* vol. 29, p. e21710, 6 2019.

[86] H. AL-Saif, M. Usman, M. T. Chughtai and J. Nasir, "Compact ultra-wide band mimo antenna system for lower 5g bands," *Wireless Communications and Mobile Computing,* vol. 2018, p. 1–6, 6 2018.

[87] B. Arumita and G. V. Rani, "Design and development of low pro-file MIMO antenna for 5G new radio smartphone applications," *Wireless Personal Communications,* vol. 111, no. 3, pp. 1695-1706, 2020.

[88] L. H, T. Y, L. BK, Y. Z and H. S., "Characteristic Mode Based Tradeoff Analysis of Antenna-Chassis Interactions for Multiple Antenna Terminals," *IEEE Transaction on Antenna and Propagation,* vol. 60, no. 2, pp. 490-502, 2012.

[89] C. Van Niekerk and J. T. Bernhard, "Characteristic mode analysis of a shorted microstrip patch antenna," in *Proceedings of the 2012 IEEE International Symposium on Antennas and Propagation*, 2012.

[90] A. B. Numan and M. S. Sharawi, "Extraction of material parameters for metamaterials using a full-wave simulator [education column]," *IEEE Antennas and Propagation Magazine,* vol. 55, p. 202–211, 10 2013.

[91] D. Gangwar, S. Das and R. L. Yadava, "Reduction of mutual coupling in metamaterial based microstrip antennas: the progress in last decade," *Wireless Personal Communications,* vol. 77,

no. 4, pp. 2747-2770, 2014.

[92] G. A. Halls, "Hiperlan: the high performance radio local area network standard," *Electronics & Communication Engineering Journal,* vol. 6, p. 289–296, 12 1994.

[93] T. Varum, M. Duarte, J. N. Matos and P. Pinho, "Microstrip antenna for iot/wlan applications in smart homes at 17ghz," in *12th European Conference on Antennas and Propagation (EuCAP 2018)*, London, 2018.

[94] R. Khan, A. Abdullah Al-Hadi, P. J. Soh, M. T. Ali, S. S. Al-Bawri and Owais, "Design and optimization of a dual-band sub-6 ghz four port mobile terminal antenna performance in the vicinity of user's hand," *Progress In Electromagnetics Research C,* vol. 85, p. 141–153, 2018.

[95] Y. Liu, M. Liu, F. Xu, J. Xu and X. Huang, "A novel four-port high isolation MIMO antenna design for high-capacity wireless applications," *Microwave and Optical Technology Letters,* vol. 60, p. 1476–1481, 6 2018.

[96] L. Zhao, A. Chen, J. Zhang, S. Zheng and Y. Yin, "A single radiator with four decoupled ports for four by four MIMO antennas and systems," in *2017 IEEE International Symposium on Antennas and Propagation & USNC/URSI National Radio Science Meeting*, San Diego, CA, USA, 2017.

[97] M. S. Sharawi, M. Ikram and A. Shamim, "A two concentric slot loop based connected array mimo antenna system for 4g/5g terminals," *IEEE Transactions on Antennas and Propagation,* vol. 65, p. 6679–6686, 12 2017.

[98] H. T. Chattha, Y. Huang, X. Zhu and Y. Lu, "An empirical equation for predicting the resonant frequency of planar inverted-f antennas," *IEEE Antennas and Wireless Propagation Letters,* vol. 8, p. 856–860, 2009.

[99] R. Khan, S. A. A. Al-Hadi, P. J., M. R. Kamarudin, M. T. Ali and Owais, "User Influence on Mobile Terminal Antennas: A Review of Challenges and Potential Solution for 5G Antennas," *IEEE Access,* vol. 6, pp. 77695-77715, 2018.

List of Publications

1. Kumar, Naveen, and Rajesh Khanna. "A compact multi-band multi-input multi-output antenna for 4G/5G and IoT devices using theory of characteristic modes." International Journal of RF and Microwave Computer-Aided Engineering 30, no. 1 (2020): e22012. [SCIE – IF:1.694]

2. Kumar, Naveen, and Rajesh Khanna. "A two element MIMO antenna for sub-6 GHz and mmWave 5G systems using characteristics mode analysis." Microwave and Optical Technology Letters 63, no. 2 (2021): 587-595. [SCIE – IF: 1.392]

3. Naveen Kumar and Rajesh Khanna, “A Four Element MIMO Antenna for 4G/5G Communication Devices using Characteristics Mode Analysis covering sub-6 GHz and mmWave bands,” AEU- International Journal of Electronics and Communications – (Under Review). [SCIE (IF: 3.183)]